

COMMITTEE CERTIFICATION OF APPROVED VERSION

The committee for Joan Louise Kenney certifies that this is the approved version of the following dissertation:

**MECHANISMS AND GENETIC DETERMINANTS OF
ALPHAVIRUS INFECTION OF MOSQUITO VECTORS**

Committee:

Scott C. Weaver, Ph.D., Supervisor

Stephen Higgs, Ph.D.

Judith Aronson, M.D.

Ilya Frolov, Ph.D.

Laura Kramer, Ph.D.

Dean, Graduate School

**MECHANISMS AND GENETIC DETERMINANTS OF
ALPHAVIRUS INFECTION OF MOSQUITO VECTORS**

by
Joan Louise Kenney, MPH

Dissertation
Presented to the Faculty of The University of Texas Graduate School of
Biomedical Sciences at Galveston
in Partial Fulfillment of the Requirements
for the Degree of

Doctor of philosophy

Approved by the Supervisory Committee

Scott C. Weaver
Ilya Frolov
Laura Kramer
Stephen Higgs
Judith Aronson

November, 2011
Galveston, Texas

Key words: alphavirus, vector ecology, arbovirus

© 2011, Joan Louise Kenney

This dissertation is dedicated to John, Ann, and Leslie for their support throughout all my endeavors and the memory of Brandon Brei.

ACKNOWLEDGEMENTS

There are so many people who need to be acknowledged for their help and support throughout my time as a graduate student. First and foremost, I thank my mentor Scott Weaver for his endless support, patience, good humor, and excellent funding. All current and former members of the Weaver Nation were my predominant teachers of various techniques and virology concepts. Special thanks goes to Paige Adams who advised me and assisted me with every one of my aims and Rodion Gorchakov who taught me the magical art of cloning with extreme patience and an unfailingly upbeat attitude. Lark Coffey, Nik Vasilakis, and Nicole Arrigo provided invaluable mosquito training and BSL3 training, without which I never would have been able to safely work with these viruses. I owe a debt of gratitude, as do all Weaver lab members, to Grace Leal who quietly manages to keep the Weaver lab running smoothly and is always willing to help students. I thank Jing Huang, for her tireless efforts at maintaining and providing mosquitoes for all my many experiments. A special thanks goes to my committee members, Judy Aronson, Steve Higgs, Ilya Frolov, and Laura Kramer who each were supportive and always willing to share their knowledge. Outside of the lab, I was guided by many faculty members including, Chuck Fulhorst, Leoncio Vergara, Steve Wikel, Gustavo Valbuena, Norbert Herzog, and many others. For non-scientific help, Dora Salinas was my primary source and she was always eager to help with a smile on her face, which was always appreciated and greatly valued. I also would like to thank Ken McManus and his baristas at Mod for letting me work in his wireless coffee shop for

multiple hours at a time, many days a week. Throughout my time at UTMB I was fortunate to be funded by the CDC Vector-Borne diseases training grant, the NIH Biodefense and Emerging Infectious Diseases training grants, the UTMB McLaughlin endowment, and the W. M. Keck Fellowship for Virus Imaging. I'll close by thanking the UTMB Graduate School for Biomedical Sciences for all the wonderful support they provided throughout my time at UTMB.

MECHANISMS AND GENETIC DETERMINANTS OF ALPHAVIRUS INFECTION OF MOSQUITO VECTORS

Publication No. _____

Joan Louise Kenney, Ph.D.

The University of Texas Graduate School of Biomedical Sciences at Galveston, 2011

Supervisor: Scott C. Weaver

Venezuelan equine encephalitis virus (VEEV) is a mosquito-borne disease that has caused hundreds-of-thousands of human and equine cases. Since epizootic strains have historically been the largest public health threat, the majority of experimental studies have focused on these strains. Recently, there has been an increase in the number of cases caused by enzootic strains, IE and ID, which illustrates the importance of understanding how these viruses interact with their mosquito vector. Studies examining the interaction between epizootic strains and their vector indicate that the primary viral determinants for successful infection of epizootic mosquito vector can be mapped to the E2 glycoprotein region. I hypothesized that in addition to the E2 glycoprotein, regions outside of the E2 glycoprotein determine successful infection by enzootic strains of their mosquito vector, *Culex taeniopus* and examined this hypothesis utilizing chimeric viruses of epizootic IAB and enzootic IE VEEV strains. My findings support my hypothesis that the regions of the E2 glycoprotein are not solely responsible for enzootic vector infection and suggest that the 3' UTR might also be a determinant of enzootic vector infection.

The second focus of this dissertation was to examine the particular characteristics of initial midgut infection and dissemination by IE VEEV in *Cx. taeniopus*. Given

previous findings suggesting that the epizootic mosquito vector has a limited number of susceptible midgut cells, I hypothesized that the enzootic vector would not have a restricted population of susceptible midgut cells and orally infected *Cx. taeniopus* mosquitoes with replicon particles to examine this hypothesis. My findings suggest that there is not a restricted population of susceptible midgut epithelial cells and enzootic IE virions do not have a predilection for infection of a particular region of the posterior midgut epithelium.

I additionally proposed to elucidate the route of enzootic viral escape from the *Cx. taeniopus* midgut and hypothesized that the virions utilized the mosquito tracheal system to bypass the basal lamina associated with the midgut. I utilized a IE virus encoding a green fluorescent protein (GFP), but was unable to determine the route of dissemination due to attenuation of the virus as a result of the GFP inclusion.

TABLE OF CONTENTS

TABLE OF CONTENTS.....	VIII
LIST OF TABLES.....	XIV
LIST OF FIGURES	XV
LIST OF ABBREVIATIONS	XVII
CHAPTER 1: INTRODUCTION	1
Alphaviruses	1
Classification	1
Virion entry and translation	3
Transcription and Replication.....	6
Virion assembly and budding	7
Conserved sequence elements	8
Venezuelan equine encephalitis virus (VEEV).....	10
Disease.....	11
Emergence and outbreaks	11
Vaccine	13
VEEV Ecological Cycles.....	15
Epizootic Cycle.....	15
Enzootic Cycle	16
Virulence and equine-amplification models	19
Mosquitoes as vectors.....	21
Mosquito Biology	21

Anatomy.....	22
Mosquito-Virus Interaction.....	27
Infection	27
Dissemination from the midgut.....	29
Culex taeniopus and VEEV	33
Project summary and significance	34
Summary	34
Significance	36
CHAPTER 2: GENERATION OF INFECTIOUS CLONES.....	38
Chimeric viruses between IAB and IE VEEV Strains.....	38
Purpose	38
Mismatching <i>cis</i> -acting element cloning.....	41
Tth111I fusion cloning.....	41
Generating matching <i>cis</i> -acting chimeras.....	44
From plasmid to replicating virus.....	47
Large scale DNA preparation	47
Cesium Chloride Purification.....	48
Transcription and Electroporation	49
IE 68U201 Expressing Green Fluorescent Protein.....	50
Fusion Cloning Strategy	50
Characterization	53
Replication <i>in vitro</i>	53
Statistical analysis of replication <i>in vitro</i>	54

Replicons and helpers	56
Purpose	56
IE 68U201 GFP and CFP replicon	59
IAB V3000 Helper.....	59
Linearization and Electroporation	60
cloning summary and conclusions	61
CHAPTER 3: GENETIC DETERMINANTS OF VEEV INFECTION OF THE ENZOOTIC VECTOR, <i>CULEX TAENIOPUS</i>	64
Background.....	64
Methods.....	68
Viruses	68
Mosquitoes.....	68
Mosquito Exposure	69
Artificial Viremia.....	70
Natural Viremia.....	70
Artificial Blood Meal	71
Plaque and CPE Assays	72
Statistics.....	72
Results.....	73
Mosquito Exposure	73
<i>Cx. taeniopus</i> Infection and Dissemination	75
<i>Ae. taeniorhynchus</i> Infection and Dissemination	77

Conclusions and Summary	80
CHAPTER 4: CHARACTERIZING THE MIDGUT INFECTION OF <i>CULEX TAENIOPUS</i> .87	
Background.....	87
Materials and methods	90
Cells and replicon particles.....	90
Replicon titration	91
In vitro infection control	92
Tail vein inoculations.....	92
Mosquito exposure.....	93
Midgut dissection and processing.....	94
Microscopy	96
Results.....	96
Tail vein inoculations.....	96
<i>Cx. taeniopus</i> midgut infection.....	100
<i>Cx. taeniopus</i> midgut epithelial susceptibility	101
Conclusions and summary	105
CHAPTER 5: MIDGUT ESCAPE OF ENZOOTIC SUBTYPE IE VEEV IN <i>CULEX TAENIOPUS</i>.....110	
Introduction.....	110
Methods.....	115
Virus and cells	115
Oral infection of <i>Cx. taeniopus</i>	115
Viremic exposure	115

Artificial viremia exposure	115
Intrathoracic inoculation of <i>Cx. taeniopus</i>	116
Sampling and cryosectioning.....	116
Fluorescent microscopy	117
Results.....	117
Intrathoracic exposure.....	117
Oral exposure.....	117
Dissemination.	118
Cryosectioning and Microscopy.....	118
discussion.....	121
CHAPTER 6: TRANSMISSION POTENTIAL OF TWO CHIMERIC WESTERN EQUINE ENCEPHALITIS VACCINE CANDIDATES IN CULEX TARSALIS	126
Introduction.....	126
Methods.....	131
Viruses	131
Oral mosquito infections.....	132
Intrathoracic mosquito infections.	132
Transmission to mice.....	133
Statistical analyses	134
Results.....	135
Orally exposed <i>Cx. tarsalis</i> infection and dissemination.	135
Intrathoracic exposure to WEEV-McM and SIN/EEE/McM.....	135
Mosquito transmission following oral exposure.....	137

Mosquito transmission following intrathoracic inoculation	139
Conclusions and Summary	140
CHAPTER 7: FINAL CONCLUSIONS AND FUTURE DIRECTIONS	148
Summary	148
Viral determinants of enzootic infection	150
Initial midgut infection and cell susceptibility	154
Dissemination pathway	159
Final Conclusions	160
REFERENCES.....	162

LIST OF TABLES

Table 1-1: Summary of important alphaviruses around the world.	2
Table 3-1: Natural and artificial viremias.....	75
Table 3-2: Rates of infection and dissemination of each virus in <i>Cx. taeniopus</i>	78
Table 3-3: Infection, dissemination, and disseminated infection in <i>Ae. taeniorhynchus</i> .	80
Table 4-1: Infection and location within <i>Cx. taeniopus</i> midgut	101
Table 4-2: Dual infection <i>in vivo</i> and <i>in vitro</i>	102
Table 6-1: Rates of infection and dissemination.....	136
Table 6-2: Probing status and survival of suckling mice exposed to IT inoculated mosquitoes	146

LIST OF FIGURES

Figure 1-1: Depiction of alphavirus genome and virion structure	4
Figure 1-2: Alphavirus replication and conserved sequence elements	9
Figure 1-3: VEEV ecological cycle	18
Figure 1-4: Depiction of mosquito anatomy with structural labels.	24
Figure 1-5: Illustration of tracheoblasts and tracheoles	25
Figure 1-6: Junction of foregut and midgut at site of intussuscepted foregut.	31
Figure 2-1: Parent and chimeric viruses	40
Figure 2-2: Tth111I fusion PCR strategy and primers for IAB/IE and IE/IAB.....	45
Figure 2-3: Final Fusion PCR strategy for IE/IAB and IAB/IE	46
Figure 2-4: Fusion PCR strategy for 3' UTR and primers	47
Figure 2-5: 68U201 GFP plasmid clone.	51
Figure 2-6: Fusion primers for 68U201 GFP.....	52
Figure 2-7: Chimera replication curves	55
Figure 2-8: Electroporation of replicons.....	57
Figure 3-1: Change in artificial viremia.....	74
Figure 3-2: Regression of infection, dissemination and disseminated infection	79
Figure 3-3: Clearance of rates after intracardiac inoculation.....	83
Figure 4-1: 68U201 replicon particles expressing GFP and CFP.....	90
Figure 4-2: Change in circulating artificial viremia	95
Figure 4-3: Adapted tail-vein inoculation technique	99

Figure 4-4: Sites of 68UGFP midgut infection (10x).....	103
Figure 4-5: Examples of dual 68U201 replicon infection	104
Figure 4-6: Dose response of <i>Cx. taeniopus</i> compared to <i>Ae. taeniorhynchus</i>	107
Figure 5-1: Mosquito anatomy and dissemination.....	111
Figure 5-2: GFP in <i>Cx. taeniopus</i> at serial time points.....	120
Figure 5-3: Example of high levels of background and nonspecific fluorescence	123
Figure 6-1: Western equine encephalitis ecological life cycle	127
Figure 6-2: SIN/CO92 and SIN/EEE/McM chimeric vaccine candidates.....	130
Figure 6-3: Survival of suckling mice from orally exposed <i>Cx. tarsalis</i>	138
Figure 6-4: Survival of suckling mice from IT inoculated <i>Cx. tarsalis</i>	140

LIST OF ABBREVIATIONS

ANOVA	analysis of variance
BSA	bovine serum albumin
CFP	cherry fluorescent protein
CIP	calf intestine phosphatase
CPE	cytopathic effects
DEPC	diethyl pyrocarbonate
EtOH	ethanol
GFP	green fluorescent protein
INA	1,5 – iodonaphthyl-azide
IP	intraperitoneal
M	molar
ml	milliliter
MOI	multiplicity of infection
PFU	plaque forming units
PPO	2,5 – diphenyloxazole
rcf	relative centrifugal force
TB	terrific broth

CHAPTER 1: INTRODUCTION

ALPHAVIRUSES

Classification

The viral family *Togaviridae* contains two genera, *Alphavirus* and *Rubivirus*. While the *Rubivirus* genus only includes one virus, there are 29 recognized virus species within the *Alphavirus* genus, many of which are considered to be a growing risk to public health. Alphaviruses are primarily defined by their antigenic complex, geographic distribution, and the type of human disease they cause (table 1-1). Species of the *Alphavirus* genus persist in nature in Australia, Asia, Africa, North and South America, New Zealand, and have been identified in seals in Antarctica [1]. Old World species, such as chikunguna virus (CHIKV), o'nyong-nyong virus (ONNV), and Semliki Forest virus (SFV), are more likely to cause an arthralgic disease, which is frequently characterized by arthralgia and in some cases a rash [1]. New World species such as eastern equine encephalitis virus (EEEV), Venezuelan equine encephalitis virus (VEEV), and western equine encephalitis virus (WEEV), are associated with encephalitic disease and are more likely to cause a fatal outcome [1]. While not all representatives persist in an insect-vertebrate host life cycle, invertebrate hosts, predominately mosquitoes, vector the majority of alphavirus strains known to have an impact on human health. The types of vertebrate hosts primarily include avians or mammals, although aquatic alphaviruses utilize fish as hosts [1].

Virus (Abbreviation)	Antigenic Complex	Principal Vertebrate Reservoir Host	Geographic Distribution	Human Disease
Aura (AURA)	WEE	?	South America	
Barmah Forest (BF)	BF	Birds	Australia	Fever, arthritis, rash
Bebaru (BEB)	SF	?	Asia	
Cabassou (CAB)	VEE	?	French Guiana	
Chikungunya (CHIK)	SF	Primates	Africa, Southeast Asia, Philippines, Indonesia	Fever, arthritis, rash
Eastern equine encephalitis (EEE)	EEE	Birds	North America, South America, Caribbean	Fever, Encephalitis
Everglades (EVE)	VEE	Mammals	Florida	Fever, encephalitis
Fort Morgan (FM)	WEE	Birds	Colorado	
Getah (GET)	SF	Mammals	Asia	Fever
Highlands J (HJ)	WEE	Birds	North American	
Kyzlagach (KYZ)	WEE	Birds	Azerbaijan	
Mayaro (MAY)	SF	Mammals	South America	Fever, arthritis, rash
Middelburg (MID)	MID	?	Africa	
Mucambo (MUC)	VEE	?	South America, Caribbean	
Ndumu (NDU)	NDU	?	Africa	
O'nyong-nyong (ONN)	SF	?	East Africa	
Pixuna (PIX)	VEE	Mammals	Brazil	
Rio Negro (AG80)	VEE	Mammals	Argentina	
Ross River (RR)	SF	Mammals	Australia, South Pacific	Fever, arthritis, rash
Salmonid	?	Fish	North Atlantic	
Semliki Forest (SF)	SF	?	Africa	Fever, encephalitis
Sindbis (SIN)	WEE	Birds	Australia, Africa, Northern Europe, Middle East	Fever, arthritis, rash
Southern Elephant Seal (SES)	?	Seals	Antartica	
Trocara		?	South America	
Una (UNA)	SF	?	South America, Trinidad	
Venezuelan equine encephalitis (VEE)	VEE	Mammals	South America, North America	Fever, encephalitis
Western equine encephalitis (WEE)	WEE	Birds, mammals	North America, South America	Fever, encephalitis
Whataroa (WHA)	WEE	Birds	New Zealand, Australia	

Table 1-1: Summary of important alphaviruses around the world.

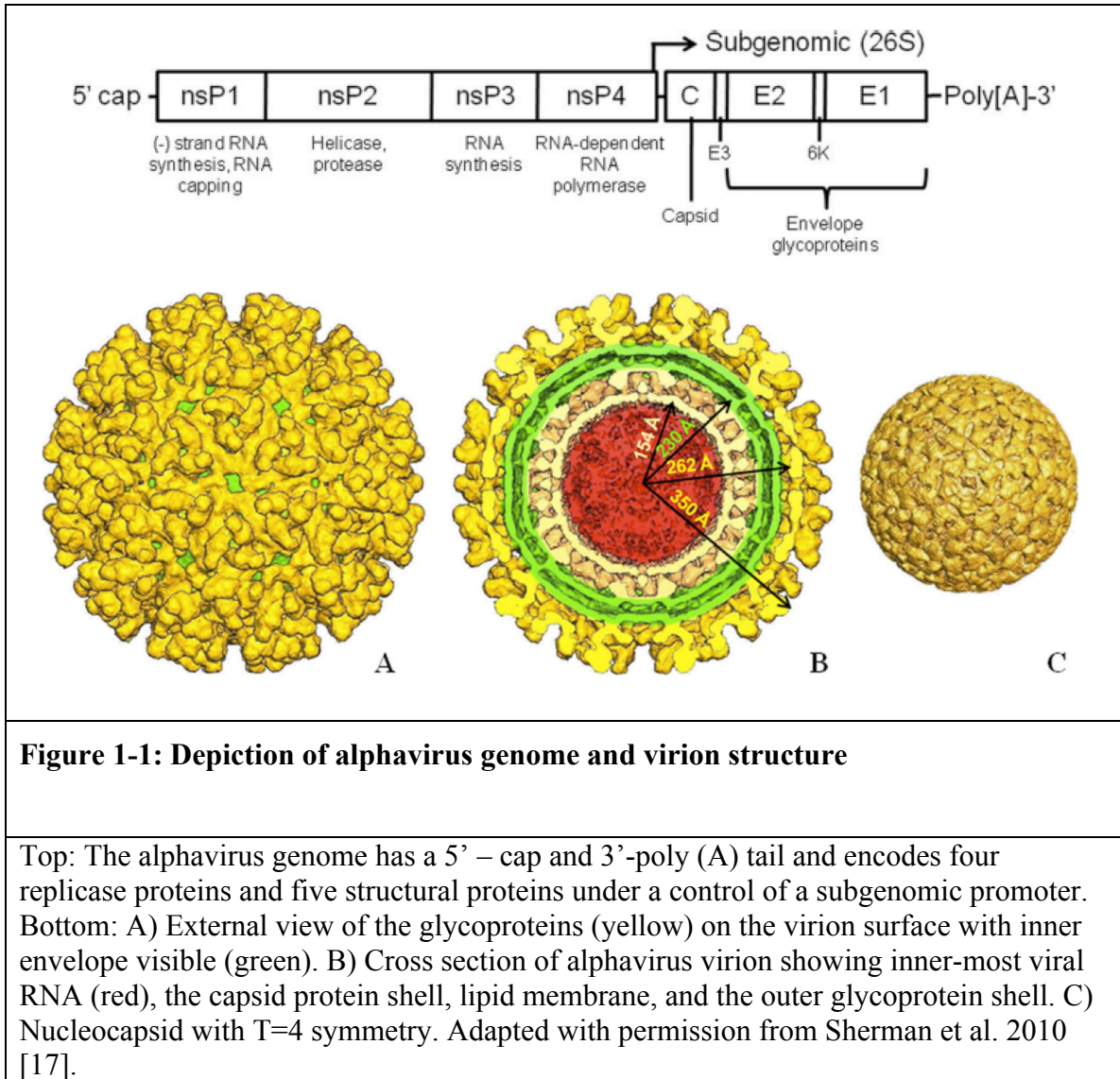
Adapted with permission from Griffin 2007 [1].

Virion entry and translation

Alphavirus virions have a diameter of approximately 700 Angstroms with a host derived lipid bilayer envelope. The nucleocapsid consists of a positive sense, single stranded RNA genome of approximately 11.7 kilobases (KB). Like cellular mRNA, the alphavirus genome has a 5' methylguanylate cap and a 3' polyadenylated tail [2]. Two glycosylated glycoproteins, E1 and E2 form stable heterodimers that in groups of three make up the spike-like protrusions on the virion surface [3,4]. Alphaviruses are capable of infecting a wide range of cell types both *in vitro* and *in vivo* indicating that either the E2 glycoprotein has many receptor-binding sites for various cell receptors or the virus utilizes a highly available receptor that is common on multiple cell types [5].

Alphaviruses have been shown to utilize the laminin receptor for entry into mammalian cells and mosquito cells *in vitro* [6]. However, it has been shown repeatedly that serial passaging of alphaviruses *in vitro* results in acquisition of specific, positively charged mutations in the E2 glycoprotein that confer the ability to bind heparin sulfate, which engenders improved attachment to cells [7-12]. Although recent isolates of EEEV have been found to have the ability to bind heparin sulfate, which is potentially correlated to the high neurovirulence of these strains [13]. Once virions have bound to a receptor, they are endocytosed into vesicles using a clathrin dependent mechanism [14]. The virion membrane joins with the host cell membrane following a change in pH in which the vesicle becomes acidic [15]. As a result of the low pH, the glycoprotein heterodimer

disassembles resulting in exposure of a fusion peptide on the E1 glycoprotein, which allows for E1 trimers to form and release of the viral nucleocapsid into the cytoplasm [5,16].



Some studies of SINV suggest that nucleocapsid core interacts with ribosomal RNA which facilitates uncoating in preparation for translation [18].

Genomic RNA serves as the template for translation of first polyprotein, which makes up the replication or nonstructural proteins. They consist of four individual proteins (nsp1-nsp4), which are translated as a polyprotein nsP123 or nsp1234 with nsp123 being the more common species [19]. Read through of p1234 occurs due to an opal codon at the termination codon of nsp3 and is thought to act as a feedback mechanism for control or shut off of minus strand template synthesis that occurs three to four hours following infection [20-22]. Nsp1234 and nsp123 undergo autocatalytic cleavage by a proteinase encoded in nsp2 to yield the individual nonstructural proteins [23,24]. Nsp1 functions as a methyltransferase and guanylyltransferase and plays a role in formation of m⁷GpppA cap structures on genomic and subgenomic viral RNA species [25]. Nsp1 has also been shown to associate with the host cell membrane [26,27] and play a role in minus strand RNA synthesis [28]. Nsp2 appears to play a role in many enzymatic processes including regulation of subgenomic and minus strand RNA synthesis [29-31], helicase activity [32,33], proteolysis and cleavage of the nonstructural polyprotein [34-36], has a nuclear localization signal, and has been implicated in neuropathogenicity of SFV [37,38]. The amino terminus of nsp3 is conserved in alphaviruses, although the importance of this conservation is unknown. The carboxy-terminus consists of a hypervariable region that varies in length and sequence among

alphaviruses, is a frequently phosphorylated on serine and threonine residues, and has been shown to play a role in modulating nsp3 degradation [39,40]. Nsp4 is the catalytic RNA dependent RNA polymerase and its translation is highly regulated [41-43]. Translation of the structural polyprotein utilizes the subgenomic 26S mRNA which encodes the five structural proteins (capsid-E3-E2-6K-E1). Like the nonstructural proteins, the structural polyprotein is post-translationally cleaved by a protease encoded within the capsid [44], cellular signalase proteins, and a furin-like protease [5].

Transcription and Replication

Alphavirus replication utilizes three highly controlled species of RNA: a) positive strand genomic RNA, b) complementary minus strand RNA, and c) positive strand subgenomic RNA. Replication initiates with synthesis of the minus strand RNA, which requires the viral 3' UTR and nonstructural polyprotein cleavage products nsp123 and nsp4 [45-49] (Figure 1-2). Plus strand RNA synthesis initiation coincides with the occurrence of post-translational cleavage of individual nsp1, nsp2, and nsp3 proteins and continues as long as protein synthesis is occurring. A model for initiation of minus strand synthesis entails joining of the 5' and 3' ends of the genomic RNA, although experimental systems to irrevocably demonstrate this phenomenon are lacking [5,45]. While the total minus strand RNA generated is significantly less than the plus strand RNA synthesized, subgenomic RNA encoding the structural proteins is transcribed at a

rate approximately three-fold higher than plus strand genomic RNA, although the particular ratio varies depending on the alphavirus [5].

Virion assembly and budding

Post-translational cleavage of the structural polyprotein is necessary for individual structural proteins to be functional. Cleavage of the capsid from the polyprotein exposes a signal sequence on the new amino terminus that promotes translocation across the endoplasmic reticulum membrane [50]. The polyprotein is modified by attachment of oligosaccharides [51] and subsequent cleavage by host-cell signalase proteins [52] resulting in PE2, E1, and 6K proteins. The carboxy termini of PE2 and 6K encode a signal sequence that facilitates migration of the PE2, E1, and 6K proteins [5]. PE2 and E1 fold into intermediates and then form a heterodimer [53] prior to being transported to the Golgi network. Before reaching the plasma membrane PE2 is cleaved into E3 and E2 by a furin-like protease [54]. Prior to budding, a specific interaction between capsid proteins and glycoprotein dimers takes place. Structural examination of these interactions has indicated that the cytoplasmic domain of the E2 glycoprotein binds to a hydrophobic pocket in the amino terminus of the capsid core [55,56]. The 6K protein has also been shown to play an essential role in release of new virus particles on the cell surface [57]. Finally nucleocapsids interact with the cell plasma membrane and trans-membrane viral glycoproteins in an action that encapsulates the virion particle in the host cell bilayer lipid membrane [58].

Conserved sequence elements

In addition to the many protein interactions required for efficient alphavirus replication, there are several less clearly observable RNA interactions that occur between different regions of the viral genome. Typically, the regions involved have been shown to be highly conserved RNA elements present in all members of the genus. There are four conserved sequence elements (CSE) described in alphaviruses (figures 1-2). The first two, located near the 5' end of the genome, consist of the 5' terminal sequence within the UTR, which encodes the core promoter [59], and a 51-nt CSE in the nsp1 gene, which is believed to act as a replication enhancer [59,60]. Despite not having stringent conservation of the entire nucleotide sequence, there are structural aspects of the alphavirus 5' UTR that are conserved and necessary for initiation of replication [45,61-63]. Specifically, the UTR has an initial AU dinucleotide sequence for the first two nucleotides and a structurally relevant G-C rich RNA stem that appear to act in tandem to allow for genome replication initiation [64]. The third element, a 24-nt sequence at the junction between the nonstructural cassette and structural cassette, is required to instigate transcription of the subgenomic RNA [65,66]. The fourth CSE of 19-nt immediately precedes the 3' poly (A) tail and has been established as a promoter [46,47,67].

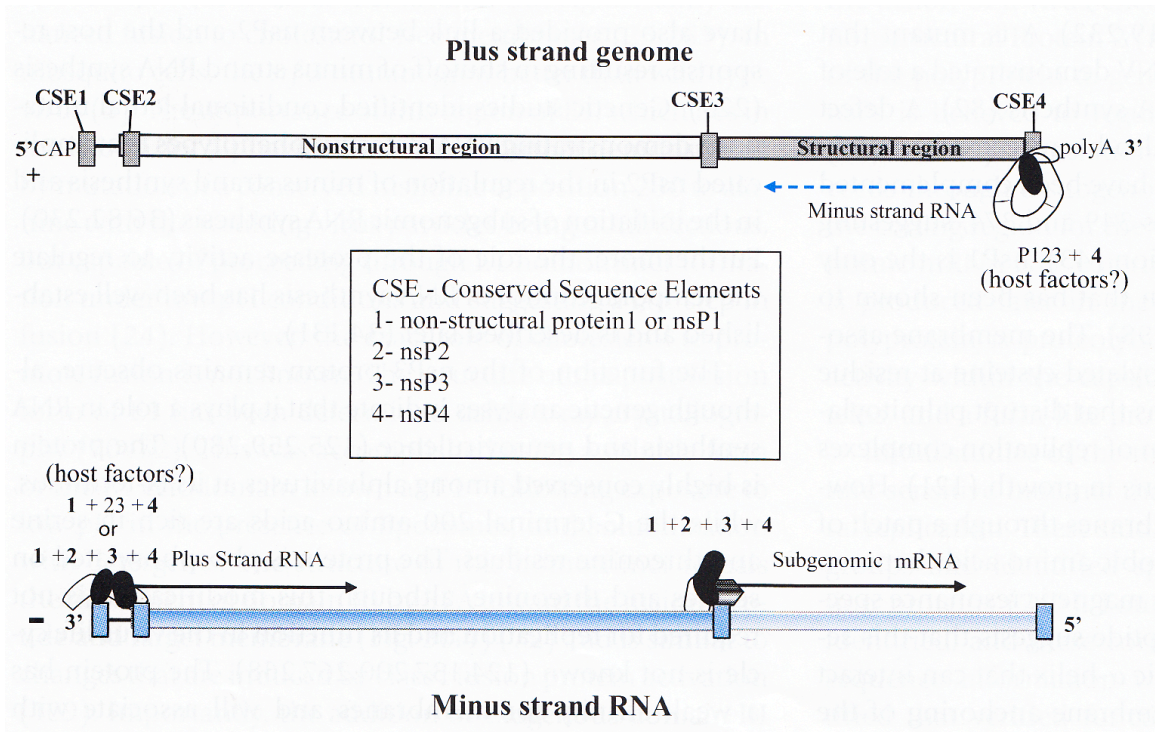


Figure 1-2: Alphavirus replication and conserved sequence elements

Top: The genome has four conserved sequence elements (CSE1-CSE4). Replication initiates with minus strand RNA synthesis, which takes place at the 3' UTR with the presence of P124 and nsP4. Bottom: Cleavage between nsP1 and nsP2 provides material necessary for synthesis of plus strand genomic synthesis. Further cleavage of nsP2 and nsP3 allows for synthesis of subgenomic mRNA. Image from Kuhn 2007 with permission [5]

VENEZUELAN EQUINE ENCEPHALITIS VIRUS (VEEV)

Venezuelan equine encephalitis virus (VEEV) is an example of a new world alphavirus that is vectored by mosquitoes and causes fatal encephalitis in horses and humans. The VEE antigenic complex is made up of six subtypes (I-VI) representing VEE complex viruses, Everglades virus (EVEV), Mucambo complex viruses, Pixuna virus, Cabassou virus, and Rio Negro viruses, respectively. Of all of these subtypes, only the VEEV group (subtypes IA-E) contains viruses with epizootic and/or virulent phenotypes [68]. Within VEE, subtype I, are five varieties: IAB, IC, ID, IE, and IF distributed throughout the Americas. Strain IF is the only virus in the subtype that is not a strain of VEE, but rather is Mosso das Pedras Virus [68]. VEEV has a unique ecology when compared to other alphaviruses in that it cycles in two clearly distinct cycles: epizootic and enzootic. As defined by the Medline Plus Merriam Webster dictionary, an enzootic virus is “of animal diseases: peculiar to or constantly present in a locality” while epizootic is defined as “an outbreak of disease affecting many animals of one kind at the same time.” Typically, subtypes IAB and IC have been responsible for major outbreaks in humans and horses and therefore are thought of as the epizootic strains. ID, IE, and IF have historically been thought of as enzootic as they do not cause disease in humans or horses, but persist in sylvatic cycles [68]. The only exception to these typical characterizations are some recent IE VEEV strains from Mexico that appear able to cause

disease in horses and are compatible for infection and transmission of the primary epizootic vector *Aedes taeniorhynchus* [69,70].

Disease

VEEV has caused hundreds-of -thousands of human and equine cases in regions of Mexico, Central, and South America [68]. Clinical signs include tachycardia, depression, circling and anorexia. Encephalitis tends to develop within 5-10 days of infection and death follows soon thereafter [71]. In humans the disease can be sub-clinical, but more often has a high attack rate and is very pathogenic. Cases with self-limiting disease tend to present with malaise, fever, chills, retro-orbital or occipital headache, and myalgia. Clinical signs include leucopenia, tachycardia, fever, nausea, vomiting, and diarrhea. Less typical signs indicative of involvement of infection of the central nervous system are convulsions, somnolence, confusion, and photophobia. Lethal human VEE, which occurs in less than 1% of cases, is characterized by diffuse congestion and edema in the brain, gastrointestinal tract, and lung [72]

Emergence and outbreaks

VEE disease has a large impact on South American countries that rely on equids for agriculture and transportation. Epidemics were first detected in Venezuela in the 1920s and continued periodically through the 1960s affecting hundreds-of-thousands of people [73]. The virus was first isolated from an equine brain in 1938 and examination of replication and virulence models showed the isolate to differ from previously

described Eastern and Western encephalitic virus [74]. The first documented outbreak began in Colombia in 1935 and is believed to have spread into Venezuela by the following year [68]. VEEV continued to spread north and emerged on the Island of Trinidad in the early 1940s. The virus continued to migrate and spurred massive outbreaks in Colombia, Venezuela, and Peru through the 1960s [75]. Phylogenetic studies examining outbreak isolates from this time period suggest that some of these outbreaks originated from vaccine strains, that were likely not inactivated properly [76]. It has been estimated that outbreaks in Colombia and Peru during this time period accounted for over 200,000 human cases and 100,000 equine deaths [73,77]. The next most notable outbreak started in Central America in 1969, spread north through Mexico, and into southern Texas over the next few years [68]. Interestingly, following that epizootic, VEEV went largely undetected until 1992, when the virus re-emerged in Venezuela [78]. Despite imperceptible activity of subtypes IAB and IC from 1973 to 1993 persistence was confirmed by phylogenetic studies of enzootic and epizootic strains obtained during the period from 1992-1993 [78,79]. Since then, outbreaks in equids in Mexico and a severe outbreak in Venezuela and Columbia (1995) have reinforced the potential for this disease to re-emerge. The Mexican outbreaks involved subtype IE, which was previously established to be enzootic and not known to cause equine disease, and affected approximately 157 horses with 75 deaths [70,80]. This outcome of a historically enzootic virus strain producing significant outbreaks raises concerns for potential emergence of more epizootics. VEEV has also been developed into a biological weapon by the United

States as well as the former Soviet Union and is now classified as a CDC/NIH category B select agent due to its infectivity via the aerosol route, severe pathogenicity, and absence of a licensed human vaccine or proven therapeutic treatment [81,82].

Vaccine

In the early 1960s a live attenuated vaccine strain, TC-83, was developed using serial passaging of the wild-type Trinidad donkey subtype IAB VEEV strain (TrD) through guinea pig heart cells [83]. Comparison of the attenuated product and the original TRD strain, revealed seven amino acid changes as well as one nucleotide change in each of the 3' - and 5' -UTRs [84]. While never licensed for humans, TC-83 has been used as an investigational drug to vaccinate at risk military and laboratory personnel [85-88]. Summary findings from these vaccinated groups indicated that when vaccinees do generate an immune response, TC-83 induces a robust hemagglutination inhibition (HI) and neutralizing antibody responses. While the generated immunity provides protection against challenge with other IAB VEEV strains, it evokes poor protection against VEEV subtype ID, IE, and other alphaviruses in the VEE complex (subtypes III, VI) [89]. However, TC-83 has a high seroconversion failure rate and approximately 20% of recipients fail to mount a humoral immune response [90]. Similarly, 25-38% of vaccinees develop viremia and clinical symptoms similar to those observed after wild-type VEEV infection [85,88]. The attenuation of TC-83 virus has also been shown to be unstable. For instance, as little as three serial intracranial (i.c.) passages in infant mice results in

reversion to a neurovirulent phenotype characteristic of the wild type parent IAB strain [83,87,91].

A more recent live attenuated approach is exemplified by the VEEV 3526 candidate, in which a full-length cDNA VEEV TrD strain was modified to contain two independently attenuating mutations. In this candidate there is a deletion of the four amino acid furin recognition site between structural proteins E3 and E2 as well as a Phe to Ser attenuating change at amino acid 253 within the E1 glycoprotein [92]. The latter mutation is required to rescue viability of the cleavage site mutant, which provides a lethal control against reversion. Previous studies examining neurovirulence of this vaccine candidate indicated it does not gain virulence following five serial i.c. passages in adult mice or five cell culture passages. Also, V3526 replicates poorly in adult mouse brains and causes less histopathology when compared to TC-83 [20]. However, when this candidate was tested in non-human primates, it caused clinical symptoms in vaccinated primates [93], so to date there is still no licensed vaccine available for VEE. However, recent work with a novel inactivating agent, 1,5-iodonaphthyl-azide (INA) has shown inactivated V3526 to be immunogenic and protective in adult mice and cause no disease in suckling mice [94].

VEEV Ecological Cycles

Epizootic Cycle

Epizootic strains, primarily characterized by IAB and IC, have a long history of causing severe illness in humans and equines, which has allowed for ample opportunities to isolate and study these strains. When epizootic viruses are active, they persist in a dual host life cycle primarily between mosquito vectors and equine hosts, with humans being tangentially involved. Epizootic viruses are distinct from their enzootic counterparts in that they cause a high (up to 10^7 suckling mouse LD₅₀/ml) viremia in equines and utilize a contrasting set of mosquito vectors from those of the enzootic strains [95]. Similarly, epizootic mosquito vectors generally have a higher threshold of infection (defined as the concentration of virus necessary to infect 1-5% of exposed mosquitoes) as compared to enzootic vectors, although these values vary depending on the mosquito vector and virus in question [96]. Incriminated epizootic vectors include *Psorophora columbiae*, *Ps. confinnis*, *Ps. discolor*, *Ae. sollicitans*, *Mansonia indubitans*, *Cx. (Dienocerities) spp.* and *Cx. pseudes* [68,97-100]. However, *Ae. taeniorhynchus* is believed to be the most important epidemic vector in coastal areas of South America [101,102]. Although not all epizootic mosquitoes have the same natural history, they generally are found near brackish water, can fly long distances from breeding sites, prefer to feed on humans or other large mammals, and can tolerate feeding in sunny areas, which makes them ideal transmitters of epizootic strains.

Enzootic Cycle

Enzootic VEEV strains persist in a disparate ecological cycle from IAB and IC strains. These viruses are thought to primarily cycle between a mosquito vector and sylvatic rodent hosts from various genera including *Sigmodon*, *Oryzomys*, *Zygodontomys*, *Heteromys*, *Peromyscus*, and *Proechimys* [89,100]. Recent studies examining host viremia have implicated *Baiomys musculus*, *Liomya salvini*, *Oligoryzomys fulvescens*, and *Oryzomys couesi* as competent reservoir hosts for IE viruses as they generate high enough titers to allow for transmission to susceptible vectors [103]. Similar experiments with *Proechimys seimispinosus* and *S. hispidus* with a ID VEEV strain resulted in peak viremia titers ranging from 3.3 to 7.0 \log_{10} PFU/ml, which are likely sufficient to infect *Cx. (Melanoconion)* spp. vectors in areas where ID circulates [104,105]. Enzootic vectors, *Cx. (Melanoconion)* spp. of the Spissipes section, have never been implicated during an epizootic outbreak, although they have been shown to be transmission-competent for some recently emerging epizootic-like IE strains in Mexico [106]. Experimental studies have shown *Cx. taeniopus* to be a highly competent vector of enzootic IE VEEV strains [107-110]. Interestingly, these enzootic vectors are highly permissive to sympatric enzootic strains, but refractory to all VEEV (including enzootic ID) strains except those that are IE-like, as well as most allopatric enzootic strains [111]. Unlike epizootic mosquito vectors, *Cx. (Melanoconion)* spp. prefer larval habitats that have abundant shade, which are typically found in forested regions with stable pools of water for larval development. Field studies in Colombia have shown that *Cx. pedroi*, *Cx.*

vomerifer, and *Cx. adamesi* transmit circulating enzootic ID virus to naïve hamsters [112]. While this was the first example of the virus utilizing multiple enzootic vectors efficiently in the same region, *Cx. portesi* [113], *Cx. cedecei* [114], *Cx. ocosa* and *panocossa* (formerly *Cx. aikenii sensu lato*) [115,116] had been previously identified as vectors of enzootic VEEV as well. To date, only *Ps. confinnis* has been shown to efficiently acquire, disseminate, and show transmission potential (virus in the salivary material) for both epizootic IC and enzootic ID strains [117]. Although, as previously mentioned, *Cx. taeniopus* mosquitoes are able to acquire and transmit recent emergent IE strains that have epizootic characteristics [106].

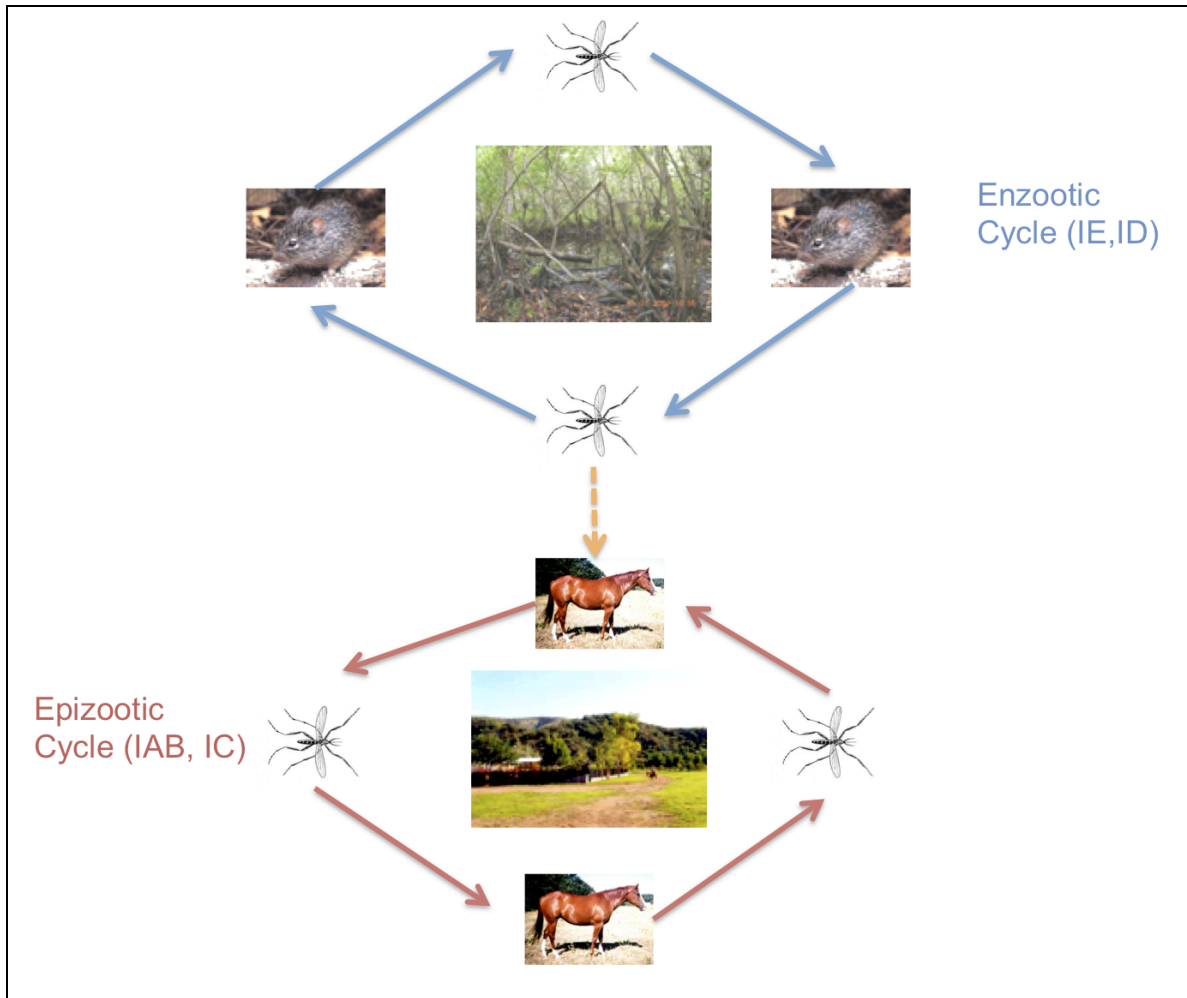


Figure 1-3: VEEV ecological cycle

Epizootic VEEV strains (red) cycle between epizootic mosquito vectors and equine hosts and cause incidental disease in humans in landscapes adjacent to sylvatic regions or sites recently adapted from sylvatic to an agricultural purpose. Enzootic VEEV strains (blue) cycle between *Cx. (Melanoconion)* spp. mosquitoes and primarily rodent hosts in shaded forest regions with pools for larval habitat.

Virulence and equine-amplification models

During the 1970's there was a strong need to be able to differentiate emerging, equine virulent VEEV from strains circulating in enzootic foci or from the attenuated vaccine strain, TC83 [118,119]. Initial studies characterizing the virulence of different VEEV strains utilized experimental models to distinguish strains with an epizootic phenotype from those with an enzootic phenotype. Equids are the most ecologically relevant model, although using equids to determine viral phenotype is an extremely expensive method. Nevertheless, several experiments have examined the virulence of different VEE complex viruses comparing known enzootic VEEV strains and closely related viruses with known epizootic VEEV strains. Typically, enzootic or attenuated strains in the VEE complex (including EVEV, TC83 vaccine strain, IE VEEV, and ID VEEV) caused no clinical illness, and if a viremia was generated it was typically under $3.0 \log_{10}$ suckling mouse LD_{50}/ml [120,121]. Epizootic viral challenges, including IAB and IC strains caused clinical illness in all horses, although not all cases were fatal. IC viruses caused mortality 62% of the time, whereas IAB viruses caused mortality ranging from 22-75% of challenged horses [121]. Examination of the virulence of emergent IE strains in Mexico that have shown the potential to cause disease in horses, did result in mild to moderate fever in the majority of horses, but a viremia level below the limit of detection by Vero cell plaque assay, and only caused encephalitis in 1/10 examined horses [122].

Other laboratory animals utilized to distinguish epizootic VEEV from enzootic strains include hamsters, and guinea pigs. Hamsters were shown to be highly susceptible to both epizootic and enzootic strains and are not useful models for distinguishing virulence types within subtype I strains [123,124]. Studies testing the usefulness of guinea pigs as models of virulence showed that lethality appears to correlate with equine virulence of a given VEEV strain [118,119], although enzootic ID viruses still are lethal to guinea pigs with a greater survival time as compared the virulent strains [125].

When cultured on Vero cells, epizootic VEEV strains develop characteristically smaller plaques than enzootic viruses [126], which has typically correlated to equine virulence. Similarly, equine-virulent viruses are more likely to be alpha/beta interferon (IFN- α/β)-resistant as compared to equine-benign strains of the subtype I VEE viruses. However, this correlation is not without exceptions because ID viruses may have an intermediate interferon resistance phenotype [127]. Another technique proposed as a method for easily distinguishing equine-virulent epizootic viruses from enzootic viruses was to evaluate the ability of each virus to infect, replicate, and be transmitted by representative vector mosquitoes. For example, when examining the transmission potential of *Ae. taeniorhynchus*, it was observed that this mosquito could transmit 80-100% of IAB viruses whereas it was only capable of transmitting less than 40% of IE VEEV strains. It was also noted that the threshold of infection was nearly 3.0 log₁₀ PFU/ml higher for enzootic viruses in this mosquito vector [102]. Similar studies in *Cx. taeniopus* mosquitoes have shown this mosquito to be highly susceptible to IE enzootic

viruses, but not epizootic viruses. However, *Cx. taeniopus* also is shown to only transmit enzootic ID viruses at very low levels indicating that poor infection capability for this mosquito is not necessarily a good predictor of equine virulence [108].

MOSQUITOES AS VECTORS

Mosquito Biology

Mosquitoes are the largest group of medically important arthropods. Within the order Diptera, meaning two-winged, the Culicidae family is closely related to midges and sand flies. Within the family Culicidae exists three subfamilies: Toxorhynchitinae, Anophelinae, and Culicinae. The mosquito species important for VEEV transmission fall under the Culicinae subfamily [128]. Although mosquitoes can be found in any place in the world with water present for the immature stage development, they primarily subsist in tropical and subtropical locations, where the weather is typically warm and humid throughout the year.

Mosquitoes undergo a complete metamorphosis in which they are laid as eggs, and transition to larval and then pupal stages before emerging as winged adults. Female mosquitoes lay up to 500 eggs either directly onto the surface of water or in areas that will become submerged with water periodically depending on the species of mosquito and preferred habitat [129]. Eggs develop into the water-dependent larval life stage typically after a few days of fertilization; however this is largely dependent on temperature and other environmental conditions. Different species of mosquitoes have

various requirements for the ideal larval habitat. For example, epizootic VEEV mosquito vectors such as *Ae. sollicitans* or *Ae. taeniorhynchus* mosquitoes tolerate brackish or saline water in salt marshes near the coast [130], whereas *Cx. (Melanoconion) spp.* larvae are more likely to be found in freshwater ground pools or slowly moving rivers [131]. Mosquito larvae feed on aquatic microorganisms that are readily available in their habitat, but require access to atmospheric oxygen so are frequently found near the water surface. After molting multiple times, the larvae transform into the third life stage, the pupae. Pupae remain in the water until emergence typically one to two days following metamorphosis into the pupal stage. Adults emerge on the surface of the water, where they remain until their exoskeleton hardens. Typically the adult female requires a blood meal for egg maturation and copulation with a male for collection of spermatozoa prior to oviposition.

Anatomy

Exoskeleton

The mosquito body is made up of a head, thorax, and abdomen region. On the head resides the compound eyes, antennae, and proboscis and is connected to the thorax by a narrow region consisting of two chitinous plates. The thorax is divided into the pro-, meso-, and meta-thorax, with the meso-thorax being the largest section. The pro-thorax is collar like in shape and lies between the head and meso-thorax [132]. Pairs of three-lobed salivary glands reside in the thorax. Wings emerge from the meso-thorax portion. The

meta-thorax forms the posterior-most portion of the thorax and is narrow like a ring and is adjacent to the abdomen, which consists of eight segments. Each segment of the thorax holds the origin of a leg.

The alimentary canal

The alimentary canal of mosquitoes is adapted for hematophagy and expands to allow for maximal intake. The foregut of the canal is made up of the mouth, pumping organ at the base of the proboscis, the esophagus, and dorsal and ventral diverticula. These regions develop from ectodermal tissues and therefore have a modified cuticular intimal lining of a single layer of cuboidal cells. The midgut, or stomach of the mosquito, initiates at the intussuscepted foregut (sometimes referred to as the homologue of the proventriculus), the narrow portion of the midgut or anterior midgut, and the expandable posterior midgut. The intussuscepted foregut represents the fold in tissue where the foregut of ectodermal origin and the midgut of endodermal origin join [132]. Blood can be observed in the posterior midgut and sometimes in the intussuscepted foregut immediately following feeding; however no blood is observed in the anterior portion of the midgut [133]. The midgut epithelium consists of a single layer of columnar cells that change shape dramatically when the midgut is distended with blood. The midgut is tapered posteriorly and transitions to the hindgut. The hindgut consists of the five malpighian tubules, rectum, and anus [132]. Malpighian tubules function in osmoregulation and excretion.

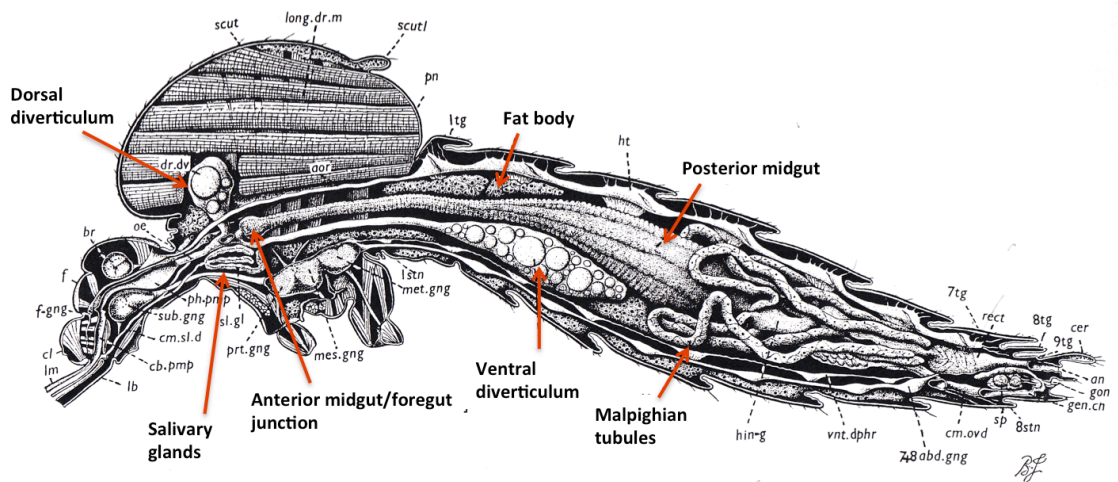


Fig. 138 *Aedes aegypti*, ♀; general organisation.

Copyright ©1985 Wellcome Trust

Figure 1-4: Depiction of mosquito anatomy with structural labels.

Adapted with permission from Jobling and Lewis 1987 [134]

The tracheal system

Oxygen exchange is carried out by the tracheal system, which is analogous to branching bronchi of the human lung. Tracheae develop from ectodermal invaginations and are lined with a chitinous cuticle, which is secreted by surrounding tracheal epidermal cells [132,135]. Tracheal epidermal cells divide and migrate in a linear fashion so the terminal cells give rise to tracheolar cells, which have many tapered branches. Air is initially taken in through openings in the chitin exterior called spiracles and drawn into smaller and smaller branches to eventually be delivered to insect tissues by the terminal

tracheoles [135,136]. Tracheoles have been shown to penetrate the basal lamina of the midgut to deliver oxygen to depleted areas [137].

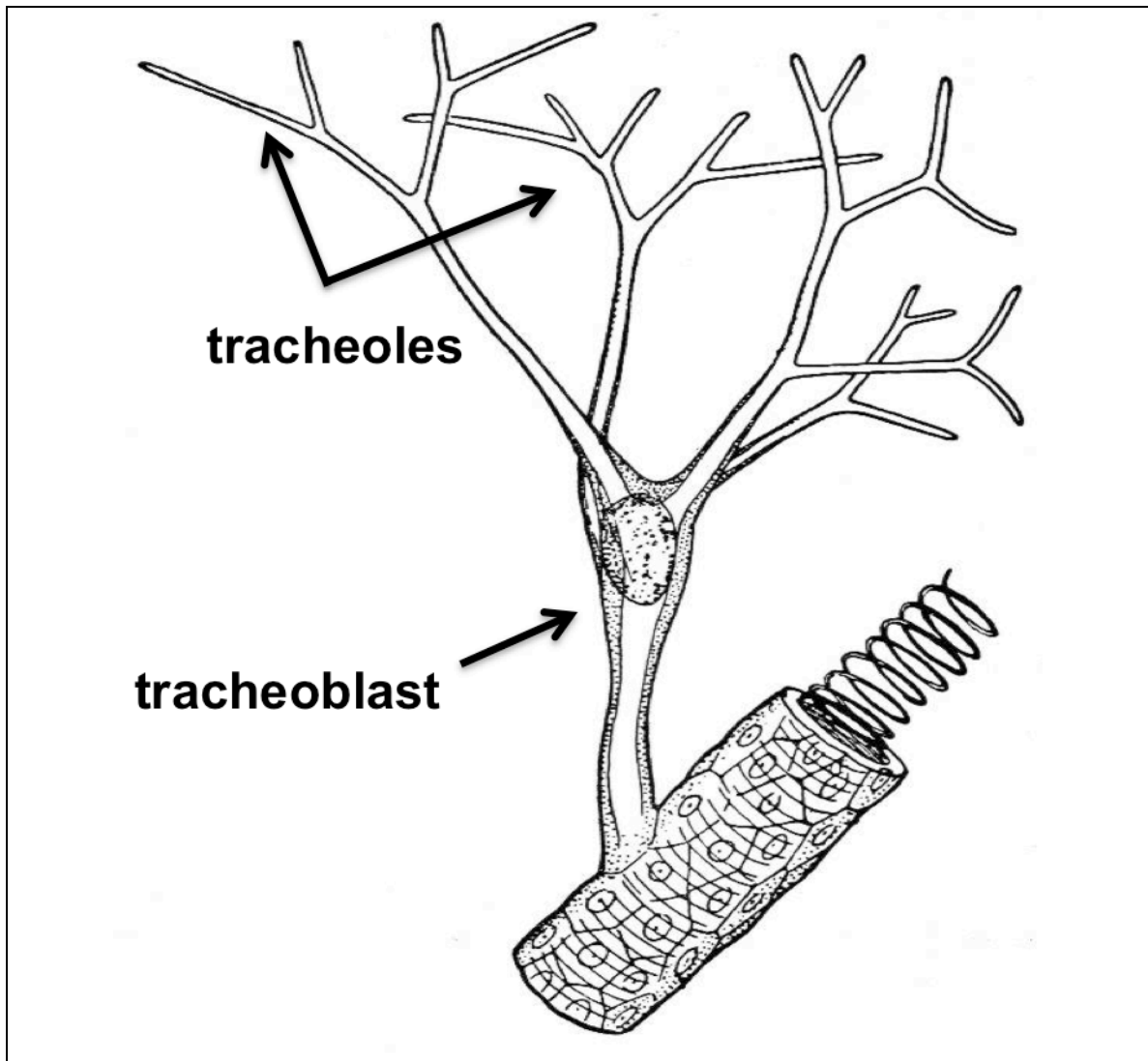


Figure 1-5: Illustration of tracheoblasts and tracheoles

Tracheoblasts are cells with tracheolar endings that penetrate and deliver oxygen to depleted tissues. Figure acquired from of http://www.public.asu.edu/~icjfh/edu/trachea/TS_Tr11.html

Nervous system

The mosquito nervous system consists of a number of ganglionic centers throughout the head, thorax, and abdomen. Near the pharynx is a ring of ganglia from which nerves to the eyes, antennae, and mouthparts are derived. In the thorax, near the ventral diverticulum, is another ganglionic center. Two nerve cords connect this center in the thorax to the ganglionic ring found in the head. The concentration of ganglia in the thorax yields large nerves, which connect to the legs as well as to the next ganglionic center in the abdomen. Ganglia in the abdomen are found near the oviducts and provide nerve branches to the final segments of the abdomen [132].

The female reproductive system and fat body

The size of ovaries changes considerably throughout the gonotrophic cycle. However, in a recently emerged female, the ovaries are small and found in the fourth and fifth abdominal segments near the midgut/hindgut junction. However, after a female has taken a blood meal and eggs begin to develop, the ovaries rapidly increase in size and force the midgut, hindgut, and fat body ventrally within the abdomen. Each ovary is made up of several follicular tubes. Oviducts are tube-like structures passing from the ovaries to beneath the anus from which eggs are deposited. The spermatheca, which contains the male spermatozoa for egg fertilization, is adjacent to and joins the oviduct near the anus to allow for fertilization of ova as they are deposited. The fat body is a mass

of adipose tissue found in the abdomen in where excess lipids can be stored for biological uses [132].

Mosquito-Virus Interaction

When a mosquito imbibes an infectious blood meal, the volume of blood is drawn into the posterior midgut where it is encased in a peritrophic matrix within 24 hours after the blood meal [138]. Any virus present in this blood meal must be able to replicate and translocate to the mosquito salivary glands prior to being successfully transmitted to the next susceptible host. Virions must initially infect the midgut epithelium layer, penetrate or circumvent the basal lamina in order to gain access to the hemocoel for replication and dissemination to other organs including the salivary gland, and gain access to the salivary gland before it can be transmitted.

Infection

It has been commonly observed and is well documented for alphaviruses that one strain of a virus may be infectious for one species of mosquito and yet not for another. For example, it has been repeatedly observed that epizootic VEEV strains have very poor infection rates or are unable to infect the enzootic mosquito vector *Cx. taeniopus* [102,107,108,139]. Several theories have been put forth to explain this phenomenon, however experimental evidence suggested that these differences are likely due to the types or modification of receptors available on the susceptible midgut epithelial cell. The most compelling example is that described by Hardy et al. where they compared the

infection threshold of a WEEV strain in various laboratory colony strains as well as wild strains of *Cx. tarsalis* mosquitoes and saw a very distinct infectivity difference between mosquito strains [140]. To test the hypothesis that binding specificity is the determinant for infection, Houk et al. extracted the sites of binding (brush borders) from the different *Cx. tarsalis* strains and performed binding affinity studies with a radiolabeled WEEV strain and observed that WEEV susceptible mosquitoes showed high binding affinity, whereas previously identified refractory *Cx. tarsalis* mosquitoes showed only non-specific WEEV binding [141]. That raises the question as to what type of difference is occurring in the receptors on epithelial cells from the same species of mosquito that could result in one mosquito being refractory and one being highly susceptible to the same virus. *In vitro* studies with SINV have suggested that the C-type lectins DC-SIGN and L-SIGN can act as receptors, while *in vitro* studies with epizootic VEEV propose a 32-kDa laminin binding protein functions to bind viral particles [6,142]. However, it is unclear how important these receptors are *in vivo* in either vertebrate or invertebrates. The other aspect of compatible binding is that of the structure and charge of the viral antigen. For instance, in the epizootic vector *Ae. taeniorhynchus*, it has been determined that specific mutations in the E2 glycoprotein of a VEEV virus strain that increase the positive charge of the E2 epitope will allow for enhanced infection rates in this vector.

Dissemination from the midgut

Before an infected mosquito can transmit a virus, it must gain access to the salivary glands. However, it is unclear as to how viruses escape the midgut epithelial cells, which are lined by an apparently virus-impenetrable basal lamina [143]. While it has largely been shown that virus replication occurs before exiting the midgut, enzootic VEEV has been observed in the fat body of *Cx. taeniopus* within one hour of exposure, which suggests that virus particles escaped the midgut prior to viral replication [109]. However, since the majority of disseminated virus in this case was seen two to four days after infection, it is likely that escape to the fat body was incidental. Another alphavirus, Whataroa virus, has been described to disseminate through the nervous tissue [144]. However it should be noted that these experiments were done in a mosquito model not known to be of ecological importance and mosquitoes were subjected to an extrinsic incubation temperature of 20°C, which is unusually low. It has been repeatedly demonstrated that extrinsic incubation temperature (the interval between the time of exposure and the time at which the vector is able to transmit the pathogen), along with other environmental factors can have a dramatic effect on the efficiency of dissemination [145,146] and it cannot be ruled out that route of dissemination might also be affected by temperature. The route that is most obvious, yet the hardest to explain is dissemination through the midgut epithelium and surrounding basal lamina. The midgut epithelium basal lamina has been described as consisting of multiple layers and being organized in a grid-like pattern with pores up to 100 Angstroms [147,148]. Studies examining whether

engorgement and subsequent structural changes in the basal lamina might result in pore sizes large enough to permit viral particles showed that, while basal lamina thickness and ultrastructure is temporarily changed, neither cell-cell junctions nor changes in the grid pore sizes were observed [147]. Some alphaviruses, like EEEV and WEEV have been shown to cause cytopathic effects (CPE) in the midgut epithelium, which could cause a loss of integrity and subsequent viral escape [149,150]. However, since the majority of alphaviruses are not known to cause pathologic changes, this is not likely a primary method of midgut escape.

Another site of potential midgut escape the intussuscepted foregut. In some cases, ingested blood may be diverted to the ventral diverticulum (which normally functions to collect sugar water between blood meals) during feeding and later regurgitated back into the anterior midgut at the site of the intussuscepted foregut. It has been proposed that if virions infect at the midgut/foregut junction site and spread cell-to-cell to the dorsal diverticulum, then they will bypass the basal lamina and the chitinous intima of the foregut to gain access to the hemocoel [133]. This has been proposed to be an important route of dissemination has been observed for EEEV [151], and to a lesser degree for VEEV [152,153], and WEEV [154].

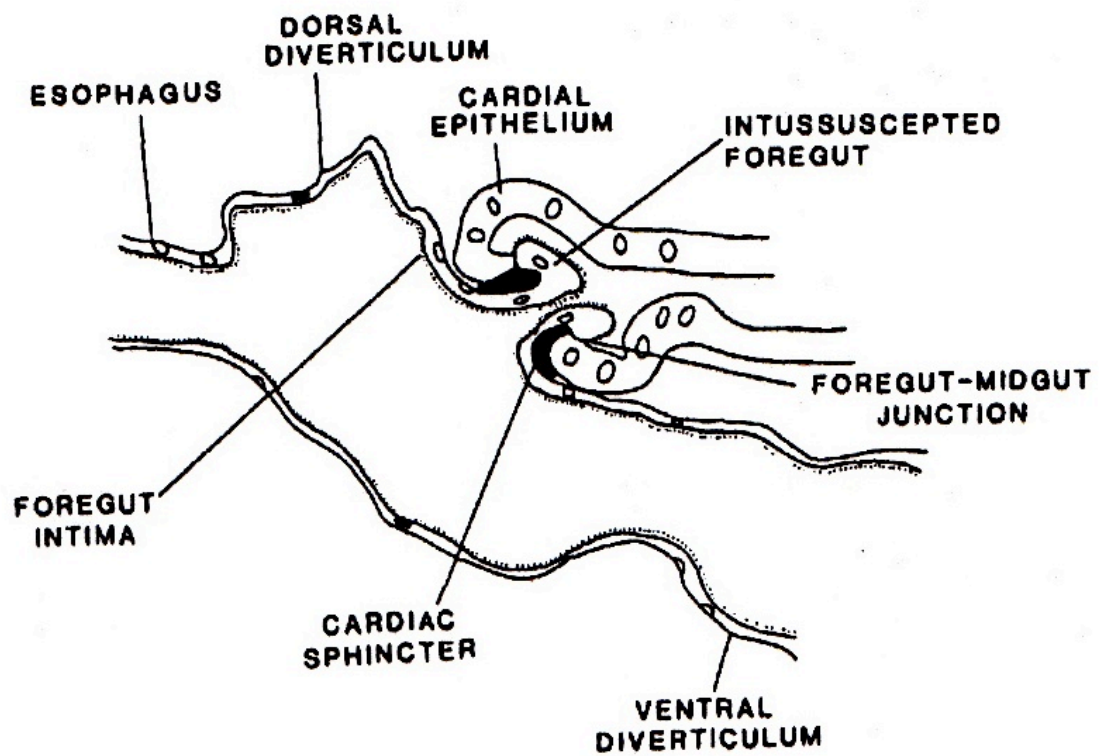


Figure 1-6: Junction of foregut and midgut at site of intussuscepted foregut.

A depiction of the junction between the midgut and foregut. The midgut is of endodermal origin and has a basal lamina, whereas the foregut is ectodermal and has a modified cuticle layer on the luminal side. Figure adapted with permission from Romoser et al. 1987 [133].

Romoser et al. have since suggested that viruses bypass the basal lamina by taking advantage of the tracheal system that penetrates through the basal lamina and into the midgut [152]. Midgut tracheae have been shown to be closely associated with muscle fibers that penetrate into the basal lamina. While it has been shown in other insects that these tracheae completely penetrate the basal lamina [137,155], ultrastructural studies done specifically on mosquitoes indicate only partial penetration into the basal lamina [148,156]. Romoser et al. [152] used VEEV replicons expressing green fluorescent protein (GFP) to identify the first tissues initially infected upon circumventing the midgut barrier by intrathoracic (IT) inoculation into the hemocoel and oral introduction. Following the IT route of infection with replicons, relevant tissues found to be infected included the midgut muscles, and tracheal cells corresponding to the alimentary canal, but no virus was found in the midgut epithelial cells. However, when replication-competent virus was inoculated IT, the virus progressed through the initial cells shown to be infected by replicons and also progressed into the midgut. While the typical route of alphavirus dissemination is from the midgut to the hemocoel, this study suggests a conduit that allows for passage out of the midgut as well as back in, however, unlikely in a natural infection. Romoser et al. concluded that tracheae act as the conduits that allows virus to penetrate the basal lamina pore size obstacle and gain access to the hemocoel [152]. The close association between tracheae and the midgut epithelium in various types of arthropods also contributes to this theory [135,152]. Similar studies examining the

pathway that arthropod-borne baculoviruses use to spread within their host indicate use of a tracheal route as well [157-159]. Findings by Bower et al. further support the close association with alphaviruses and tracheae, as they showed the presence and persistence of SINV in tracheal cells of infected *Cx. pipiens* mosquitoes [160].

Culex taeniopus and VEEV

Cx. taeniopus was first shown experimentally to be a competent vector for VEEV strains with a hemagglutination inhibition subtype IE strain in the early 1980s [108,111,139]. However, it was quickly discovered that *Cx. taeniopus* mosquitoes are not susceptible to other subtypes of VEEV, even enzootic ID strains [107], which suggests that a high degree of co-adaptation developed between IE viruses and *Cx. taeniopus* mosquitoes. This theoretically steady relationship is highly different from the occasional and transient interaction that occurs between epizootic virus strains and their corresponding vectors.

Electron microscopy studies of IE VEEV dissemination throughout *Cx. taeniopus* have shown that virus is initially detected in the midgut within the first hour following the blood meal and the majority of particles remain within the midgut for two days. The virus is found in the hindgut starting on day two after infection and remains for at least 21 days. Virus was detected in the abdominal fat body throughout the entire study, from the first hour to 21 days after infection. This suggests that virus particles penetrate the midgut and accumulate in the abdominal fat body prior to replication within the vector. This

pattern differs from that reported for other arbovirus-vector pairs and the mechanism by which dissemination occurs is unclear [109].

PROJECT SUMMARY AND SIGNIFICANCE

Summary

The goal of this research was to elucidate the mechanisms by which enzootic VEEV interacts with the enzootic vector. With the exception of a few studies, the majority of research on VEEV in the vector has been done with epizootic laboratory models. I anticipated that the interaction between this highly co-adapted vector-virus pair would prove to be very different from the epizootic model. Since the survival and continued outbreaks caused by this virus are dependent on the maintenance of the enzootic cycle. By understanding the enzootic model, we can gain an understanding of how VEEV is maintained in nature, what types of selective pressures it is regularly subjected to, and possibly gain insights into mechanisms of emergence.

Aim 1. Identify regions in the VEEV genome that affect *Cx. taeniopus* infectivity and dissemination. Understanding of which regions of the genome are most important in viral fitness within the enzootic mosquito vector will provide insight as to how the virus thrives in the enzootic life cycle. *I hypothesized that structural regions of the genome, particularly the E2 region, play the largest role in initial infectivity, however; nonstructural genes will play a role in viral replication.* Awareness of the contribution of

viral genes to the evolutionary fitness within the natural enzootic host will supplement our current knowledge and provide insight into recent VEEV IE emergence into an epizootic cycle. Similarly, understanding of these determinants will aid in the origination of environmentally safe vaccine development strategies towards disease causing VEEV strains.

Aim 2. To examine the initial midgut entry barrier of enzootic strains utilizing replicon particles. Examination of the epizootic VEEV strains in the primary epizootic vector, *Ae. taeniorhynchus*, indicates initial infection occurs only within a limited number of susceptible midgut cells [161]. *Because Cx. taeniopus has theoretically coevolved throughout time with sympatric enzootic strains, I hypothesize that there will be more susceptible posterior midgut epithelial cells to initial enzootic infection than what has been previously observed in the epizootic vector.* Explicit knowledge of the selective pressures exerted by the primary enzootic vector will refine our knowledge on the mechanisms responsible for VEEV maintenance in nature.

Aim 3: Determine the mechanism by which enzootic VEEV virus escapes the midgut and gains access to the hemocoel in *Cx. taeniopus*. Studies employing fluorescent replicon particles and surveying ultrastructural surfaces of *Ae. taeniorhynchus* mosquitoes, the primary vector of epizootic VEEV strains, suggest that tracheal cells penetrate the midgut and basal lamina and are utilized by viral particles to circumvent

these barriers [152]. *I hypothesize that enzootic VEEV particles initially infect the posterior midgut epithelium of Cx. taeniopus, spread cell-to-cell into the tracheoles, and utilize the tracheoles as conduits to bypass the basal lamina and emerge into the hemocoel for further dissemination.* Comprehension of how VEEV virus escapes the midgut will provide unique knowledge of how the virus has adapted to overcome barriers of infection in naturally infected *Cx. taeniopus* mosquitoes in an ecologically maintained cycle.

Significance

Because VEEV outbreaks are often devastating to equine populations, this virus is considered a great risk to agriculture in addition to a public health risk where it circulates. The virus has been detected in many countries, ranging from the United States (Texas and Florida) to Peru with foci in Mexico, Venezuela, Central America, and Colombia. While the virus showed little activity from 1972-1991, equine epizootics in Mexico, Venezuela, and Colombia since 1991, and recent enzootic-derived human cases in Peru, Bolivia, and Ecuador [162,163] have only reinforced the importance and potential of this virus as an emerging infection [122]. Emerging studies indicate that endemic VEE represents a large burden of disease in Latin America. Potentially, tens of thousands of endemic VEE cases are being misdiagnosed as dengue [162]. This represents a large potential for generation of epizootic cases. Similarly, the alarming emergence of equine virulent strains in Mexico that can be readily transmitted by *Cx. taeniopus* underscores

the importance of understanding how VEEV is maintained in nature and how changing ecology can affect emergence. Characterizing infection of the enzootic as well as the epizootic vector may help understand and predict the determinants of outbreaks. In addition to having no approved human vaccine and being classified as a Category B priority agent by the National Institute of Allergy and Infectious Disease (NIAID) within the NIH [81], the repeated examples of widespread epizootic outbreaks arising from persistently circulating enzootic strains exemplifies this virus as a significant threat to public health. Presently, there is a lack of understanding of the dynamic interface between the enzootic virus strains and the enzootic mosquito vector in nature. Awareness of these interactions will move us closer to understanding how persistent enzootic cycles can precipitate epizootic outbreaks.

CHAPTER 2: GENERATION OF INFECTIOUS CLONES

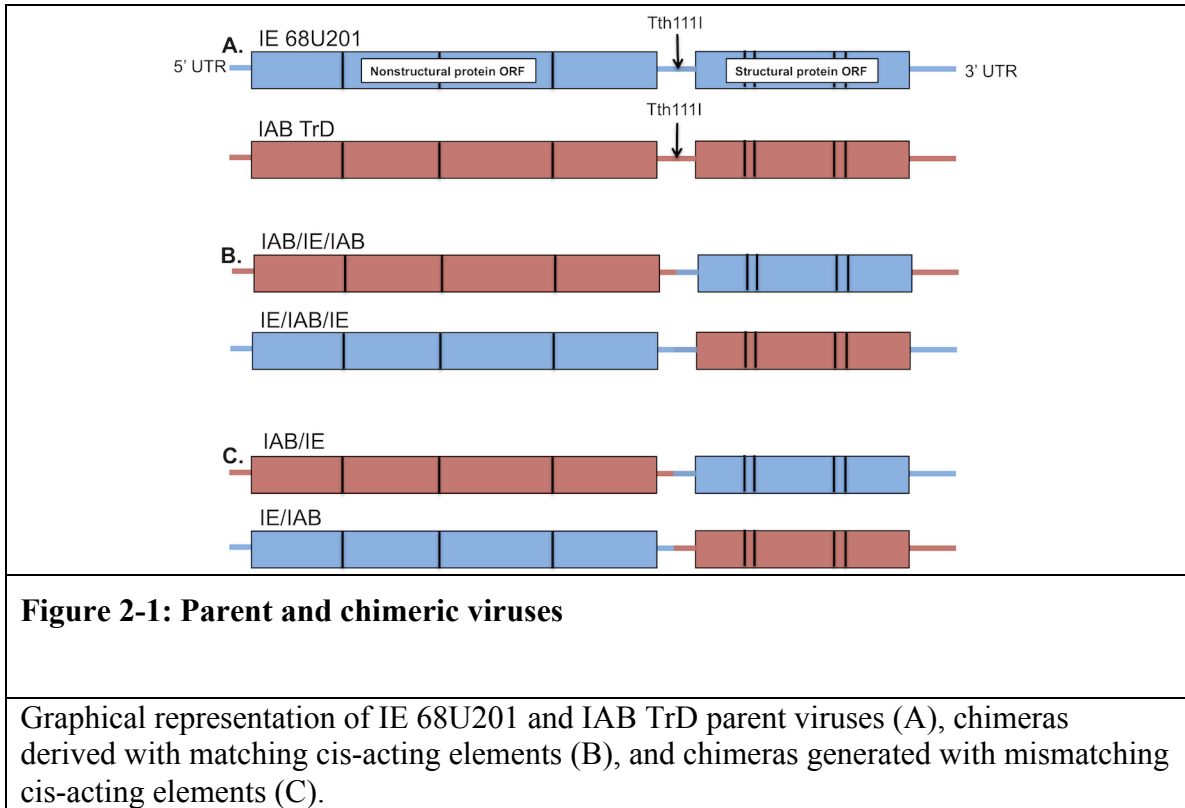
CHIMERIC VIRUSES BETWEEN IAB AND IE VEEV STRAINS

Purpose

One large benefit to studying a small, positive strand virus is the ability to utilize reverse genetics to systematically examine the contribution of each region of the genome. This strategy has been repeatedly utilized to characterize the essential structures and function for ideal replication of alphaviruses [45,46,60,63]. Comprehension of the regions essential for replication allowed for development of chimeric alphavirus vaccine candidate strains that are replication competent although attenuated for safety [164-169]. Similarly chimeras between less divergent alphavirus strains have been generated to characterize the epizootic and enzootic phenotype in vertebrates and mosquito models [69,125,170,171]. Considering the value of these previous studies, I determined that chimeric vaccine strains would be the most efficient way to isolate the contribution of specific viral regions to infection capability in *Cx. taeniopus* mosquitoes. It has been previously shown that while *Cx. taeniopus* mosquitoes are highly susceptible to enzootic IE subtypes, IAB strains are unable to infect and disseminate in this species of mosquito [106-109]. The stark contrast in infectivity of these viruses in *Cx. taeniopus* provides a valuable tool for examining the contributing viral regions for infection in this mosquito

vector. Similar studies with chimeras between IE and IAB VEEV strains have been performed in the epizootic mosquito vector, *Ae. taeniorhynchus* [69]. Initially I proposed to utilize these chimeras, which had been previously described [69,171], however, the chimeras utilized for those studies were generated utilizing a different IAB infectious clone, IC-109. This IAB clone was originally derived to evaluate attenuating mutations from the IAB wild type strain to the attenuated TC-83 vaccine strain [172] and had point mutations from TC-83 that could potentially affect how the virus infects and disseminates in mosquitoes. Additionally, detailed examination of the IE-IAB chimeric infectious clones from Powers et al. [171], showed multiple point mutations suspected to be cloning errors throughout the genomes, including one in the T7 promoter that drastically affected transcription efficiency. Therefore, I chose to generate new chimeras utilizing an infectious cDNA clone derived from a wild type IAB Trinidad Donkey strain with no introduced mutations, V3000 described by Davis et al. [173]. Prior to generation of the clone, this IAB VEEV strain was passaged once in guinea pig brains and 14 times in embryonated eggs. The phenotype of virus derived from this infectious clone was shown to be as virulent as wild-type IAB strains in rodents [173]. I also utilized an infectious clone made from VEEV IE 68U201 for the enzootic parental virus and IE regions of the chimeras. Prior to incorporation into the cDNA clone, the 68U201 virus strain was passaged once in newborn mice and twice in BHK-21 cells [171]. The IE virus derived from this infectious clone has been previously demonstrated to exhibit the characteristic

enzootic phenotype of the parental strain in both vertebrate models and invertebrate models [69,106,171]



Chimeric clones previously utilized by Powers et al. [171] and Brault et al. [69] were derived with mismatching *cis* – acting elements between the 5’ UTR/nonstructural regions and the 3’ UTR. A number of studies have since demonstrated that regions of the of the 5’ UTR and 3’ UTR work in tandem to maximize efficient minus strand initiation and plus strand RNA synthesis [45,46]. It was decided that generation of two pairs of chimeras, those with mismatching and matching *cis* – acting elements, would allow for an independent evaluation of the contribution of each of the nonstructural, structural, and

3' UTR regions as determinants for infection of the enzootic mosquito vector, *Cx. taeniopus* (figure 2-1).

Mismatching *cis*-acting element cloning

***Tth111I* fusion cloning**

This strategy involved utilizing the *Tth111I* restriction site located in the 26S 5' UTR as the junction between the IAB and IE portions of the mismatching *cis*-acting element chimeric viruses. This strategy was originally described by Powers et al. when they examined the interferon response induced by VEEV chimeras in animal models [171]. It was determined that keeping the subgenomic promoter strain-matched with the 5' UTR and 3' UTR *cis*-acting element species (whenever possible) would be less likely to result in aberrant replication and therefore, I decided to use the *Tth111I* site in the 26S UTR for the site of fusion between the two genomes..

As shown in figure 2-2 the fusion PCR was performed using a pair of long primers (about 40 nt) with one half complimentary to each of the two VEEV strains of the chimera that cover the junction between the two species. The first fusion PCRs were performed using the forward fusion primer and a downstream reverse primer and the reverse fusion primer and an upstream forward primer to generate two fragments (see figure 2-2 for primers utilized). Both the fusion and joining PCRs were performed using the Phusion® High Fidelity DNA Polymerase kit (NEB, Ipswich, MA) according to the product insert instructions. Briefly, annealing temperatures for primers were determined

utilizing the NEB Tm calculator, which utilizes thermodynamic theory described by Breslauer et al. [174] and a salt correction reported by Owczarzy et al. [175]. In cases in which the calculated annealing temperatures of the two primers were greater than 5 °C apart, two degrees were subtracted from the lower temperature and that value was utilized as the annealing temperature for the reaction. Elongation times were determined allowing 30 seconds for each kb of amplicon. Product from each of the joining PCRs was used as template for the second set of PCRs, which were used to join the two fusion fragments together and generate the chimeric junction with the outer joining primer pairs (the upstream forward primer and downstream reverse primer) (figure 2-2). The reactions were also performed using the Phusion® High Fidelity DNA Polymerase kit using the NEB Tm calculator. The fusion pcr fragment and plasmid inserts were digested with restriction endonucleases.

Digestion

Plasmid DNA digestions in general were performed with an estimated 1 µg/µl of vector plasmid or cloning insert, 5 µl of 10x buffer, 0.5 µl of 100x bovine serum albumin (BSA) (if required), 39.5 µl water and 1 µl of each enzyme. Additionally, 0.2 µl of CIP (calf intestinal phosphatase) was added to one of the vector fragments to prevent self-ligation. For the IAB/IE chimera, the restriction enzymes utilized included XbaI, BssHI, and PspOMI for IAB/IE and EcorI, NheI, and Bsu36I enzymes for IE/IAB (figure 2-3). NdeI and SacI enzymes were used in addition to help distinguish the fragment sizes

during gel electrophoreses of IAB/IE fragments. For the IE/IAB fragments, AvrII and RsrII were used to help correctly isolate the Bsu36I – EcorI band from extraneous digested fragments. Gel extracted fragments were phenol/chloroform purified prior to ligation.

Extraction and Phenol Chloroform Purification

Digested fragments were gel-extracted utilizing the QIAquick Gel Extraction Kit (Qiagen, Valencia, CA), and eluted in 100 µl of the provided elution buffer, EB. 100 µl of phenol chloroform and 2 µl of 5 M NaCl were added to the eluted DNA, vortexed, and centrifuged for five minutes at 16,600 relative centrifugal force (rcf). The upper phase was transferred to a fresh tube with 0.5 µl GlycoBlue™ (Ambion, Austin, TX) and 250 µl of 100% EtOH and pulse vortexed. The sample was transferred to -20°C and incubated for a minimum of one hour prior to centrifugation for 16,600 rcf for 10 minutes. The resulting pellet was washed and centrifuged for three minutes at 16,600 rcf twice with 70% ethanol prior to suspension in 11 µl of RNase-free water. The purification was confirmed by running 1 µl of the purified sample with 1 µl of 10x loading buffer and 8µl of water on an agarose gel.

Ligations and Transformation

Ligations were performed using 1 µl of T4 DNA ligase (NEB, Ipswich, MA), 2 µl of ligation buffer, the three ligation fragments at an approximate ratio of 1:3 vector to insert, and enough DNase free water to bring the final volume to 20µl. The reaction was

incubated at 16° overnight. Ligations were transformed in One Shot® OmniMAX competent cells (Invitrogen, Carlsbad, CA). Multiple colonies were selected for each clone and mini-prepped using the QIAprep Spin Mini kit (Qiagen, Valencia, CA). Each clone isolate was digested with enzymes to determine which clones were of the expected size. Clones confirmed to have the correct fragments were then sequenced across the fusion PCR fragment using the joining PCR primers.

Generating matching *cis*-acting chimeras

In order to create the second pair of chimeras, a fusion PCR strategy was again utilized to create a junction between the E1 glycoprotein and 3' UTR (figure 2-4). The Phusion® High Fidelity DNA Polymerase kit, NEB Tm calculator, and listed primers (figure 2-4) were used for this strategy. The restriction enzymes utilized for the IE/IAB/IE chimera were SgrAI that cut in the E1 glycoprotein, and EcoRI, which was used for linearization. Fragments generated from digestions were purified and ligated in a two-piece ligation reaction. A three-piece ligation was used to manufacture the IAB/IE/IAB chimera. The strategy included digestion with EcoRI, SpeI, and SacII to generate the necessary fragments for ligation.

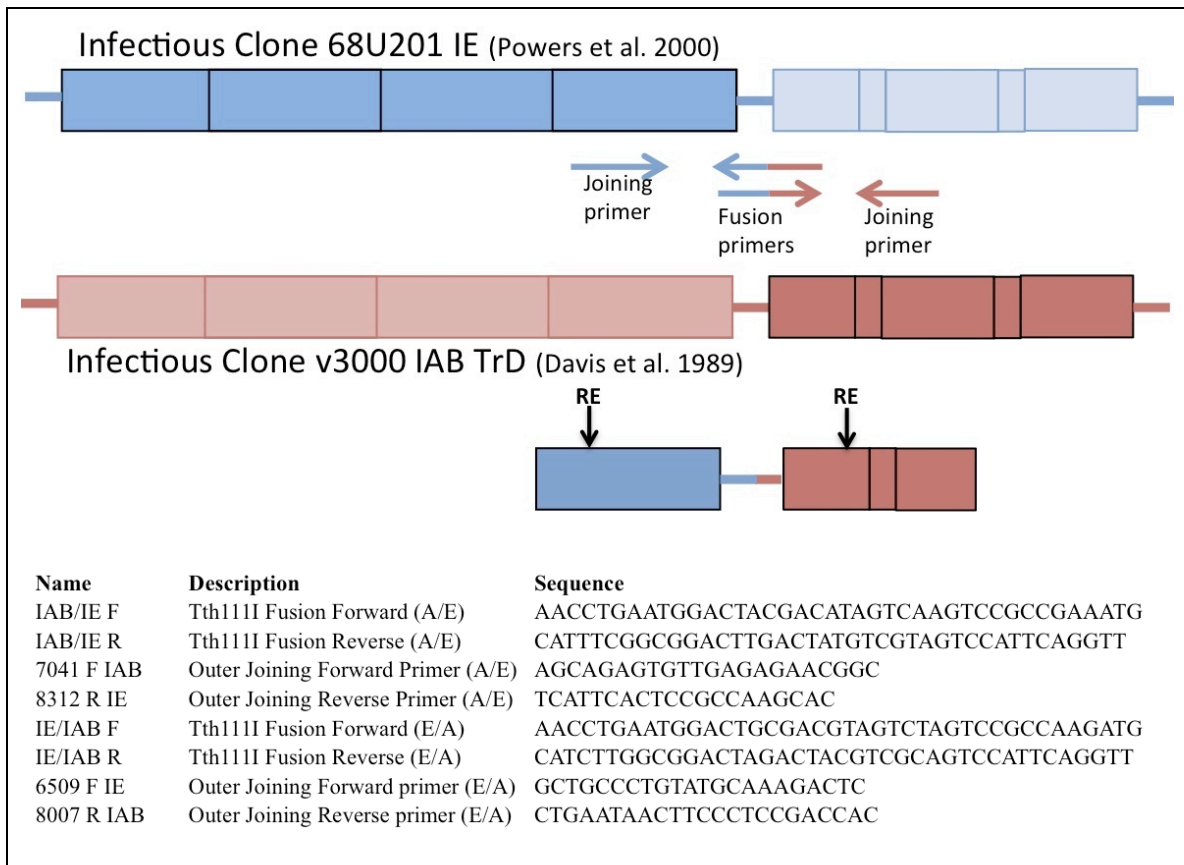


Figure 2-2: Tth111I fusion PCR strategy and primers for IAB/IE and IE/IAB

For each chimera two fusion fragments were initially generated utilizing an outer joining forward primer paired with a Tth111I fusion reverse primer or a outer joining reverse primer and a Tth111I fusion forward primer. The two fragments were joined in a single reaction using the two outer primers and both templates, and the final fragment was cleaved prior to ligation.

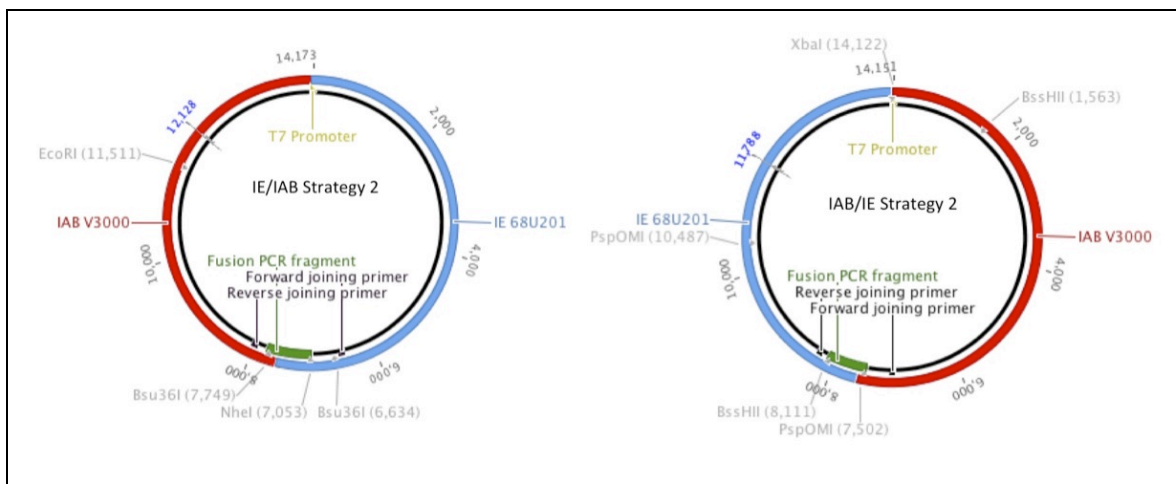


Figure 2-3: Final Fusion PCR strategy for IE/IAB and IAB/IE

The IE/IAB chimera was generated with a 3-piece ligation between EcoRI, NheI, and Bsu36I, while the IAB/IE chimera was generated with a 3-piece ligation between XbaI, PspOMI, and BssHI

Individual clones obtained from transformed competent cells were screened for the presence of the fusion fragment and positive samples were further minipreped (Qiagen, Valencia, CA), and digested to confirm the presence and size of the remaining clone fragments. Confirmed samples were further sequenced for confirmation of polymerase fidelity prior to the large DNA preparation of each clone.

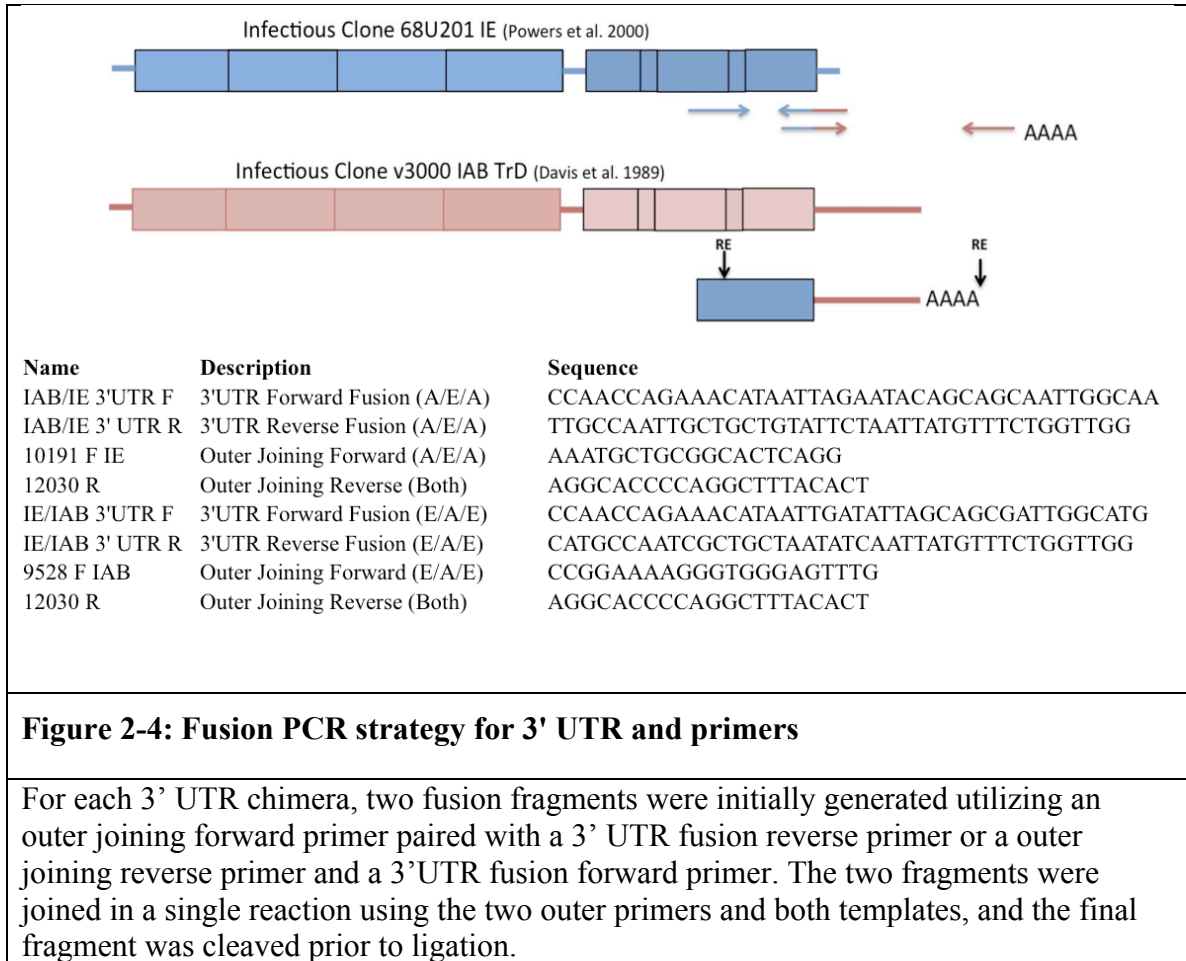


Figure 2-4: Fusion PCR strategy for 3' UTR and primers

For each 3' UTR chimera, two fusion fragments were initially generated utilizing an outer joining forward primer paired with a 3' UTR fusion reverse primer or a outer joining reverse primer and a 3'UTR fusion forward primer. The two fragments were joined in a single reaction using the two outer primers and both templates, and the final fragment was cleaved prior to ligation.

From plasmid to replicating virus

Large scale DNA preparation

DNA from the four chimeras and two parental viruses were all prepared in the same manner. Liquid cultures of 250 milliliters (ml) in Terrific Broth (TB) (Sigma Aldrich, St. Louis, MO) were grown at 37° C overnight, prior to nucleic acid isolation and purification. The liquid culture was centrifuged at 4070 rcf at 4°C to pellet the

bacterial cells, which were resuspended in 8 ml of BF1 buffer¹. Sixteen ml of BF2 buffer² were added and each sample and vortexed until the solution was homogeneous. Twelve ml of BF3 buffer³ were added and samples were thoroughly mixed and stored on ice for 15 minutes. Samples were centrifuged at 14515 rcf at 4°C for 10 minutes. The supernatant was collected and transferred to a fresh tube for nucleic acid precipitation with 100% isopropanol. Samples were incubated a -20°C for 30 minutes to overnight and then centrifuged at 1020 rcf for 10 minutes at 4°C. Nucleic acids were reconstituted in 2 ml of TE buffer, treated with 2 ml 5M lithium chloride, vortexed, and incubated on ice for 10 minutes. RNA was centrifuged out at 29,131 rcf for 10 minutes and supernatant was transferred to a fresh tube containing 8 ml of ethanol (EtOH) and incubated at -20°C for at least 15 minutes. DNA was pelleted with a 1020 rcf centrifugation step for 10 minutes. Pelleted DNA was washed with 70% ethanol (EtOH).

Cesium Chloride Purification

DNA was pelleted, allowed to dry, and resuspended in 1 ml of TE buffer in a fresh 15 ml conical tube. The resuspended DNA was mixed with 4.8 g of cesium chloride and 40 µl of 10 mg/ml ethidium bromide, plasmid solution, and filled to 9.1 grams total (including the tube) with TE buffer . Samples were carefully balanced to within 0.01

¹ 12.5 ml of 1M Tris, ph 7.5, 10 ml of 5M NaCl, and 10 ml of 0.5 M EDTA

² 20 ml of 1M NaOH, 10 ml 10% SDS, 70 ml water

³ 150 g KAc, 100 ml glacial acetic acid , bring to 500 ml with DNase-free water

grams of one another, transferred to OptiSeal ultracentrifuge tubes (Beckman Coulter, Brea, CA), and centrifuged at 339,158 rcf (70,000 rpm in a Beckman NVT™ 90 rotor) at 20°C for at least four hours. The DNA band was aspirated with a 1 ml syringe, mixed with 1 ml TE and 3.5 ml of EtOH, and centrifuged at 1,020 rcf for 10 minutes. The supernatant was removed and replaced with 400 µl TE buffer and allowed to incubate at room temperature for 30 to 40 minutes prior to phenol chloroform treatment and spectrophotometry for determination of DNA yield.

Transcription and Electroporation

All DNA stocks were stored at a final concentration of one microgram per microliter (µg/µl). For each clone, 1 µg of DNA were linearized and phenol/chloroform purified prior to transcription with the T7 mMessage mMachine® Kit (Ambion, Austin, TX). At room temperature 1 µl of dH₂O was mixed with 5 µl of 2x NTP/CAP, 1 µl of 10x reaction buffer, 1 µl of GTP, 1 µl of linear DNA template, 1 µl of RNase inhibitor, and 1 µl of enzyme and incubated for one hour at 37°C. Transcribed samples were either used immediately for electroporation or stored at -80°C for no more than 48 hours.

Electroporation was performed in BHK cells that had been washed three times in DPBS (Gibco®, Carlsbad, CA) prior to resuspension. Cells were mixed with the full product from the transcription reaction and immediately subjected to electroporation to minimize any RNA degradation. Electroporation was performed on a BTX ECM 630 (BTX, Holliston, MA) with the following settings: HV mode, 0680 volts, a pulse length of 099s,

5 pulses, a 100 ms interval, unipolar polarity, and in a 2mm cuvette. Following electroporation the cuvette of cells was incubated on ice for 10 minutes prior to being transferred to a 75-cm² flask with DMEM (Gibco, Austin, TX) supplemented with 10% FBS, penicillin and gentamycin. Virus was harvested 48 hours after electroporations.

IE 68U201 EXPRESSING GREEN FLUORESCENT PROTEIN

Fusion Cloning Strategy

Upon sequencing of an existing stock of the IE 68U201 GFP infectious clone that I proposed to utilize in my candidacy proposal, it was determined that the 26S UTR region was actually derived from VEEV subtype IC strain 3908. As a result, I decided to recreate the IE 68U201 GFP infectious clone for use in my experiments. To derive this clone, a three-piece ligation with a fusion PCR strategy was utilized (figure 2-5).

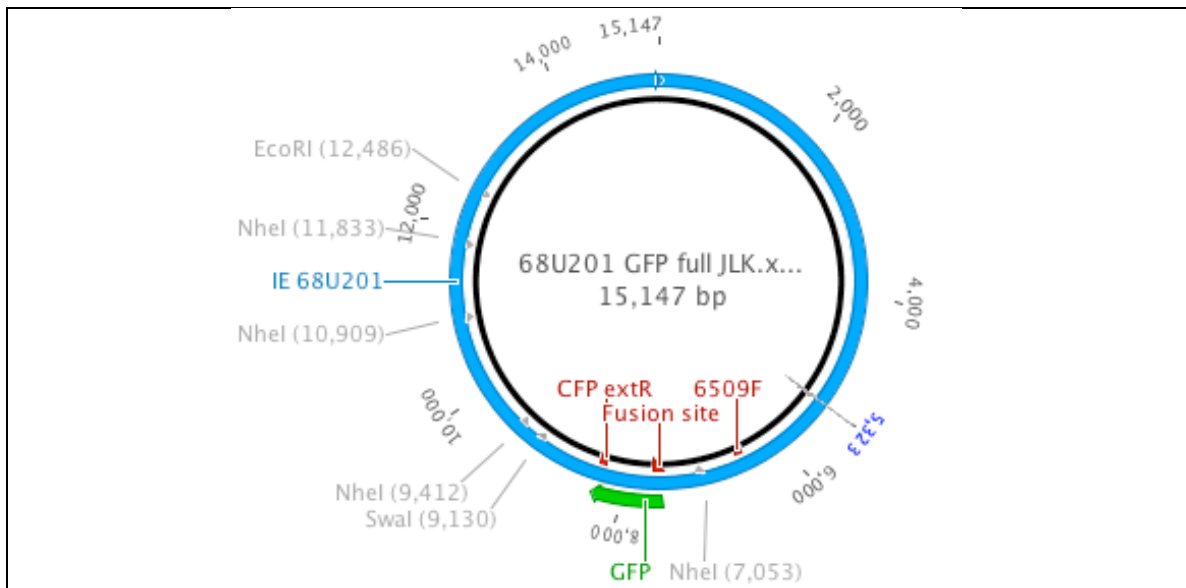


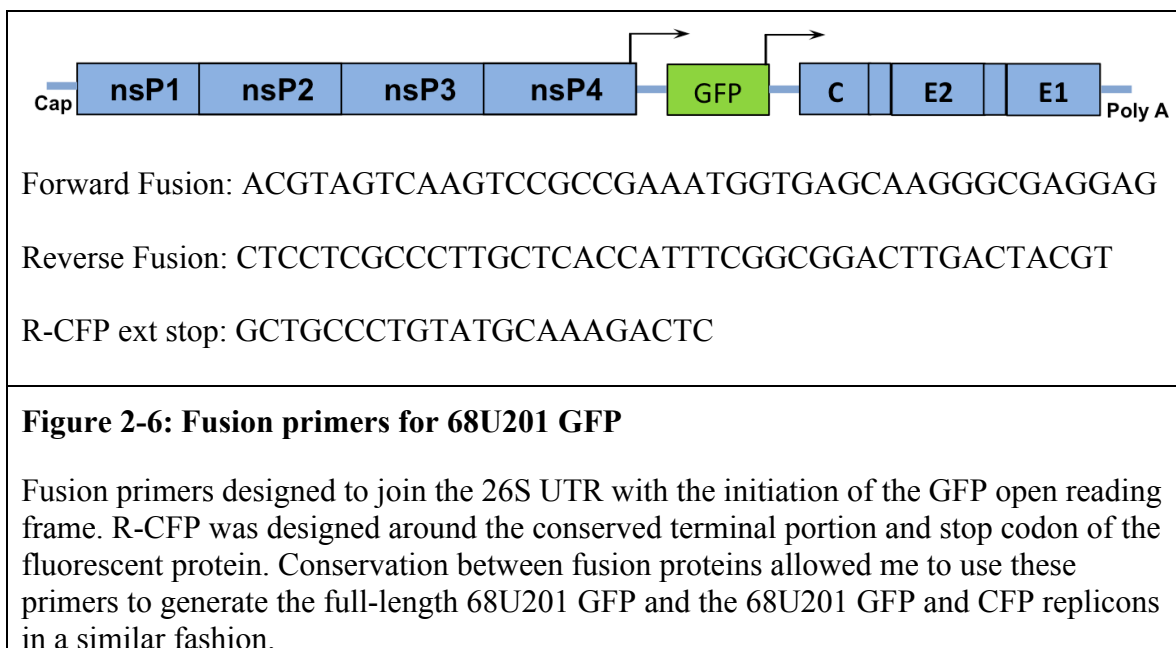
Figure 2-5: 68U201 GFP plasmid clone.

Derived using a fusion PCR and restriction enzymes EcorI, NheI, and SwaI

The first ligation piece was generated by digesting the parent 68U201 strain with EcorI and NheI sites. The second ligation piece was the fusion fragment, which was designed to fuse two amplicons generated from the parent 68U201 and the correct 68U201 GFP replicon (see below) at the junction between the 26S UTR and the start of the GFP open reading frame. Conveniently, GFP and cherry fluorescent protein (CFP), are 100% conserved for the first and last 20 nucleotides, which makes it easy to design a universal fusion primer that can be utilized for any construct with a colored fluorescent protein.

The first of the joining fragments was created by amplifying the parent 68U201 with a IE 6509F (see above) and the reverse fusion primer listed below (figure 2-6) using the Phusion high fidelity polymerase (NEB, Ipswich, MA). The second joining fragment was

generated from high fidelity amplification the correct 68U201 GFP replicon (see below) with the forward fusion fragment (figure 2-6) and R-CFP ext stop primer. These two fragments were then joined using the outermost primers and then digested with *NheI* and *SwaI*.



The third ligation piece was derived by digesting the pre-existing 68U201 GFP with *SwaI* and *EcoRI*. This was possible as the only errors in the pre-existing 68U201 GFP clone were in the 26S UTR, which were not required for this fragment. Digested fragments were isolated by gel electrophoreses and the QIAquick PCR purification kit (Qiagen, Valencia, CA). Eluted DNA was subjected to phenol/chloroform purification prior to ligation utilizing the NEB T4 DNA ligase (NEB, Ipswich, MA) according to the product insert directions. The three-piece and control ligations were transformed in One Shot

OmniMAX™ competent cells (Invitrogen, Carlsbad, CA). Colonies were screened by digestion to detect the presence of the fusion fragment and those with the fragment were further subjected to sequencing to identify any mutations. A representative clone with no identified sequence errors was chosen for large DNA prep and cesium chloride purification as described above. Linearization, transcription, and electroporation were performed as previously described.

CHARACTERIZATION

Replication *in vitro*

One-step growth curves of experimental viruses IAB, IE, IAB/IE/IAB, IE/IAB/IE, IAB/IE, and IE/IAB were performed on Vero cells to evaluate the role of chimerization on viral replication and detect differences that might bias infection and dissemination in the *in vivo* mosquito model. Replication curves were performed in triplicate at an MOI of 5, with samples at 0h, 3h, 6h, 9h, 12h, 24h, and 48h, and each time the full volume of each well (1 ml) was collected and replaced with fresh, complete media. In addition to the four chimeras and two parental strains, I also included IAB GFP and 68U201 GFP strains (figure 2-7). I infected 8 wells of a 12-well plate in triplicate with 150 µl of each diluted virus and allowed the plates to incubate for one hour while gently rocking the samples every 15 minutes. Following one hour, each well was washed carefully with pre-warmed PBS twice prior to addition of one ml of complete DMEM, which was immediately removed and replaced for time point 0 h sample. Collected samples were

stored at -80°C until titration of each sample on Vero cells. Similar replication curves were done on *Ae. albopictus* C6/36 cells with the only differences being that the complete DMEM media had 10% FBS instead of 5%, and was additionally supplemented with 1% tryptose phosphate broth (Sigma Aldrich, St. Louis, MO). C6/36 cells were incubated at 28°C with 5% CO₂ while Vero cells were incubated at 37°C with 5% CO₂.

Statistical analysis of replication in vitro

Two-way analysis of variance (ANOVA) with a post-hoc Bonferroni test was utilized to inspect the replication results in both Vero cells and C6/36 cells. For the Vero curves, the virus treatment was significant ($P < 0.0001$). In post-test analysis the parental IAB TRD virus showed significant differences compared to each of the other viruses on at least one time point with the exception of IE/IAB, which showed no replicative difference from IAB at any time point. None of the chimeras showed any replicative differences when compared to each other or to the parental IE 68U201 strain. Interestingly, the IAB TRD GFP virus showed significant differences from the IAB parent at all time points except 24 hours. This indicates that TRD GFP is more different from wild type IAB TRD than from the parental IE 68U201, which only differed from IAB TRD at time points 6h and 9h. Independent comparison of parental 68U201 to its fluorescent counterpart, IE 68U201 GFP showed no replicative differences at any time point. This indicates that while inclusion of the GFP in IAB TRD resulted in a reduced rate of *in vitro* replication, incorporation of GFP into the IE 68U201 virus appears to have

no impact on replication in Vero cells. Examination of other alphaviruses with heterologous inserts of the same design have previously shown that alphaviruses encoding a GFP show less efficient replication, decreased peak titers, and in some cases a delay in the time required to achieve the peak titer in both mammalian and insect cell lines [176,177]. Comparison between IAB TRD GFP and IE 68U201 GFP showed no significant differences at any time point.

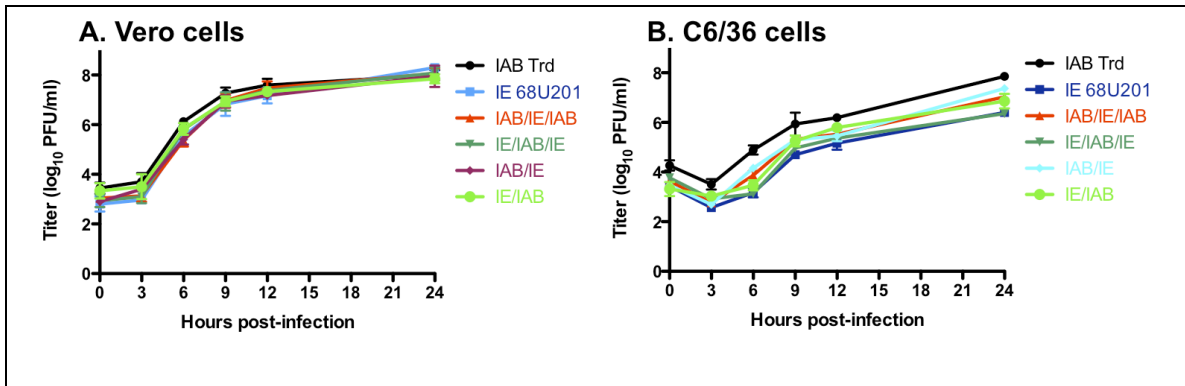


Figure 2-7: Chimera replication curves

Replication curves of both parental and four chimeric viruses on Vero cells (A) and C6/36 cells (B) at an MOI of 5

Examination of replication in C6/36 *Ae. albopictus* cells showed no major replication deficiencies for any of the viruses. Specifically, IAB TRD was found to be significantly different at all time points from 68U201 and showed differences from all the chimeras at a minimum of four time points, however the 0 hour titer was higher than all

other viruses likely contributes to the subsequent differences. IE 68U201 showed no differences from IE/IAB/IE, but showed differences at a minimum of two time points from the other chimeras. IAB/IE/IAB differed from IE/IAB/IE at 6 hours and 24 hours, but showed no differences at any time point from IAB/IE or IE/IAB. IE/IAB/IE differed from IAB/IE at 6 hours and 24 hours, but showed no differences from IE/IAB at any observed time points. As the mismatching *cis*-acting element chimeras showed no replication differences from the chimeras with matching *cis*-acting elements, I can conclude that inclusion of mismatched 3' UTR *cis*-acting elements does not adversely affect replication in a C6/36 *in vitro* model. Individual comparison of IAB/IE to IE/IAB showed a significant difference only at time point 6 hours.

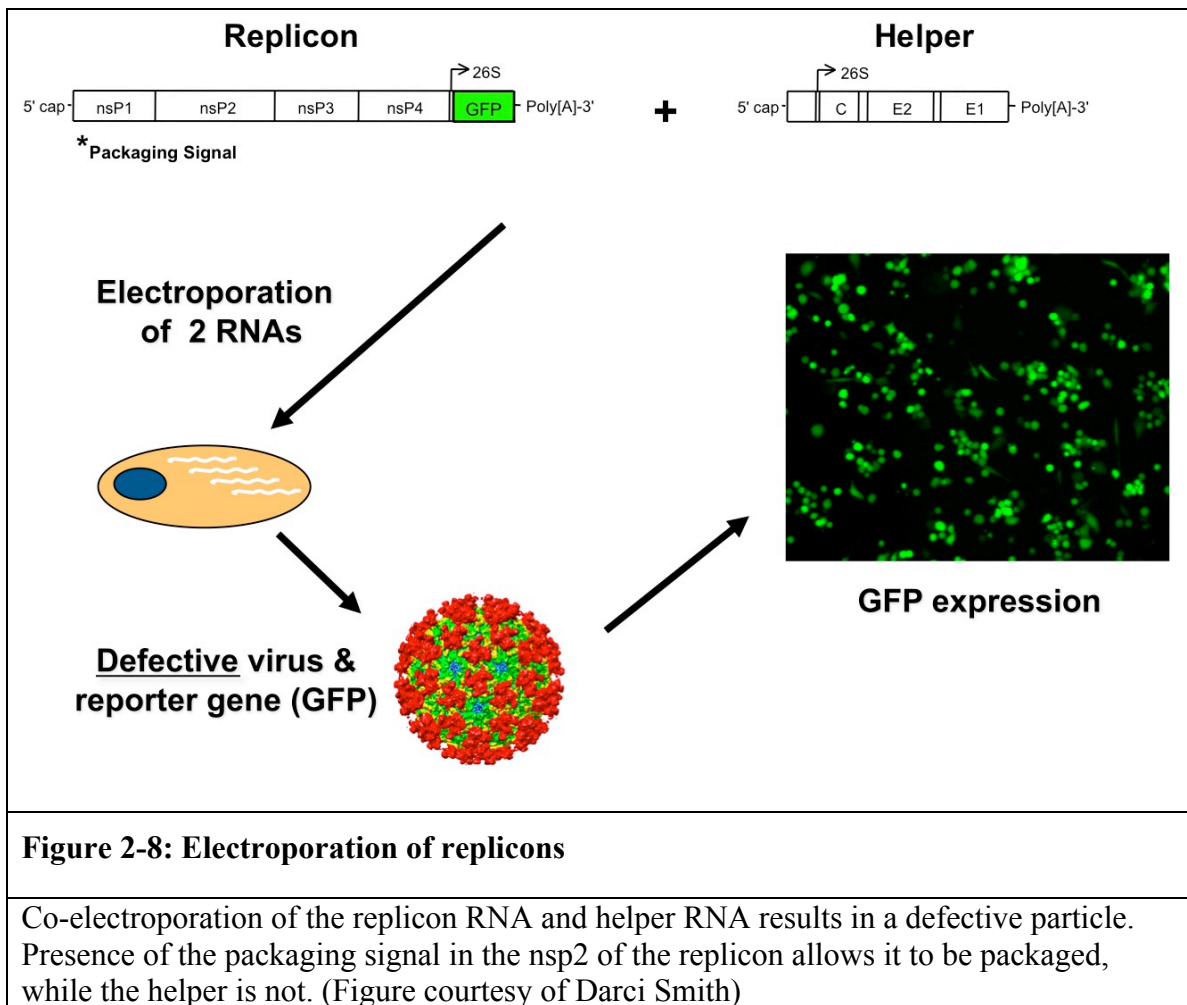
REPLICONS AND HELPERS

Purpose

Various aspects of this project were designed to evaluate the initial cell types and progression of infection following oral exposure in an enzootic mosquito vector. The most sensitive way to observe cells infected with virus is to visualize infection with a reporter. This can be done indirectly by tagging a reporter to an antibody that is specific to a viral antigen or directly by including a reporter gene within the viral genome that expresses a marker (i.e. luciferase or GFP) upon viral translation. Use of alphaviruses encoding GFP in mosquitoes has been demonstrated previously [161,178-180].

However, distinguishing the first cells infected from cells infected as a result of viral

replication and spread could be potentially challenging. However, the alphavirus genome organization allows for generation of replication-deficient virions that can infect cells initially and replicate their genomes, but are unable to generate functional progeny virions that propagate the infection by spreading beyond the initial cells infected. This was achieved with co-electroporation of two capped RNA segments (figure 2-8).



The first segment, or the replicon, consists of the 5' UTR, nonstructural polyprotein ORF, and a reporter gene such as GFP or luciferase. The second RNA species is referred to as the helper, and made up of the structural regions and *cis*-acting elements required for RNA replication. When electroporated together into cells, they interact to allow for replication of both RNAs and translation of proteins. However, the helper RNA does not include a packaging signal that is found in the nonstructural cassette and therefore will not be packaged into virion particles and results in defective particles that do not contain subgenomic RNA [181]. As a consequence those cells that are initially infected will continually express GFP, which can be easily viewed on a fluorescent microscope, but no surrounding cells will become infected. I determined that replicons would be ideal tools to study the initial infection site and number of cells infected in *Cx. taeniopus* midgut. In my original proposal, I intended to use pre-existing replicons and helpers for IE 68U201 and IAB TrD from the V3000 clone. However, it was quickly established that the IE 68U201 replicon had 12 nucleotides from IC 3908 in the subgenomic promoter regions which accounts for three nucleotide differences from IE in that region, and therefore needed to be regenerated. Additionally, my plans for co-infection studies (see chapter four) called for a IE replicon expressing GFP as well as one expressing CFP, so two versions of the replicon were generated. While the IAB TrD replicon had been previously generated from the V3000 and generously donated by Nancy Davis, I had to generate the IAB helper clone.

IE 68U201 GFP and CFP replicon

The strategy for these replicons was to do a three-piece ligation with one fragment being made by fusion PCR. In this case, because the GFP and CFP are conserved in the 5' and 3' ends of the gene, the same primers could be used for both strategies. For each clone the first ligation piece was made by digesting the parental IE 68U201 plasmid with EcorI and NheI. The second ligation fragment was made from two individual PCRs. The two joining fragments were made in the same fashion as those used for generation of the IE 68U201 GFP virus described above. The only exception being that the second fragment of the 68U201 CFP replicon was amplified from a plasmid construct encoding CFP. The third ligation piece was made by digesting the pre-existing 68U201 GFP replicon with BsgRI and EcorI. The fragments were ligated, transformed, examined for accuracy, prepared, transcribed, and electroporated as described above.

IAB V3000 Helper

Our collection of IAB V3000 clones, including the parent IAB strain, the full length IAB with a ClaI site and GFP, the IAB GFP replicon, and a bipartite helper for the replicon were generously provided by Nancy Davis and Robert Johnston from the University of North Carolina. However, for my experiments described in chapter four, I required a single species helper that included the entire structural open reading frame. To generate this clone, I initially digested the IAB V3000 clone with KpnI and RsrII and ran a small portion (2 μ l) of the digested product on an agarose gel to be sure the digestion

was complete. The remaining volume of the digestion was subjected to a filling-in reaction to generate blunt ends. This was done by adding 0.5 μ l Klenow polymerase (NEB, Ipswich, MA), 1 μ l dNTPs, and 5 μ l NEB buffer 4 (the same as used in the original digestion) and allowed the mixture to incubate at room temperature for ten minutes. The mixture was then purified by phenol chloroform treatment, resuspended in 45 μ l and digested with SmaI enzyme with NEB buffer 3 and bovine serum albumin (BSA) (NEB, Ipswich, MA). I utilized agarose gel electrophoresis to identify and isolate the RsrII-SmaI fragment, which was gel extracted and purified prior to ligation with the NEB T4 DNA ligase. The ligation product was transformed into One Shot® OmniMAX competent cells (Invitrogen, Carlsbad, CA). Five bacterial colonies were sampled and prepared using the QIAprep kit (Qiagen, Valencia, CA) and examined for accuracy by digestion with HindIII and sequencing prior to the large preparation of DNA.

Linearization and Electroporation

Ten μ g of each large DNA preparations for 68U201 GFP, CFP, and the helper, were linearized with EcoRI, while the replicon and helper derived from IAB V3000 were linearized with NotI. Linearized materials were purified with by phenol/chloroform and alcohol precipitation. One μ l of each was transcribed for one hour using the mMessage mMachine® T7 kit (Ambion, Austin, TX). A single μ l of each transcription product was examined by gel electrophoresis prior to electroporation. Those samples that were not immediately electroporated, were stored at -80°C for a maximum of 48 hours prior to

use. Each replicon was mixed with its respective helper at equal volumes prior to electroporation, which was performed in BHK cells that had been washed three times in DPBS (Gibco®, Carlsbad, CA) prior to re-suspension. Cells were mixed with the transcription products and immediately subjected to electroporation to minimize any RNA degradation. As described above, electroporation was performed on a BTX ECM 630 (BTX, Holliston, MA) with the following settings: HV mode, 0680 volts, a pulse length of 099s, 5 pulses, a 100 ms interval, unipolar polarity, and in a 2mm cuvette. Following electroporation the cuvette of cells was incubated on ice for 10 minutes prior to being transferred to a 75-cm² flask with DMEM (Gibco, Austin, TX) supplemented with 10% FBS and penicillin and gentamycin.

CLONING SUMMARY AND CONCLUSIONS

Although in my original proposed project I planned to use pre-existing infectious clones to generate low passage virus stocks for my experiments, this turned out to be unworkable as many of those clones had errors and had to be regenerated. All in all, I had to generate nine clones for this project. This was mostly achieved using fusion PCR to create these clones. An advantage for using this method is that no restriction site is required at the junction site. In most cases, a naturally occurring restriction site is rare and the junction site desired has to be artificially introduced and then removed once the desired cloning has been completed. A disadvantage of the fusion PCR cloning method is the potential for the DNA polymerase to make errors and introduce mutations into the

fusion region. However, use of a high-fidelity polymerase minimizes the chance of this occurring. Throughout these cloning projects, typically, a minimum of one out of five transformed colonies pre-established to have the fusion fragment were found to have no point mutations within that fragment upon sequencing.

In addition to sequencing the PCR fusion fragment, the full-length replicating clones and chimeras were evaluated and compared for growth characteristics. This was performed primarily to assess the effect of chimerization prior to independent comparison of infection and dissemination in an *in vivo* mosquito model. In Vero cells, replication of each of the IAB-IE chimeras appeared competent, and not statistically different from the parental IE, but, with the exception of IE/IAB, all showed differences at some time point from IAB. The growth of the chimeras was additionally tested in an *in vitro* mosquito cell line to see if any growth patterns could be correlated to that seen in the *in vivo* experiments (chapter 2). The replication was more varied in this cell line with more statistical differences observed at multiple time points, however no obvious replication deficiencies were seen in this cell line either. It did appear that IAB TrD had a more distinct replicative advantage C6/36 cells than in Vero cells, although this does not appear vital as neither chimera pair showed major replicative differences from the other.

The replication of full-length version of each parental virus expressing GFP, IE 68U201 GFP and IAB TrD GFP, was also compared to the parental strains to determine if the addition of the GFP had a deleterious effect. Interestingly, it appears that the presence of the GFP significantly affected replication of IAB in Vero cells as compared

to the wild-type IAB strain, while the IE 68U201 GFP virus did not replicate differently from the parent IE virus at any time points. It is also worth noting that the attenuated replication of the IAB GFP virus was no different than that of IE parent or the IE GFP virus.

CHAPTER 3: GENETIC DETERMINANTS OF VEEV INFECTION OF THE ENZOOTIC VECTOR, *CULEX TAENIOPUS*

BACKGROUND

Venezuelan equine encephalitis virus (VEEV) is a mosquito-borne virus in the family *Togaviridae* and genus *Alphavirus*. Initially identified in the 1920s, in the past 80 years, VEE has resulted in hundreds-of-thousands of cases of often severe and sometimes fatal encephalitic disease in humans and equids. Disease manifestations can range from a subclinical flu-like illness that is relatively minor to a fatal encephalitis with a case-fatality rate anywhere from 4-14% [68]. VEEV persists in two distinct ecological cycles. Two of the four antigenic subtypes, IAB and IC, persist in the epizootic, or outbreak ecological cycle, while the IE and ID antigenic subtypes are primarily enzootic, or endemic viruses.

The key factors distinguishing an epizootic virus strain from an enzootic virus strain are whether the virus can cause disease in horses and what mosquito species transmit the virus. With the exception of some unique IE VEEV strains that were encountered in Mexican outbreaks in the early 2000s [122], IE and ID isolates are not known to cause disease in equids and are typically vectored by *Cx. (Melanoconion) spp.* mosquitoes of the *Spissipes* section. IE VEEV strains in particular have repeatedly shown to be vectored by *Cx. (Melanoconion) taeniopus* mosquitoes, but other recognized

species within the *Spissipes* section include *pedroi*, *adamesi*, *ocossa*, *panocossa*, and *vomerifer* [112,115,182]. These mosquito species prefer to inhabit shaded, intact forests with stable pools of water available for larval development. Some also require the presence of *Pistia* spp., an aquatic plant, for respiration [131]. While these mosquito species are not necessarily limited to feeding on small rodent, small rodents such as cotton rats (*Sigmodon* spp.), spiny rats (*Proechimys* spp.) and various other species including *Liomys salvini* and *Oligoryzomys fulvescens* are thought to be particularly important for maintenance and transmission of enzootic VEEV strains in nature [103-105].

Epizootic subtypes, IAB and IC are known to cause severe disease that often coincides with a high viremia in humans or equine cases. This high viremia is what allows for transmission by a completely different group of mosquito vectors that are more likely to feed on human and equine hosts. When outbreaks occur, epizootic strains persist for the duration of the outbreak in a mosquito-equine transmission cycle. The occurrence of cases in humans or equids is dependent on the presence of a competent mosquito vector that utilizes both humans and equids as hosts. Mosquitoes such as *Aedes (Ochlerotatus) taeniorhynchus*, *Ae. (Ochlerotatus) sollicitans*, *Psorophora confinnis*, *Culex (Deinocerites) psuedes*, *Mansonia indubitans*, and *Ma. titillans*, among others have been incriminated as important vectors for epizootic VEEV [102,153,182-185]. Many of these mosquitoes flourish near coastal brackish water systems, can fly long distances from larval development sites, prefer to feed on humans or large mammals, and can

tolerate feeding in sunny areas, although they may rest in shaded regions, which makes them quite different from they typical enzootic mosquito vector.

Generally, mosquito vectors of VEEV are highly specific in their susceptibility to either epizootic or enzootic VEEV strains, and are nearly refractory to subtypes from the alternate transmission cycle. It has been shown repeatedly that mosquito vectors of enzootic strains have a lower threshold of infection than that which is required for many epizootic vectors [102,111,139]. This specificity has made a valuable tool to identify circulating strains of VEEV as epizootic or enzootic [102]. Most experimental studies examining vector competence have shown *Ae. taeniorhynchus* to be primarily competent for epizootic strains and poorly competent or refractory for enzootic strains [69,102,153,161,184-187]. Because these epizootic vectors are easily accessible and readily colonized for experimentation, the majority of previous experimental studies that focus on genetic determinants of ecological cycle specificity have been performed with these vectors. Reverse genetic studies in these model systems have shown that epizootic vector specificity depends heavily on the E2 envelope glycoprotein [69,187], which forms the tips of spikes on the alphavirus surface [188]. Further studies comparing epizootic subtype IC and enzootic subtype IE VEEVs in *Ae. taeniorhynchus* have shown that specificity pertains directly to virus binding to mosquito midgut epithelial cells; epizootic subtype IC viruses bind at significantly higher rates than enzootic strains [161].

Similar differential competence has been shown for the Middle American enzootic vector, *Cx. taeniopus* [106-108,110,139]. While this mosquito is highly

susceptible to sympatric subtype IE enzootic strains, it is nearly refractory to enzootic subtype ID strains [108]. This differential susceptibility suggests a long co-circulation of IE viruses and *Cx. taeniopus* mosquitoes and subsequent adaptation of subtype IE VEEV to this mosquito species. Phylogenetic studies indicate that IE viruses diverged from other subtype I and II viruses well before strain IAB, IC, and ID diverged from a common ancestor at least 150 years ago [189], potentially allowing for IE strains to become established in a well-defined niche. Such a relationship might foster a different interaction between enzootic VEEV strains and their vectors as compared to the epizootic virus strains and their vector counterparts. The specificity of the epizootic VEEV strains to epizootic vectors is strongly dependent on the amino acid sequence of the E2 protein, and unlike the enzootic virus-vector interaction, epizootic viruses only interact transiently (only during periods of outbreaks when mosquito populations are high and epizootic virus is present) with their epizootic mosquito vectors. The restrictive susceptibility of *Cx. taeniopus* to enzootic subtype IE suggests a long relationship of co-adaptation between the virus and mosquito. Such a co-adaptation with consistent selective pressures would likely result in the IE virus becoming more genetically stable within this theoretically established ecological cycle. Therefore I hypothesized that the restrictive susceptibility of *Cx. taeniopus* to enzootic subtype IE VEEV strains is not strictly determined by limited regions within the E2 gene, but is likely dictated by multiple elements that may be outside of the E2 glycoprotein. To test this hypothesis, I generated four chimeric VEEVs (see chapter 2), using a strain with a known high susceptibility to

Cx. taeniopus (i.e., subtype IE strain 68U201) and a strain known to be poorly infectious for *Cx. taeniopus* [i.e., the subtype IAB Trinidad donkey (TrD) strain]. These chimeras allowed me to discern the contributions of the structural and nonstructural protein regions and the 3' untranslated region (UTR) in infection and dissemination in *Cx. taeniopus*.

METHODS

Viruses

Viruses used for these experiments were generated from cDNA clones VEEV IAB TrD V3000 (generously provided by Nancy Davis and Robert Johnston) [173] and IE 68U201 generated by Powers et al. [171]. The IAB TrD virus strain had been passaged once in guinea pig brains and 14 times in embryonated eggs prior to being immortalized in cDNA clone form. The IE 68U201 viral isolate had been passaged once in newborn mice and two times in BHK-21 cells before construction of the clone. From these clones, four chimeric variants were developed: two with matching *cis*-acting RNA elements (IAB/IE/IAB and IE/IAB/IE) and two with mismatched elements (IAB/IE and IE/IAB) (fig 2-1). Specific cloning, DNA preparation, transcription, and electroporation methods are described in chapter two.

Mosquitoes

The *Cx. taeniopus* mosquito colony was established from adult females collected in Chiapas, Mexico in 2007 and were maintained in a laboratory colony as described

previously [106]. Mosquitoes used for these experiments are from estimated F₃₀ – F₃₉ generations. Ten to 15 day old mosquitoes were anesthetized by cold and sorted 48 hours prior to viral exposure. This species was determined to be very sensitive to starving and therefore was provided with a 10% sucrose solution after sorting, which was removed and replaced with fresh cotton balls soaked with water 24 hours prior to feed. The water source was removed six to eight hours prior to blood feeding. Once the feed was completed, mosquitoes were again cold-anesthetized and engorged females were separated out from unfed mosquitoes and held for a 14-day extrinsic incubation period (eip) at 27°C. It was rapidly determined that this mosquito species requires an unusually high humidity level to survive the duration of the eip. To improve survival within the incubator, mosquito cartons were held in a sealed Tupperware container and covered with minimally (to reduce mold growth) damp paper towels to maximize humidity and shade. Mosquitoes were provided a 10% sucrose solution throughout the eip.

Mosquito Exposure

Two parental viruses (IAB and IE) and four chimeras (IAB/IE/IAB, IE/IAB/IE, IAB/IE, IE/IAB) were evaluated for their ability to infect and disseminate in *Cx. taeniopus* mosquitoes. Because colonized *Cx. taeniopus* are highly fastidious feeders and do not imbibe from an artificial blood meal source regardless of the membrane type utilized, live rodent hosts had to be utilized. For *Cx. taeniopus* oral feeds, either 10-week-old female CD-1 mice (Charles River Laboratories) or five-week-old Syrian Golden

hamsters (Harlan Laboratories) were used as viral hosts. In an experiment performed with the epizootic mosquito model, *Ae. taeniorhynchus*, an artificial membrane feeder was utilized.

Artificial Viremia

Initial oral exposure experiments were done with an artificial viremia method of CD-1 mice. Mice utilized for the artificial viremic exposure were anesthetized by intraperitoneal IP inoculation of 50 mg/kg sodium pentobarbital (about .04 ml. per 10-week old mouse), and 200 µl of a stock virus was inoculated into the tail-vein of the animal (described in more detail in chapter 4). Virus was allowed to circulate for 5 minutes prior to collecting blood and exposing the animal to the mosquitoes to allow the virus chance to circulate throughout the mouse body. Mosquitoes were allowed to feed for ca. one hour after which, blood was collected from the animal again to detect any loss of circulating viral concentration. After multiple replicates with this method of exposure, the high variability of the decay of circulating virus between groups led me to perform the remaining replicates with a natural viremia exposure system.

Natural Viremia

Initially, mice were utilized as viremic hosts, but as the literature showed that hamsters develop a higher viremia [124,190], they were utilized in the later experiments to expose *Cx. taeniopus* mosquitoes to higher doses. To develop a natural viremia, mice or hamsters were inoculated subcutaneously (SC) with 1000 plaque-forming units (PFU),

held for 24 hours , and anesthetized by IP administration of sodium pentobarbital (50 mg/kg) immediately prior to mosquito exposure. Normally, before any infection, a rodent host is swabbed with a 70% EtOH solution at the site of injection. However, it was quickly determined that feed rates were significantly lower on those mice that had been swabbed with 70% EtOH prior to anesthesia than those that had not, so no alcohol pre-treatment was used prior to anesthesia. Mice and hamsters were bled from the retro-orbital sinus, and exposed to mosquitoes for approximately one hour. Immediately prior to placement on the carton, each hamster's ventral surface was shaved to improve mosquito engorgement rates.

Artificial Blood Meal

For the *Ae. taeniorhynchus* experiment an artificial blood meal exposure was used. Cohorts of 50 adult females were allowed to feed for 45 min on an artificial blood meal containing 33% (v/v) defibrinated sheep erythrocytes (Colorado Serum Company, Denver, Co), 33% (v/v) heat-inactivated fetal bovine serum (FBS) (Omega Scientific, Inc., Tarzana, CA), 33% (v/v) of each individual virus in cell culture fluid, and 1% (v/v) of 0.25 μ M adenosine triphosphate. Artificial blood meals were encased in a collagen membrane and warmed in a Hemotek feeder (Discovery Workshops, Accrington, United Kingdom)

Plaque and CPE Assays

Viral titers of rescued viruses and animal sera were determined by plaque assay on Vero cells. Plaque assays were performed by making ten-fold serial dilutions of each sample and infecting monolayers of Vero cells. Infections were incubated at 37°C for one hour with gentle rocking at 15-minute intervals prior to addition of a 4% agarose in complete DMEM overlay. Samples were incubated for 48 hours at 37°C prior and then inactivated with a 30-minute incubation in 10% formalin. Agarose plugs were delicately removed and the remaining fixed monolayer of cells was stained with a crystal violet solution.

Following 14-day eip, legs and wings were removed from mosquitoes and stored at -80°C. Samples were triturated and used to infect monolayers of Vero cells in CPE assays. Triturated body samples that generated CPE were indicative of an infected mosquito, while legs and wings were used to detect a disseminated infection.

Statistics

Statistical analysis of rates of infection and dissemination were broadly examined using a contingency analysis, and specific 2x2 comparisons were evaluated using Fisher's exact test with JMP software (SAS Institute Inc., Cary, NC). *P-values* ≤ 0.05 were considered significant.

RESULTS

Mosquito Exposure

Unlike many mosquito species commonly utilized in a laboratory setting, *Cx. taeniopus* will not feed on a membrane feeder apparatus and require a live animal. Standard methods to expose this mosquito to virus have depended on generating a natural viremia in an animal model such as a hamster or mouse [106,111]. Unfortunately, animal viremia is often variable and it is difficult to deliver a standard exposure dose across treatment groups using this method. Similarly, exposure dose titration experiments require multiple feeds throughout the 24-hour viremia curve, which is work intensive and potentially introduces bias by doing feeds at different photoperiods. To address this I compared the traditional natural viremia exposure route with a less often utilized method of artificial viremia. First described by Weaver et al. during exposure of *Culiseta melanura* to radiolabeled Eastern equine encephalitis virus [151], the method generally entails inoculating a host animal intravenously with virus allowing for a rapid, yet temporary viremia prior to natural, replicative viremia. I replicated this technique in mice and monitored the artificial viremia before and after the feed. I found that over the course of one hour the change in artificial viremia varied greatly from not changing concentration to dropping more than one log₁₀ PFU/ml (figure 3-1).

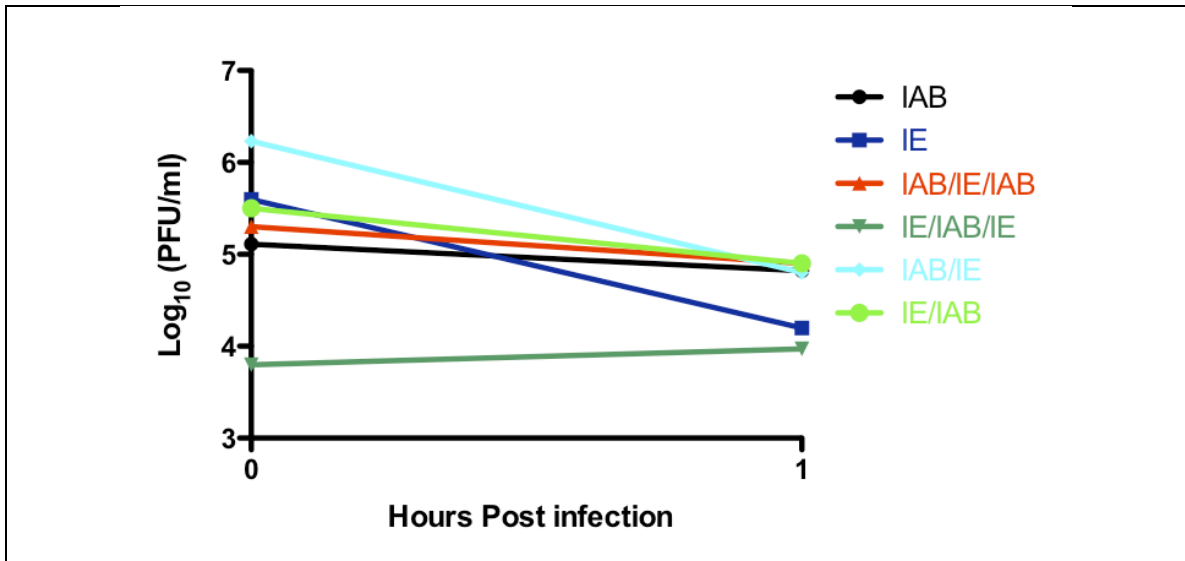


Figure 3-1: Change in artificial viremia

Comparison of circulating plaque forming units in a mouse immediately following and intravenous tail-vein inoculation and one hour after for each parental and chimeric virus

Similarly, I found it easier and more reliable to predict a virus exposure dose based on a natural viremia curve than calculating the expected artificial viremia following an intravenous inoculation. Throughout all the experiments, I determined that natural viremia in hamsters allowed for a higher exposure dose than a natural mouse viremia, and both natural viremia methods provided higher exposure doses when compared to an artificial viremic exposure (table 3-1).

Virus	Artificial Viremia (mean dose)	Viremic Mouse	Viremic Hamster
IAB	5.0	6.2	NA
IE	4.8	5.7	NA
IAB/IE/IAB	5.8	5.7	8.6
IE/IAB/IE	4.0	6.0	8.2
IAB/IE	5.5	6.0	9.0
IE/IAB	5.2	6.0	8.3

Table 3-1: Natural and artificial viremias

Examination of the maximum exposure (log PFU/ml) dose achieved by each of three methods attempted for each virus examined. Artificial viremia represents the average titer calculated between the two time points taken from mouse blood at the initiation of the feed to the completion of the feed. The viremic mouse and hamster titers represent the titer of circulating virus 24 hours after initial inoculation, which coincides with the start of the mosquito exposure.

***Cx. taeniopus* Infection and Dissemination**

Adult female *C. taeniopus* were orally exposed to a range of doses for each of the parental and chimeric strains of VEEV and tested for infection and dissemination into the hemocoel following a 14-day eip (table 3-2) Two pairs of chimeras with matched and mismatched *cis*-acting RNA elements were utilized to independently evaluate the roles of the nonstructural and structural polyprotein open reading frames as well as the 3' UTR in mosquito infection and dissemination. As expected, the parental IAB TrD virus was unable to infect *Cx. taeniopus* at blood meal titers as high as 6.2 log₁₀ PFU/ml, which is in agreement with previous work [110,139]. Similarly, as predicted based on previous

studies [106,110,111], *Cx. taeniopus* mosquitoes were highly susceptible to infection with the parental subtype IE 68U201 strain at oral doses as low as 4.2 log₁₀ PFU/ml. In support of my hypothesis that determinants of infection will not be limited to the E2 glycoprotein, all four chimeras showed an intermediate ability to infect and disseminate in *Cx. taeniopus* when compared to the parental IAB and IE strains (figure 3-2). The effect of the exposure dose on infection rate was evaluated by contingency analysis for each of the chimeric viruses (IAB/IE/IAB, IE/IAB/IE, IAB/IE, and IE/IAB) and found to be significant for each ($p < 0.05$; $p < 0.001$; $p < 0.05$; $p < 0.0001$, respectively) (figure 3-2A). In order to compare individual virus strains, a Fisher's exact test was utilized to determine differences in infection rates (table 3-2) As expected, comparisons between the parental viruses and the chimeric viruses were all highly significant ($p < 0.0001$), with the exception of the comparison between the IE parental virus and IE/IAB chimera, for which the IE strain had a less notable infectious advantage than the chimera ($p < 0.0071$). Interestingly, infection rates did not differ significantly among three of the four chimeras: IAB/IE, IAB/IE/IAB, and IE/IAB/IE. However, IE/IAB showed a significantly higher infection rate when compared to each of the other three chimeras ($p < 0.0001$; $p < 0.0049$; $p < 0.0025$, respectively). Although each chimera showed the ability to disseminate into the hemocoel after midgut infection, the dissemination rates among the chimeras were low overall (figure 3-2B); therefore, no transmission experiments were performed. Fisher's exact tests between the rates of infected mosquitoes with dissemination showed no differences between the four chimeric strains. Previous studies

of alphaviruses as well as other arboviruses have shown that infected mosquitoes often have virus restricted to the midgut, which is likely explained by a commonly recognized but poorly understood barrier to viral escape of the mosquito midgut [110,143,191,192]. While dissemination rates increased as the exposure dose was increased, the overall rates of dissemination were too low to perform reliable statistical analysis.

***Ae. taeniorhynchus* Infection and Dissemination**

In order to confirm the expected phenotype of the four chimeras based on previous publications, I exposed an epizootic mosquito model, *Ae. taeniorhynchus* using an artificial feeding apparatus. Each group was exposed to an about 6.0 log (PFU/ml) of each virus (table 3-3). Although the engorgement rates were quite low, the IE/IAB chimera appeared to have the highest infection rate (33%) and was the only virus to disseminate in the group. Despite having an epizootic derived E2 glycoprotein, IE/IAB/IE virus had very low infection rates in *Ae. taeniorhynchus*. This is likely partially due to the fact that while, *Ae. taeniorhynchus* is a strong vector of epizootic IC VEEV strains [153,161], it has been shown to be a less competent vector of IAB VEEV strains [69,184]. Although, it is interesting to note that the IE/IAB chimera showed higher infection and dissemination than the other chimera with IAB derived structural regions, which suggests that there is a role for the 3' UTR as that is the only difference between the two viruses.

Virus	BM Titer	no. infected (%)	No. with disseminated infection (%)	No. infected with dissemination (%)
IAB	3.87	0/17 (0)	0/17 (0)	0/0 (0)
	5.11	0/18 (0)	0/18 (0)	0/0 (0)
	6.17	0/2 (0)	0/2 (0)	0/0 (0)
IE	4.18	13/16 (81)	7/16 (44)	7/13 (53)
	5.60	12/12 (100)	11/12 (92)	11/12 (92)
	5.72	3/3 (100)	3/3 (100)	3/3 (100)
IAB/IE/IAB	3.85	3/8 (38)	0/8 (0)	0/3 (0)
	4.90	4/8(50)	0/8(0)	0/4 (0)
	4.81	0/16 (0)	0/16 (0)	0/0 (0)
	5.77	2/4 (50)	0/4 (0)	0/2 (0)
	5.81	10/19 (53)	3/19 (16)	3/10 (30)
	8.50	13/23(57)	3/23(13)	3/13 (23)
	8.60	3/4 (75)	2/4(50)	2/3 (66)
IE/IAB/IE	3.20	0/10 (0)	0/10 (0)	0/0 (0)
	3.98	9/17 (53)	0/17 (0)	0/9 (0)
	3.60	4/20(20)	0/20(0)	0/4 (0)
	5.30	1/4 (25)	0/4 (0)	0/1(0)
	6.00	5/16 (31)	2/16 (13)	2/5 (40)
	8.20	2/2 (100)	0/2 (0)	0/2 (0)
	8.40	16/20(80)	7/20(35)	7/16 (43)
IAB/IE	4.20	8/32 (25)	0/32 (0)	0/8 (0)
	4.70	7/20(35)	0/20(0)	0/7 (0)
	6.00	8/18 (44)	0/18 (0)	0/8 (0)
	6.23	2/22 (9)	0/22(0)	0/2 (0)
	8.30	10/20(50)	7/20(35)	7/10 (70)
	9.00	5/10 (50)	4/10 (40)	4/5 (80)
IE/IAB	4.60	8/27(30)	0/27(0)	0/8 (0)
	5.10	11/32 (34)	0/32 (0)	0/11 (0)
	5.50	22/24 (92)	7/24 (29)	7/22 (31)
	5.72	3/5 (60)	2/5 (40)	2/3 (66)
	8.20	30/34(88)	11/34(32)	11/30 (36)
	8.30	4/4 (100)	2/4 (50)	2/4 (50)

Table 3-2: Rates of infection and dissemination of each virus in *Cx. taeniopus*

Infection represents the number of infected mosquito bodies out of those exposed and alive at the end of the extrinsic incubation period. Dissemination infection represents the number of exposed mosquitoes with positive legs and wings. Infected disseminated

infection refers to the number of infected mosquitoes with positive legs/wings.

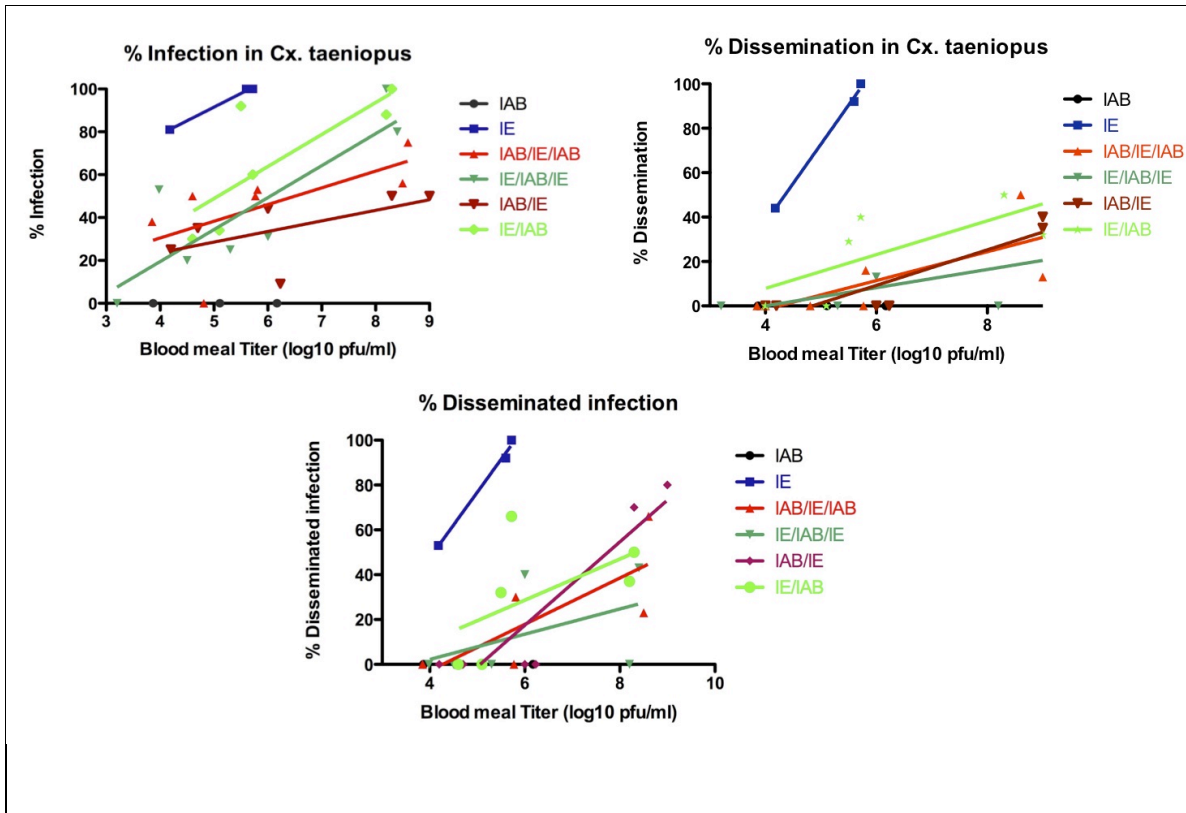


Figure 3-2: Regression of infection, dissemination and disseminated infection

Regression lines were generated for each virus for the purpose of visualizing the results. (A) represents percentage of infection at a given dose. The goodness of fit R^2 values were 0.995, 0.421, 0.725, 0.340, and 0.617 for IE, IAB/IE/IAB, IE/IAB/IE, IAB/IE, and IE/IAB, respectively. Figure (B) represents percentage dissemination at a given dose (B) and yielded R^2 values of 0.996, 0.535, 0.465, 0.820, and 0.500. Graph (C) represents the percent disseminated infection and resulted in R^2 values of 0.992, 0.606, 0.2397, 0.838, and 0.305, respectively.

Virus	# Engorged	Blood Meal (PFU/ml)	# Infected (%)	# Disseminated (%)	# Diss Infection (%)
A/E/A	16	6.6	0/8 (0)	0/8 (0)	0/0 (0)
E/A/E	26	6.64	1/8 (6)	0/18 (0)	0/1 (0)
A/E	21	7.15	1/11 (9)	0/11 (0)	0/1 (0)
E/A	19	7.2	4/12 (33)	2/12 (17)	2/4 (50)

Table 3-3: Infection, dissemination, and disseminated infection in *Ae. taeniorhynchus*

CONCLUSIONS AND SUMMARY

As human populations continue to expand into previously uninhabited areas, we will continue to see more emerging and re-emerging zoonotic pathogens. Arboviruses in particular, such as chikungunya, dengue, yellow fever, and Japanese encephalitis virus have already seen a surge in incidence [193]. Similar trends have also been observed with enzootic strains of VEEV that have caused human cases in regions of Peru, Central America, and Mexico [163,194]. Historically, studies of VEEV emergence have focused on epidemic strains in subtypes IAB and IC; however, enzootic ID and IE strains, which are responsible for a significant number of human cases, warranted further examination. Studies by Deardorff et al. have recently shown *Cx. taeniopus* to be capable of transmitting newly emerged IE VEEV strains that exhibit epizootic phenotypes such as causing severe disease in humans and readily infect an epizootic model vector, *Ae. taeniorhynchus*. Considering the growing risk of enzootic VEEV strains for causing human disease, I

developed chimeric viruses to analyze the molecular determinants for VEEV specificity to the enzootic mosquito vector.

Utilizing two viruses with distinct phenotypes for these chimeras, allowed me to confidently identify the major genome regions that contribute to specific infection of the enzootic vector. Because these viruses show a high level of divergence (10.2% at the amino acid level), extrapolation of this method to clarify the roles of each gene during enzootic mosquito infection could be prone to bias from incompatibilities between open reading frames within each chimera. However, replication curves comparing each of these chimeras to the respective parental strain (see chapter 2) indicated that none of these viruses had significant replicative deficiencies. Specifically, in Vero cell monolayers all viruses showed indistinguishable replication kinetics. *In vitro* replication C6/36 mosquito cells, also indicated that chimerization did not inhibit replicative capabilities.

A significant amount of time and effort went into establishing ideal conditions for *Cx. taeniopus* mosquitoes to engorge on presented hosts and survive throughout the incubation period with high enough survival rates. Eventually, it was determined that these mosquitoes cannot be starved of sucrose for more than six hours before the feed and require shade and high humidity within the cartons throughout the incubation period. Methods of exposure were also evaluated to determine the most consistent and effective method for delivering a high titer blood meal to *Cx. taeniopus* mosquitoes. Experimental studies with sympatric rodent hosts indicate that epizootic IE viruses cause viremia

ranging from 2.5 to 5.5 log₁₀ PFU/ml [103], and although these findings were for epizootic IE strains, it suggests that a *Cx. taeniopus* mosquito would rarely be exposed to titers higher than 6.0 log₁₀ PFU/ml. However, since these studies were examining the potential for infection, higher exposure doses were utilized. For experiments with a replicating VEEV virus strain, it was determined that a viremic hamster was the best method for delivering a maximum exposure dose to *Cx. taeniopus*. A mouse viremia was also very efficient, although the maximum exposure dose achievable (viremia) was approximately 6.0 log₁₀ PFU/ml, which is near the upper limit of exposure titers a *Cx. taeniopus* vector would encounter in nature [103]. I was able to achieve a minimum of 8.0 log₁₀ PFU/ml for all viruses replicating in hamsters. While the artificial viremia method was a viable method for exposing *Cx. taeniopus* mosquitoes to an infected blood meal, this method had a limited exposure dose and lacked consistency over time and between virus groups. Specifically, I observed on average a 2.0 log PFU/ml decrease from the stock virus titer used for the inoculation, to the peak amount of virus circulating within the mouse. This is logical as only 200 µl could be safely inoculated into the mouse without risking the mouse's survival. Similarly, that 200 µl was further diluted by the volume of the mouse blood (approximately 1.5 ml) and therefore resulted in an overall reduction in the concentration of circulating virus.

I additionally observed a high degree of variability in the clearance of each virus that occurred during the one hour feed. Initially, I assumed this to be a random occurrence that was not dependent on the viral strain; however, this phenomenon had

been documented before between various VEEV strains inoculated intracardially into hamsters. Although, Jahrling et al. [124] did not cite a statistically significant difference between the rate of disappearance from the blood between a IAB and IE VEEV strain, one can observe a trend similar to what I have seen (figure 3-3).

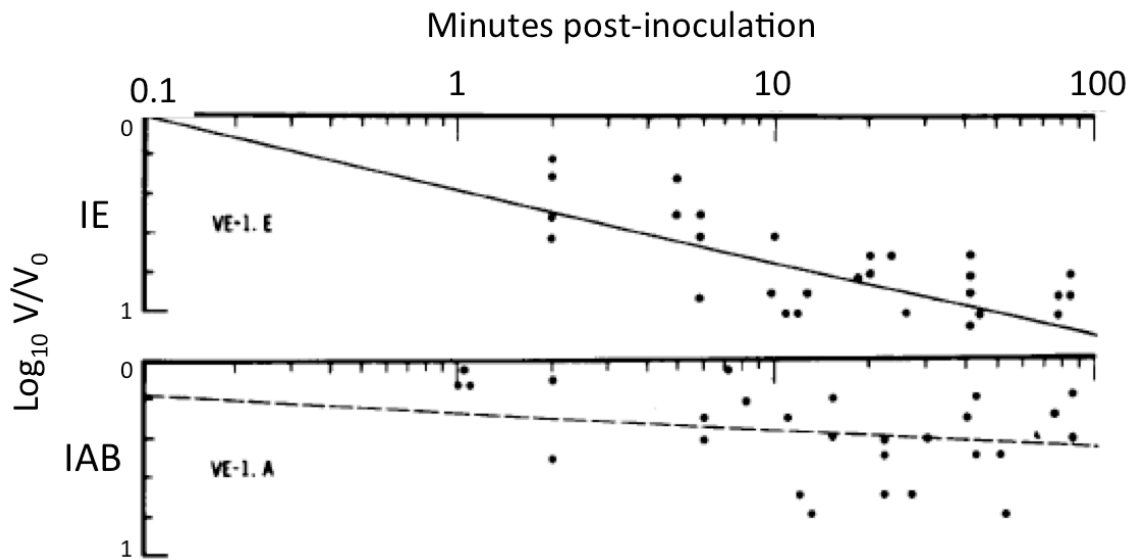


Figure 3-3: Clearance of rates after intracardiac inoculation.

Both IE and IAB viruses were inoculated intracardially into hamsters and followed at time points for clearance. Each point represents the V/V_0 or $-\log_{10}$ PFU cleared. Modified with permission from Jahrling et al. 1973 [124].

Considering this differential clearance in addition to the limit of maximal dose, I determined that a natural viremia exposure method was the best for competently replicating viruses. Despite its inconsistency between viral groups, the artificial viremia was utilized for exposing *Cx. taeniopus* to non-replicating viral particles such as replicons and GFP expressing replicating viruses to control for any potential confounding

factors due to replication attenuation as a result of inclusion of the heterologous protein (see chapter 4 and 5).

I orally exposed *Cx. taeniopus* to a range of doses of the two parental strains, IE and IAB, as well as the four chimeras, IAB/IE/IAB, IE/IAB/IE, IAB/IE, and IE/IAB to evaluate the role of the nonstructural and structural protein genes and the 3' UTR as determinants of infection and dissemination. I hypothesized that, unlike the epizootic virus strains and their vectors, genetic determinants for enzootic infection would include multiple genes and would not be restricted to the E2 envelope glycoprotein. I anticipated that chimeras with mismatched 3' UTR regions would show diminished infection and dissemination rates based on previous alphavirus studies examining the effects of mismatched *cis*-acting elements [170,195]. However, I observed that the IE/IAB chimera showed a significantly higher rate of infection than that of the other three chimeras. This suggests that the 3' UTR plays an important role in infection of the enzootic vector. A closer examination of the effect of the 3' UTR on infection shows that the chimera with IAB structural and IAB 3' UTR (IAB-IAB) has the highest infection, while the chimeras with a mixed structural-3' UTR makeup (IE-IAB or IAB-IE) have intermediate infection abilities, and the chimera with IE in the structural and the 3' UTR (IE-IE) actually had the lowest rate of infection. This suggests that there is a synergistic effect between the 3' UTR and other parts of the genome. This likely warrants further examination and in the future should be evaluated with 3'UTR-specific chimeras such as a IAB virus backbone with a IE derived 3'UTR and a virus with a IE backbone and a IAB derived 3' UTR. It

was surprising to see that the chimera with the IAB 3' UTR infected mosquitoes more readily than the mismatched chimera with the IE 3' UTR. While the role of these regions was not mimicked in the *in vitro* mosquito infection and replication study, our C6/36 data was based on cells from *Ae. albopictus*, which in laboratory experiments has been shown to be equally competent for epizootic IC and enzootic ID VEEV strains [196]. Previous studies examining chimeras between Ross river virus (RRV) and Sindbis virus (SINV), two genetically distant alphaviruses, have shown that mismatched 3' UTR regions can result in depressed RNA synthesis *in vitro*, although the effects on replication *in vivo* have not been examined [170]. Examination of alphavirus vaccine candidate made from distantly related chimeras have repeatedly shown that chimerization has an attenuating affect on viral replication in model mosquito vectors [197-199]. However, studies of chimeras between more closely related alphaviruses, such as o'nyong-nyong (ONNV) and chikungunya (CHIKV) viruses, indicate that chimerization does not have a deleterious affect on the infection of the CHIKV mosquito vector, *Ae. aegypti*, there was also no indication that mismatched 3' UTRs increased infection rates [200].

There were no statistical differences in the infection rates between chimeras IAB/IE, IAB/IE/IAB, and IE/IAB/IE, indicating that both the structural and nonstructural protein regions of the enzootic virus play a role in vector competence. However, I observed a trend in which the two chimeras with IE derived nonstructural regions showed higher rates of infection at higher doses. Specifically, the chimeras with IE derived structural were shown to reach 100% infection at the highest doses, while the chimeras

with IAB derived nonstructural regions were unable to reach 100% infection at the highest exposure doses. The diminished, yet not ablated infection for all chimeras, implies that there are likely multiple important determinants for infection that reside in different regions of the genome that may act synergistically with other regions of the genome. My conclusions support the hypothesis that infection determinants for VEEV in the enzootic mosquito vector differ from those of an epizootic vector. These findings have important implications for future vaccine development of live attenuated vaccines. Considering that the determinants for infection appear to differ between the two vector types, vaccine strains that are derived from epizootic VEEV and depend the ablation of potential mosquito infection and dissemination may not necessarily reflect how effective these vaccine candidates would be if exposed to enzootic vectors. Similarly, vaccine candidates based on enzootic strains need to be evaluated in both vector types, and not solely on epizootic vectors to ensure that genetically engineered VEEV strains are unable to persist in enzootic cycles. Recent emergence of IE epizootic strains that do cause disease in horses and are able to efficiently infect and be transmitted by the primary enzootic and epizootic mosquito vectors illustrates the importance of considering the determinants of vector infection. A vaccine generated against these strains would need to be examined for its ability to infect and replicate in both vectors to prevent accidental introduction into the natural cycle.

CHAPTER 4: CHARACTERIZING THE MIDGUT INFECTION OF *CULEX TAENIOPUS*

BACKGROUND

Epizootic strains of mosquito-borne Venezuelan equine encephalitis virus (VEEV) have a long history of causing severe disease and death in equids and humans of South America, Central America, and Mexico. Enzootic viral strains are distinct from those of the epizootic cycle in that they utilize a different set of insect vectors and do not typically cause apparent disease in equids. Recent findings, however, indicate the human disease burden of enzootic VEEV is likely higher than previously recognized, which incriminates enzootic VEEV as an important public health threat [162]. When a mosquito imbibes an infectious blood meal, virions are taken in through the proboscis, travel through the esophagus and alimentary canal, and settle within the mesenteron or midgut. Although the greatest mass of the blood meal resides in the posterior midgut, the initial sites of virion infection can vary depending on the virus. Studies of epizootic VEEV, EEEV, RVF, and yellow fever virus (YFV), have shown that these viruses have a proclivity to initiate infection in the cardiac epithelium of the anterior midgut as well as sites in the posterior midgut [133,151,153,201]. Interestingly, WEEV was rarely found to infect the anterior midgut portions in its enzootic vector, *Cx. tarsalis* [154]. Similarly, enzootic VEEV has not been shown to initially infect sites other than the posterior midgut.

The highly specific vector competence exclusivity between enzootic and epizootic strains has been documented repeatedly [102,106-108,202,203], although the mechanisms for this exclusivity has yet to be explained. This exclusivity is particularly pronounced for *Cx. taeniopus*, which appears uniquely susceptible to IE VEEV strains [108,139]. While multiple hypotheses have been presented to explain why one mosquito would be susceptible to only one VEEV subtype, but remain refractory to another, the explanation with the most support predicts that selective infection is due to different characteristics of highly specific receptor sites on the insect midgut epithelial cells that may account for the dissimilar infection capabilities [138,141,204,205]. This theory has been supported by directly comparing binding capabilities of both WEEV and VEEV strains in susceptible and refractory mosquito species [141,161]. For VEEV specifically, it has been shown that the binding of enzootic IE VEEV particles is significantly lower than that of an epizootic IC VEEV strain in an epizootic mosquito vector, *Ae. taeniorhynchus*.

Further examination of the infection of an epizootic mosquito vector, *Ae. taeniorhynchus*, has indicated that there is only a small population of susceptible cells in this vector and thus the midgut infection is initiated by a very small number of infected cells [161]. Evolutionary theory would suggest that a restriction in replicating viral genomes might deleteriously affect the fitness of the population through founder's effect and Muller's ratchet [206-209]. The founder's effect is the loss of genetic heterogeneity that occurs as a result of a genetic bottleneck. Muller's ratchet occurs as a result of

accumulation of deleterious mutations as a result of repeated bottlenecks and a high mutation rate. Eventually the mutation-free individuals are lost through genetic drift and the population fitness loss is irreversible. Mosquito midgut infections that are only initiated by a small population of viruses are susceptible to both of these factors. However, this population restriction in *Ae. taeniorhynchus* might also allow for epizootic strains to repair the fitness damage through recombination events [161]. This is a plausible strategy for an epizootic virus, which only interacts transiently with its mosquito vector during outbreak events. During an epizootic there is an abundance of vector mosquitoes that are being exposed to large sources of high titer blood meals, so even if only a small proportion of mosquitoes are infected with a viable population, they are still able to perpetuate the outbreak. However, for the enzootic strain, which needs to maintain a certain level of fitness to persist in nature over centuries or longer, such a genetic restriction would likely be highly deleterious. Previous examination of enzootic VEEV infection of *Cx. taeniopus* reports observing a large number of virions in the posterior midgut prior to advancing beyond the mesenteron [109], indicating that enzootic infection of the mosquito is initiated by more than a few cells. Given these findings and the likely deleterious effects of a restriction in viral population size on viral fitness, I hypothesized that all midgut epithelial cells in *Cx. taeniopus* are equally susceptible and, therefore, the population of enzootic VEEV virions that infect the midgut epithelium does not undergo a population restriction during infection of the midgut. Similarly, I expected to observe only portions of the posterior midgut initially infected,

and wanted to establish if there is any particular region of the posterior midgut in which the virions converged.

MATERIALS AND METHODS

Cells and replicon particles

Vero cells were utilized for replicon titration and BHK-21 cells were utilized for electroporation and virus-like particle (VLP) rescue. Cells from an *Ae. albopictus* mosquito cell line, C6/36, were utilized for co-infection experiments. Specifically designed, replication deficient VLPs, were utilized to analyze the initial sites of infection without the complication of cell-to-cell spread. These deficient particles, also referred to as replicon particles, are generated by electroporating two RNA species simultaneously into cells. The first RNA, the replicon, consists of the nonstructural open reading frame expressing a fluorescent reporter and associated *cis*-acting elements. The second RNA species, or helper, contains the structural portions of the genome (figure 4-1). Co-electroporation of these two species generates deficient particles that are unable to

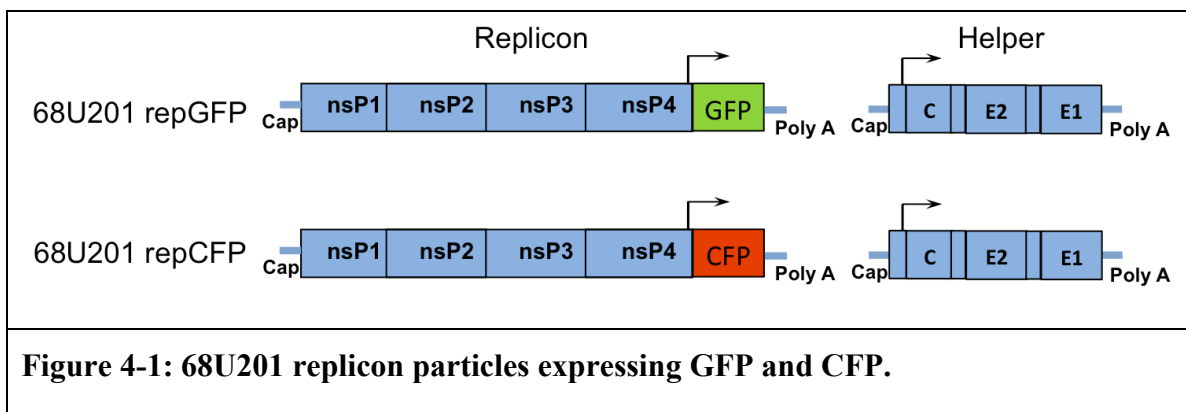


Figure 4-1: 68U201 replicon particles expressing GFP and CFP.

package the structural genes, but continue to express only the nonstructural genes packaged into the particle. For this study, the two IE 68U201 replicons were derived from a full length IE 68U201 clone (described in chapter two). The IE 68U201 viral isolate had been passaged once in newborn mice and twice in BHK-21 cells prior to generation of the cDNA clone [171]. Replicons and helpers were transcribed using a T7 mMessage mMachine® (Ambion, Austin, Texas) and electroporated into BHK-21 cells (as described in chapter 2). Electroporated replicons were harvested after 24 hours.

Replicon titration

Replicon titration is done in a similar fashion to the plaque assay method for replicating virus, with the primary exception that these virions do not produce plaques, but instead express fluorescent particles in the single cells that they infect. To titer each stock, ten-fold serial-dilutions were plated on a monolayer of Vero cells and allowed to incubate for one hour prior to an overlay with DMEM media complete with 5% FBS, gentamycin, and penicillin. After 24 hours, the medium was removed and the monolayer was fixed with 4% paraformaldehyde (PFA) (Affymetrix, Santa Clara, CA) for one hour. The number of fluorescent cells per well was counted using an Olympus Is71 inverted fluorescent microscope using filters for DAPI 360/340, FITC 488/520, and TRITC 566/600, and reported as fluorescing units (FU).

In vitro infection control

In order to establish the probability of the proportion of mosquito cells that can be dually infected by 68U201 replicons, an *in vitro* *Ae. albopictus* (C6/36) cell line was utilized as a control. C6/36 cells were maintained in DMEM supplemented with 10% FBS, 1% TPB, gentamycin, and penicillin. For each infection, a C6/36 cell monolayer in a 25cm² flask was infected at an MOI of 5 FU/cell. For the dual infection, 68U201 GFP and 68U201 CFP were mixed 1:1 and the infection was allowed to incubate for 24 hours prior to fixation with 4% PFA and analysis.

Tail vein inoculations

Cx. taeniopus mosquitoes are notoriously difficult to maintain and manipulate in a laboratory, as they will not, under any circumstance, imbibe a blood meal from an artificial membrane feeder (see chapter 3). Traditionally, this has been managed by using a viremic animal to expose mosquitoes to virus. However, since the replicon particles utilized for this study do not replicate beyond the initial cell infected, I utilized an artificial viremia system in which I inoculated an animal intravenously allowing for an immediate circulation of the virus particles in the blood stream. An intravenous model in birds specifically for mosquito infection has been described previously [151]. Since *Cx. taeniopus* had already been shown to feed on CD1 mice [106] and CD1 mice have a small blood volume that would minimize the dilution of the injected virus particles, I decided to utilize this model. I quickly determined that injecting virus particles into a

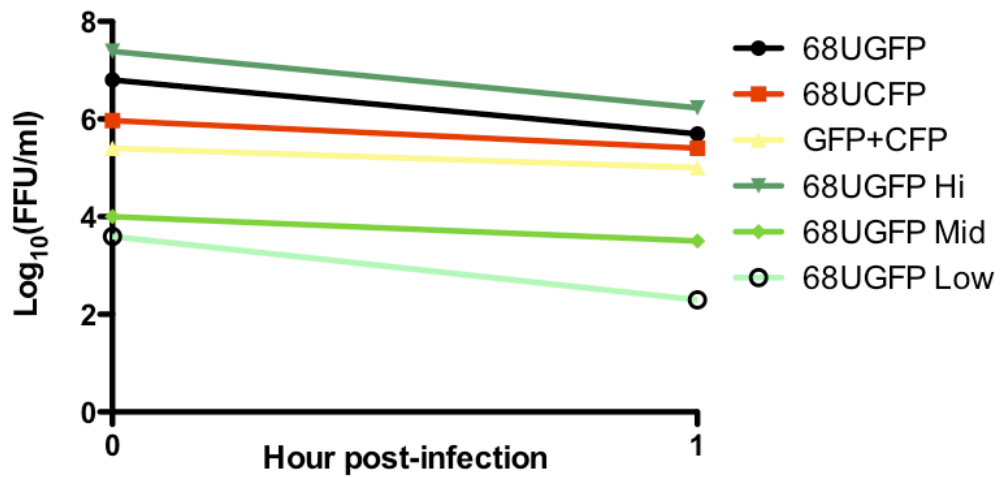
murine tail vein is challenging and required many trials in order to become consistently successful and to perform the experiments safely. The basic technique consisted of restraining a mouse in an apparatus designed to expose the tail and allow access to the vein. Initially, injection attempts started nearer to the tip of the tail and moved up towards the base of the tail if more attempts are required. If necessary, a second tail-vein was utilized. Then, using a small gauge needle, fluid was directly inoculated into the tail vein. Before I perfected this technique, I experimented with the restraining apparatus, anesthesia of the mouse, gauge of the needle, size of the syringe, various vasodilation techniques, and I added Evans blue to the virus mixture in an attempt to aid verification of the injection into the vein.

Mosquito exposure

Oral exposure experiments were performed with an artificial viremia of CD1 mice (Charles River, Wilmington, MA). Mice utilized for the artificial viremic exposure were anesthetized by IP inoculation of 50 mg/kg sodium pentobarbital (about .04 ml. per 10-week-old female mouse), and 200 μ l of a stock replicon or 1:1 mix of replicons was inoculated into the tail-vein of the animal. Particles were allowed to circulate for 1-2 minutes before blood was collected from the retro-orbital sinus to estimate the artificial viremia level achieved, and the animal was then exposed to the mosquitoes. Mosquitoes were allowed to feed for ca. one hour after which blood was collected again from the retro-orbital sinus to detect any loss of circulating replicon concentration (figure 4-2).

Midgut dissection and processing

Cx. taeniopus mosquitoes have visible, intact red blood cells in their midgut for up to 72 hours following a blood meal. Therefore, mosquito samples were not processed until 72 after the initial intake of blood to minimize chances of damaging the midgut and to allow for clear images of the midgut epithelia. At the time of processing, mosquitoes were cold anesthetized, and submerged for 30 seconds to 1 minute in 70% EtOH prior to being transferred to a PBS solution. Midguts were extracted with the assistance of a



	Pre-Titer (FFU)	Post-Titer (FFU)	Average Titer
68UGFP	6.8	5.7	6.2
68UCFP	6	5.4	5.7
68UGFP + CFP	5.4	5	5.2
68UGFP Hi	7.4	6.2	6.8
68UGFP Mid	4	3.5	3.7
68UGFP Low	3.6	2.3	2.9

Figure 4-2: Change in circulating artificial viremia

The observed drop in titer ranged from 0.3 – 1.3 log₁₀ PFU/ml for 68U201 replicons.

dissecting microscope and covered with a drop of 4% PFA on a glass slide. As GFP is very sensitive to light, samples were protected from light as much as possible. Each midgut was allowed to incubate for 30 minutes and was rinsed twice with PBS before the addition of ProLong® Gold Antifade with 4',6-diamidino-2-phenylindole (DAPI) (Invitrogen, Carlsbad, CA) as a nuclear counterstain. Slides were carefully overlain with a glass coverslip and stored in a dark place overnight.

Microscopy

Mosquito midgut samples were analyzed on an Olympus BX61 fluorescent microscope and high-resolution images were taken on an Olympus FluoView FV1000MPE confocal microscope. Fluorescent cell counting was aided using Image J software. *In vitro* dual infection experiments were visualized on an Olympus DSU-IX81 spinning disk confocal microscope and analyzed with MetaMorph® Software (Molecular Devices, Sunnyvale, CA). All microscopy analysis was performed using filters for DAPI 360/340, FITC 488/520, and TRITC 566/600,

RESULTS

Tail vein inoculations

For initial attempts to inoculate into a mouse tail-vein, I did not anesthetize the animal and quickly came to the conclusion that this method was potentially unsafe. Even though the animal was restrained, it still made jerking movements of its tail, which

greatly increased the risk of an accidental needle stick. I therefore acquired a Tailveiner® (Braintree Scientific Inc., Braintree, MA) restraining apparatus, and a cylindrical adapter to hold the tail to the side and to isolate my fingers away from the needle (figure 4-3). I used a cylinder of approximately 2 inches in diameter and taped it to the surface of the biosafety cabinet to keep it stable. Additionally, by using the cylinder I minimized the angle of the needle entry by raising the tail, which drastically improved the accuracy of the inoculation.

Initially, I found it difficult to determine whether the inoculum had gone into the vein or not. Therefore, Evans blue dye was utilized to enhance visualization of the inoculum in the vasculature. Prior to experimental injections, Evans blue was included at various dilutions within plaque assays of TC83 to determine whether it had a detrimental affect on viral replication and no effect was observed. Evans blue turned out to be a valuable tool for perfecting the technique, although once I had successfully inoculated into the tail-vein a few times, the dye was no longer necessary. I also examined multiple tail-vein vasodilation techniques including topical Methyl salicylate and various heating methods such as a heating lamp placed near the tail, submersion of the tail in warm water, a heating pad, and manual warming. The most successful technique for vasodilation was determined to be use of the heating lamp for approximately 45 seconds. I held my gloved hand adjacent to the tail during the heating process to assure the temperature generated was safe for the anesthetized mouse.

I tried various gauge needles and syringes while attempting to refine the tail-vein inoculation technique. Initially, using a 1ml. syringe and a 26 gauge, 3/8-inch needle, I had inconsistent success. I observed many cases in which the full volume of the inoculum could not be injected even after the needle had clearly entered the vein at the start of the inoculation. I tried a 28½ gauge, 1/2 –inch needle with a ½ ml syringe to reduce the pressure of the injection on the vein and found significantly more success utilizing this size needle and syringe. . In summary, I determined the preferred injection conditions to include a proper restrainer, an anesthetized animal, a stabilized cylindrical adapter, a heat lamp, and a 28.5 gauge, ½-inch needle with a ½ ml syringe.

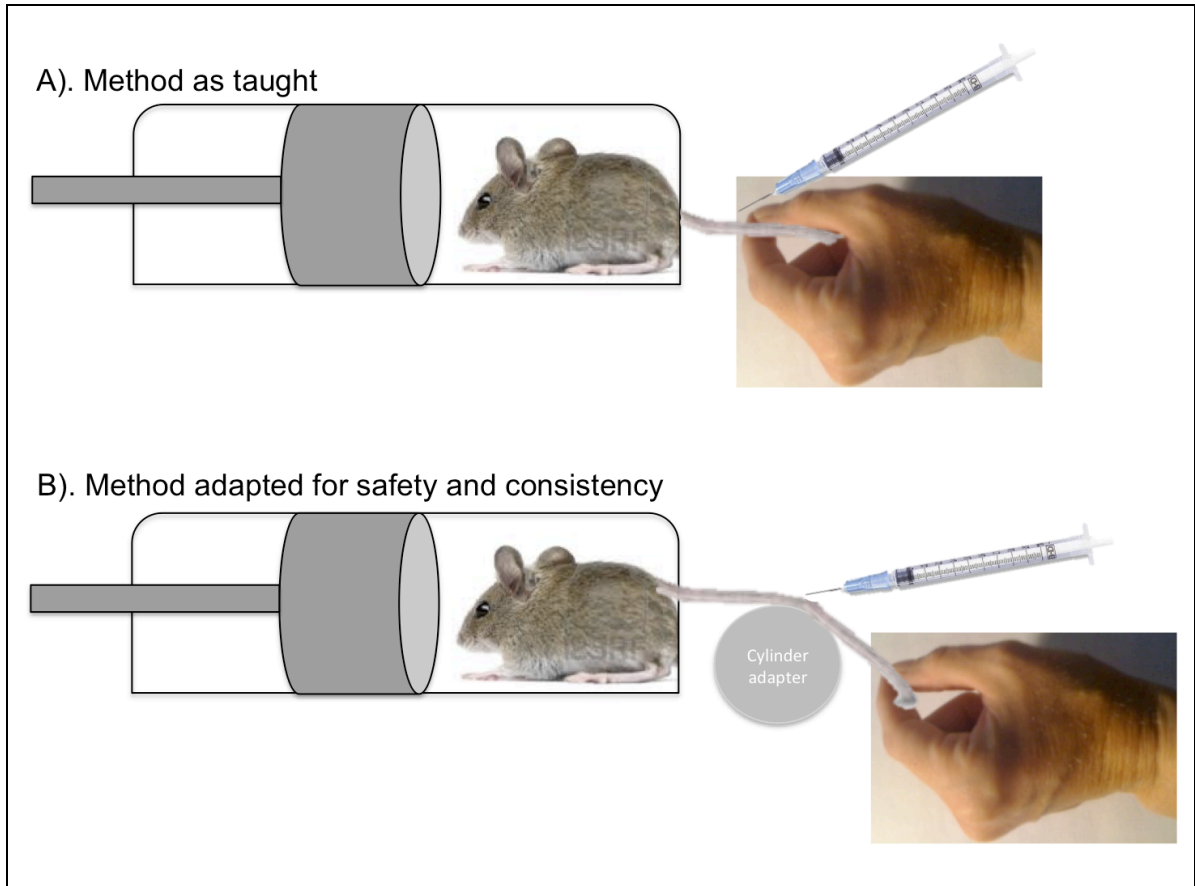


Figure 4-3: Adapted tail-vein inoculation technique

Panel A) represents the technique as I was taught by the UTMB Animal Resources Center. This technique requires your fingers under the tail directly adjacent to where the needle will be inserted and poses significant safety risks. Panel B) represents my adaptation in which, I stabilized a cylinder (something with approximately a 2 inch diameter) with tape and use it as a support for injecting the tail while keeping my fingers far away from the tip of the needle.

***Cx. taeniopus* midgut infection**

Cx. taeniopus mosquitoes were exposed to a range of doses of 68U201 replicon particles expressing fluorescent protein to observe the number of cells initially infected, the location of infected cells, and to determine whether there is a subpopulation of cells within the midgut that is more susceptible than other epithelial cells. For the single replicon infections, a clear dose-response was observed such that the lowest exposure dose (average of pre- and post- exposure titers) of 3.0 log₁₀ FU/ml infected only 11% of examined midguts with only 1-2 cells infected, whereas the highest dose 7.2 log₁₀ FU/ml infected 100% of examined midguts (range 535-1757 infected cells) (Table 4-1).

Although infected cells were not limited to any particular region of the abdominal midgut, only a minority of the midguts (9%) were found to have infection focused in the posterior portion, whereas 25% of all infected midguts showed a focused infection in the anterior portion of the abdominal midgut. The remaining 66% of infected midguts showed a mixed infection with concentrated infection within the middle portion of abdominal midgut (figure 4-4). Infection of midgut/foregut junction of the midgut was not observed.

Replicon Group	# midguts examined	Average exp titer (FFU)	# infected midguts(%)	# cells infected	Ave # cells infected	Primary location
68UGFP	9	3	1/9 (11)	1-2	na	Mixed
68UGFP	13	3.76	10/13 (77)	3-21	6	Mixed
68UGFP	4	6.79	4/4 (100)	50 - 323	130	Mixed
68UGFP	8	6.81	8/8 (100)	27 - 393	128	Mixed
68UGFP	10	7.2	10/10 (100)	535-1757	1012	Mixed

Table 4-1: Infection and location within *Cx. taeniopus* midgut

***Cx. taeniopus* midgut epithelial susceptibility**

In vitro dual replicon infection

Monolayers of *Ae. albopictus* C6/36 cells were infected with either 68UGFP, 68UCFP or a 1:1 mix of 68UGFP and 68UCFP at a mixed MOI of 0.01 in order to estimate the number of expected co-infected cells. In a sample of multiple areas containing an average of 250,000 C6/36 cells, a total of four cells were co-infected (table 4-2). Utilizing this observed proportion to generate an estimated co-infection in the *in vivo* mosquito model yields a probability of .000015, or less than one cell in a midgut of ca. 10,000 cells.

Dual infection of *Cx. taeniopus*

Cx. taeniopus mosquitoes were orally infected with a 1:1 mixture of 68UGFP and 68UCFP to determine if there was a differential susceptibility of certain midgut cells. In all 15 mosquitoes each were examined for co-infection at two different doses. The low

exposure dose achieved by artificial viremia was a mixture of 5.4 log FU/ml 68UGFP and 5.0 log FU/ml of 68UCFP and the high dose achieved was 6.5 log FU/ml of each replicon. At the low dose an average of 70 midgut epithelial cells were infected with 68UGFP and an average of 52 cells

Label	Midgut (at max dose)	C6/36 cells
GFP	896	2293
CFP	866	1806
Co-expression	<1	4

Table 4-2: Dual infection *in vivo* and *in vitro*

were infected with 68UCFP. At the high dose, an average number of cells infected with 68UGFP was 896 whereas the average number of 68UCFP infected cells was 866. At the low dose, of the five co-exposed mosquitoes examined, no co-infected cells were observed (table 4-2). At the high dose, there were a few cells with co-localization, although it was difficult to tell whether they were truly co-infected or signal bleed-through or overlap (figure 4-5). Even conservatively including these cells as co-infected, there was still an average of less than one observed co-infected cell per midgut in the highest dose group, indicating there is no subset of susceptible midgut epithelial cells.

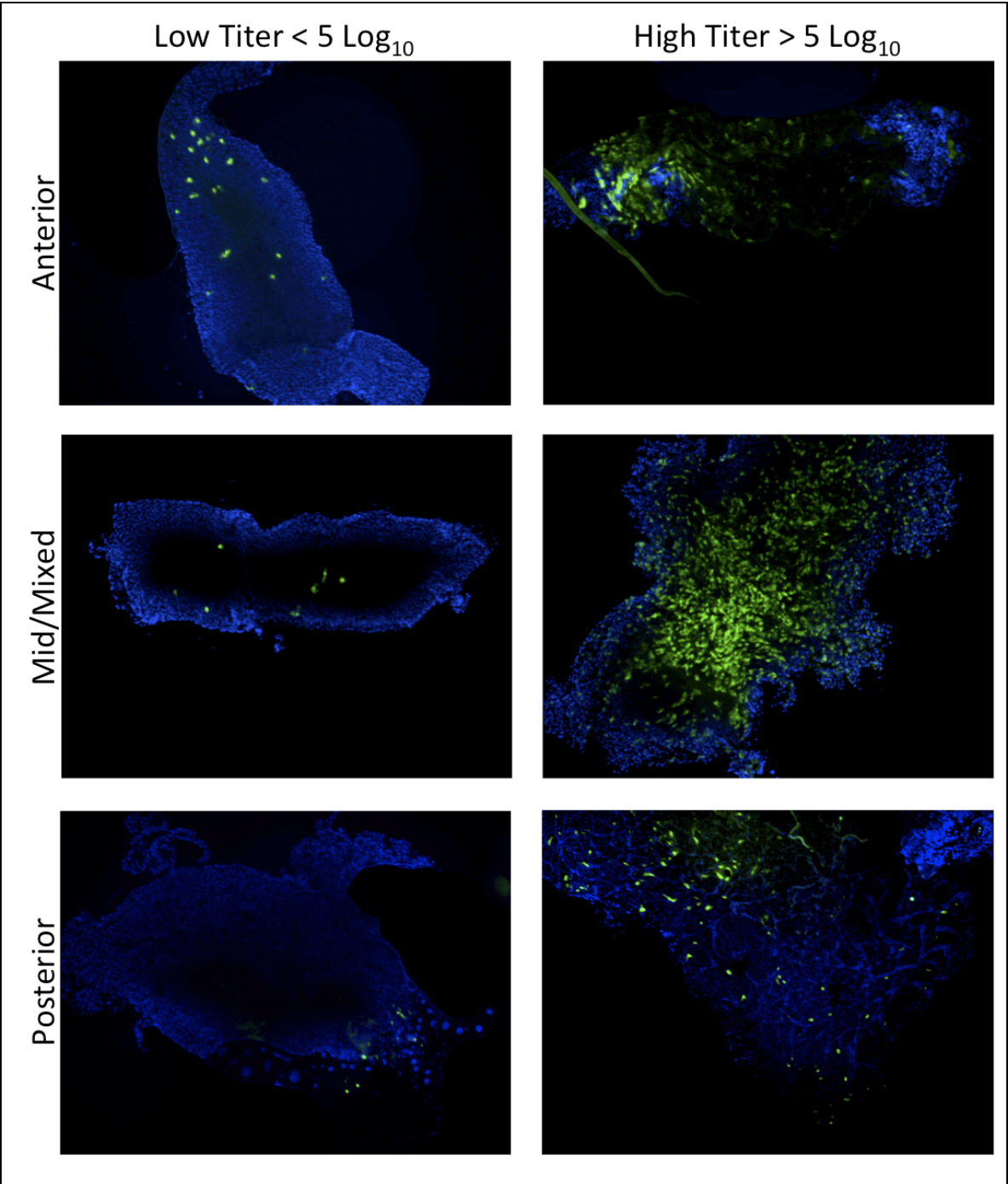


Figure 4-4: Sites of 68UGFP midgut infection (10x)

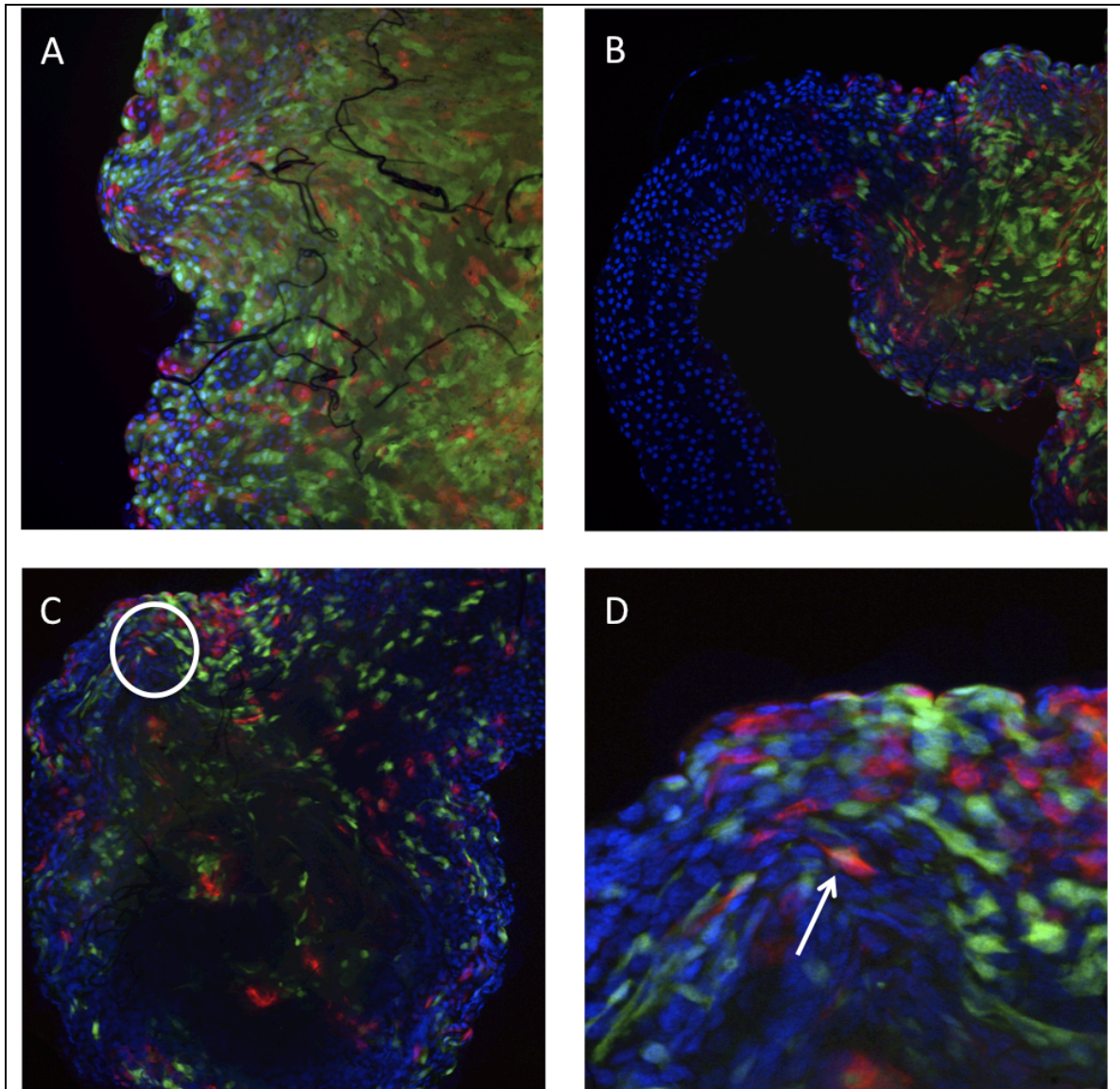


Figure 4-5: Examples of dual 68U201 replicon infection

Characteristic confocal microscopic images (20x) showing a lack of co-infection in (A)

posterior and (B) anterior midgut regions of *Cx. taeniopus*. (C) A suspected co-infected cell that when enlarged was determined to be signal overlap of two different cells (D).

CONCLUSIONS AND SUMMARY

The purpose of these experiments was to characterize the initial sites of infection and determine whether the *Cx. taeniopus* midgut epithelium has a limited population of susceptible cells to enzootic VEEV. Studies of the initial exposure of a IC epizootic VEEV strain in *Ae. taeniorhynchus* indicate that very few cells, less than 10, are responsible for establishing infection and that only approximately 100 midgut epithelial cells within the epizootic vector midgut are susceptible [161]. This, in effect, limits the heterogeneity of the genomes and potentially could deleteriously affect fitness of the VEEV population. Such a limitation may not be significant for the transient appearance of epizootic virus, which only emerges and replicates in vectors during an outbreak, but has larger implications for the enzootic virus, which must maintain a constant state of fitness to persist in nature over centuries or longer. Therefore, I hypothesized, that enzootic virus must avoid a reduction in intra-host variability that could potentially diminish fitness, and therefore no distinct, uniquely susceptible population of midgut epithelial cells would be observed.

To test this hypothesis, I exposed a primary enzootic mosquito vector, *Cx. taeniopus* to replicon particles generated from a characteristic IE enzootic virus, 68U201. Since replicon particles are deficient virions, I used an artificial viremia system in which CD1 mice were inoculated intravenously and presented to the starved mosquitoes.

Refinement of the infection method allowed for a safer and a more standardized technique that resulted in consistent and repeatable infection in all groups.

Electron microscopy studies of VEEV infection of *Cx. taeniopus* have shown that within one hour of exposure virion particles can be observed in the basal portions of the midgut, indicating that the abdominal midgut is likely the first site of infection [109]. My examination of the sites of infection of IE VEEV in the *Cx. taeniopus* midgut indicates that initial infection can occur in multiple locations of the abdominal midgut and has no predilection for either the anterior or the posterior region of the abdominal midgut, but does not initially infect portions of the anterior midgut. Similarly to what was observed in *Ae. taeniorhynchus*, a clear dose response was observed between the exposure dose and the number of midgut cells infected, although the ID₅₀ for *Cx. taeniopus* was lower and the maximal number of observed *Cx. taeniopus* infected cells was higher than the predicted 100 susceptible *Ae. taeniorhynchus* cells (figure 4-6) [161]. The infection rate of replicating 68U201 virus required to achieve 50% disseminated infection in *Cx. taeniopus* was determined to be approximately 4.4 log₁₀ PFU/ml, whereas 50% disseminated infection of IC VEEV in *Ae. taeniorhynchus* was achieved with 5 log₁₀ PFU/ml [161]. The greater number of observed infected cells (>1700) in *Cx. taeniopus* following high exposure doses indicates that a higher number of *Cx. taeniopus* midgut epithelial cells are susceptible to VEEV-IE infection than *Ae. taeniorhynchus* midgut epithelial cells susceptible to VEEV-IC.

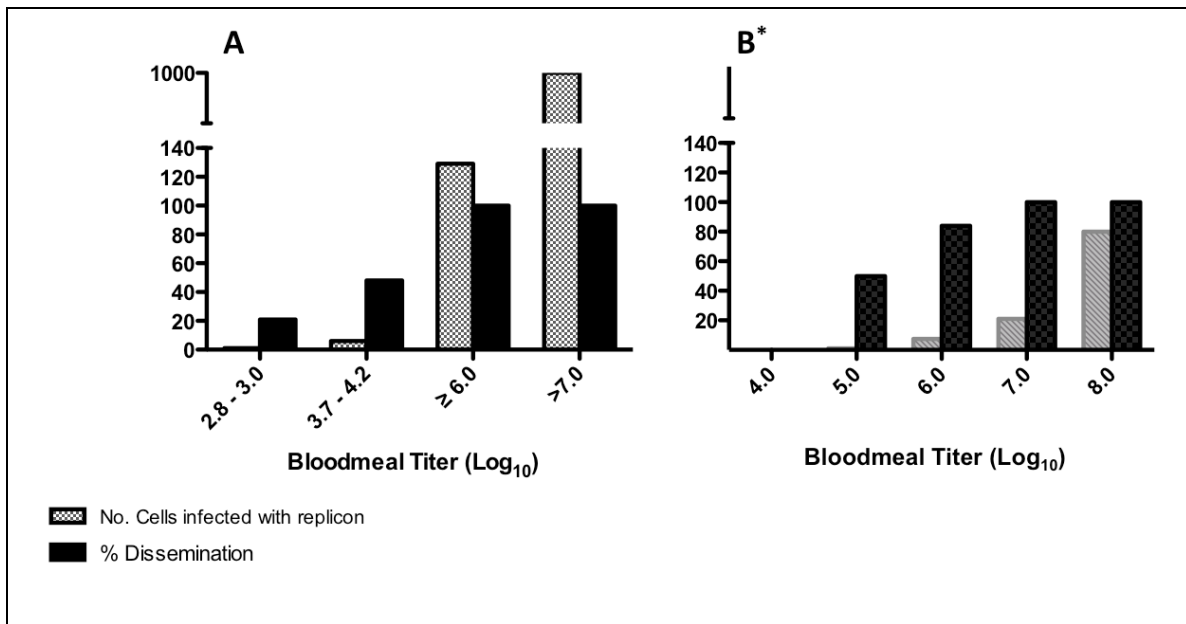


Figure 4-6: Dose response of *Cx. taeniopus* compared to *Ae. taeniorhynchus*

Comparison of the number of cells infected by replicons and the corresponding dissemination rates of wild type virus at each dose for A) *Cx. taeniopus* and IE 68U201 virus and B) *Ae. taeniorhynchus* and IC 3908 (* Graph adapted from Smith et al. 2008 [161])

This observation, in conjunction with my observation of no co-infected midgut cells in any mixed replicon experiments supports the hypothesis that the population of enzootic VEEV virions is not restricted by a limited number of susceptible *Cx. taeniopus* epithelial cells. It was also determined that the average population of cells infected by a single 68UGFP replicon at the highest dose did not differ from the average number of cells singly infected when exposed to the same dose of that replicon in the presence of the 68UCFP replicon. The same was true for the proportion of singly infected 68UCFP cells when infected in the presence of the GFP replicon. This suggests that there is no

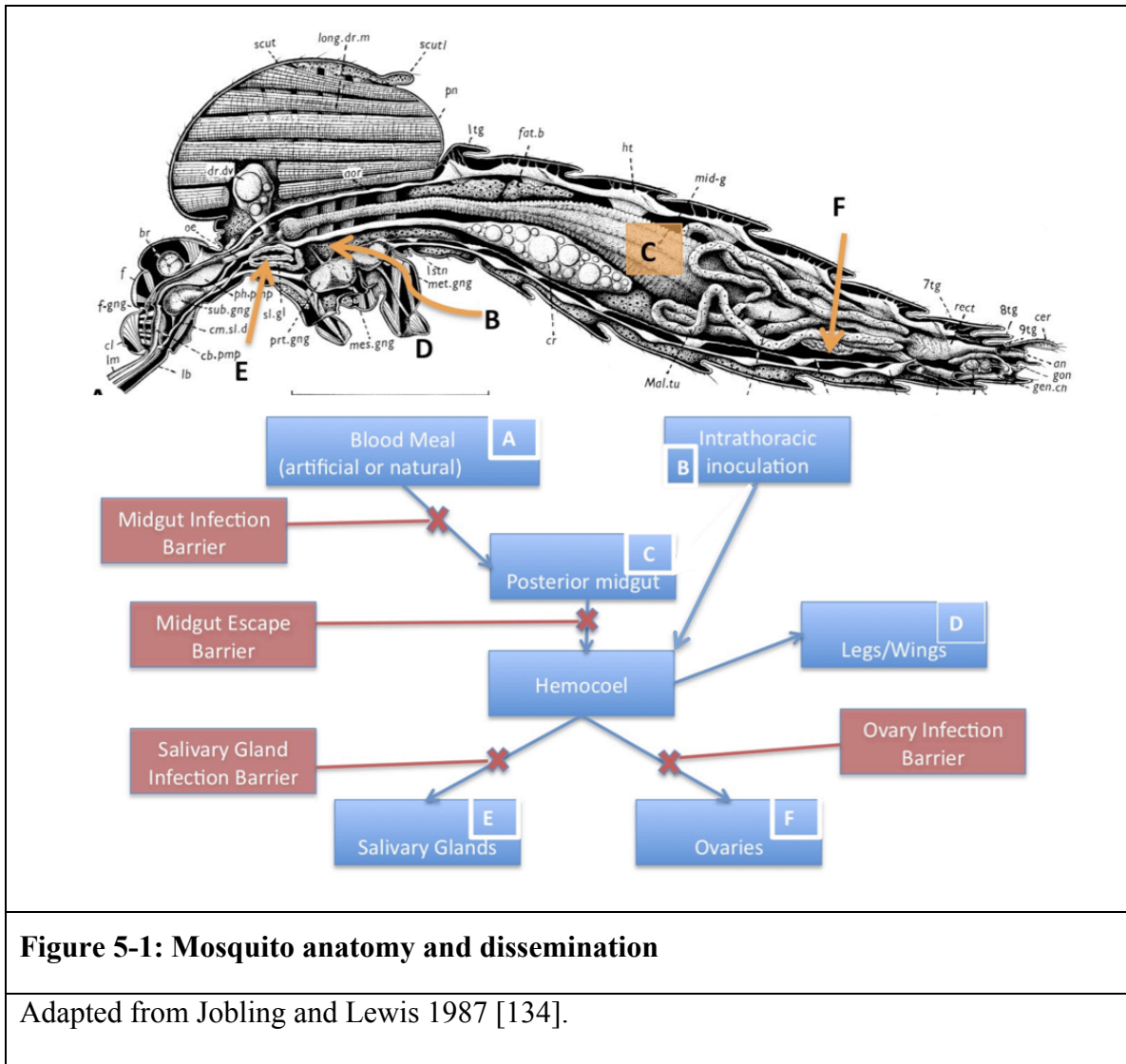
interference between replicons affecting the proportion of single replicon infection. Previous studies in an epizootic VEEV/mosquito model, found an average of 26 midgut cells co-infected utilizing this method, which is greater than what I observed in the enzootic model indicating the initial infection of the enzootic vector is different than that of epizootic model. Using the Poisson distribution and given the historical epizootic model (a model with a small population of susceptible cells) probabilities, I determined the probability of observing less than a single co-infected cell out of the five midgut replicates to be $5.1 \times 10^{(-12)}$, indicating an extremely low likelihood that there is a subpopulation of midgut epithelial cells with an enhanced susceptibility in the enzootic model. These studies illustrate the contrast between enzootic and epizootic VEEV strains. Not only do they persist in different ecological cycles and primarily infect different species of mosquitoes, but also they behave differently within their respective vector hosts. As the growing impact of enzootic VEEV on human health is becoming more apparent in addition to the recent emergence of epizootic-like IE strains, understanding how these viruses interact with competent vectors is critical to estimating their threat to human health and allow for design of more refined public health control and prevention strategies as well as yield valuable insights for VEEV vaccine development. For instance, the design strategy of a vaccine that is protective against epizootic and enzootic strains that are currently causing human disease must also consider potential susceptible mosquito vectors that could potentially acquire and transmit a vaccine should a vaccinee become viremic. If the epizootic vector only has a few susceptible midgut cells and is

examined for competence of a given vaccine strain, it may appear to be incompetent. However, the same vaccine may be able to establish an infection in the enzootic vector and this needs to be evaluated and considered. Understanding the characteristics of infection for both epizootic and enzootic mosquito vectors, could enhance the design of such a vaccine.

CHAPTER 5: MIDGUT ESCAPE OF ENZOOTIC SUBTYPE IE VEEV IN CULEX TAENIOPUS

INTRODUCTION

The interaction between arbovirus and its mosquito vector is highly complex and a complex series of events must occur before a mosquito can transmit the virus to susceptible hosts. The mosquito alimentary canal can be generally divided into four regions, foregut, thoracic or anterior midgut, abdominal or posterior midgut, and the hindgut (figure 5-1). The anterior portion of the midgut includes the midgut/foregut junction characterized by the intussuscepted foregut, cardial midgut, and dorsal and ventral diverticula. The majority of ingested blood is drawn into the posterior midgut epithelium, which is believed to be the primary site of initial infection for many alphaviruses [109,151,210-212]. The hindgut region includes the malpighian tubules, hindgut, and rectum and has not been shown to be important for alphavirus dissemination. When an infectious blood meal is imbibed, virus must initially infect cells within the midgut and this is a highly specific process. Although the particular mechanisms have yet to be elaborated, many studies have indicated that the initial midgut infection barrier is due to binding specificity to a receptor in the midgut epithelium. This highly specific interaction



has been demonstrated with a single WEEV strain's differential binding affinity to the midgut epithelium of a known susceptible and refractory strain of *Cx. tarsalis* mosquitoes [141], as well as the binding differences between epizootic and enzootic VEEV strains to the midgut epithelium of the same strain of the epizootic vector, *Ae. taeniorhynchus*

[161]. Although there have been a few documented instances of identification of virion escape from the midgut prior to replication, due to a leaky midgut [109,144,213], the majority of studies indicate that alphaviruses replicate within the alimentary canal prior to escape to the hemocoel for systematic spread. How virus manages to escape from the midgut epithelium and penetrate or circumvent the basal lamina has been a topic of much study. The basal lamina of the mosquito midgut is described as comprised of four to seven stacked layers [148] that form a grid-like structure with pores ranging from 70-100 angstroms (Å) [147]; however the number and thickness of these layers varies throughout the gonotrophic cycle [147]. Reddy and Locke tested the permeability of the basal lamina with gold particles and found that no particle larger than 15nm was able to permeate [143]. Since an alphavirus is approximately 70nm in diameter [2], it is logical to conclude that an alphavirus would also not be able to pass through the basal lamina. However, there have been several descriptions of virus “leaks” from the midgut [109,144,151,204], which may be due to structural changes occurring in the midgut epithelium and surrounding basal lamina due to stress on tissues from engorgement or leaks caused directly by cytopathology effects from virus [149,150].

Another identified pathway of escape is through the foregut/midgut junction. In some cases, ingested blood may be diverted to the ventral diverticulum during feeding and later regurgitated back into the anterior midgut at the site of the intussuscepted foregut. If the virus infects at this site and spreads cell-to-cell through it can bypass the basal lamina of the midgut and chitinous intima that lines the foregut to gain access to the

hemocoel [133]. This has been observed to be an important route of dissemination has been observed for multiple encephalitic alphaviruses [151-154].

Whataroa virus, an alphavirus found in New Zealand, has been described to have a proclivity towards infection of insect nervous tissue in experimental laboratory models. Studies indicate that this virus replicates in the mosquito central nervous system prior to replication within the salivary glands, although these studies were done in a model not demonstrated to be ecologically relevant and with a very low incubation temperature (20°C) [144]. Similarly, to date, there has been no other description of an alphavirus utilizing this route of dissemination.

One characteristic of New World alphaviruses that has been repeatedly documented is their rapid rates of dissemination, particularly enzootic mosquito vector models such as EEEV with *Cs. melanura* and VEEV with *Cx. taeniopus* [109,210]. This expeditious spread within the mosquito lends credence to another proposed mechanism of dissemination in which the virus utilizes the established network of tracheae to spread to various organs within the mosquito. The tracheae system is analogous to mammalian branching bronchioles that maximize gas exchange within the lung. Tracheae are gas filled tubes lined with chitin that bifurcate to smaller and smaller branches as they permeate tissues. They initiate at an external pore called a spiracle and deliver oxygen to insect tissues [132]. The finest branches of this system are small enough to permeate individual cells and are referred to as tracheoles. They have been found to penetrate the basal lamina of many insect organs [135,136], and have been identified as sites of

secondary infection for many viruses, including VEEV [135,152,158-161,180,214].

Engelhard et al. proposed that infection of tracheoblasts provides a direct conduit for the virus to move from within a cell to the hemocoel without having to penetrate the basal lamina [158]. Whether enzootic VEEV utilizes the tracheae to disseminate throughout the mosquito has yet to be determined.

Previous electron microscopy work on enzootic VEEV indicated that this virus does not appear in the nerve ganglia until after the virus has been found in the salivary glands, indicating nervous tissues are not the likely pathways for dissemination. Similarly, no sloughing or cytopathology of the midgut epithelium was observed to indicate the presence of a leaky midgut by which the virus can escape. Interestingly, Weaver et al. did observe viral particles within the fat body within one hour of exposure, indicating that virus is escaping the midgut prior to replication [109]. This supports the hypothesis that virions may utilize a direct conduit from the midgut epithelium to other organs. Therefore, for this study, I proposed to identify the method by which enzootic VEEV disseminates within *Cx. taeniopus* mosquitoes. I hypothesized that IE VEEV virions use tracheae to spread throughout the mosquito. To examine this hypothesis, I infected *Cx. taeniopus* mosquitoes with an enzootic IE virus expressing a GFP reporter collected mosquitoes at multiple time points following exposure to observe the location and progression of virions by microscopy. I proposed to perform IT inoculations of replicon particles and 68UGFP to identify the initial cells infected following a hemocoel

inoculation, determine the sites of secondary infection, and resolve whether replicating virus can disseminate into the midgut lumen.

METHODS

Virus and cells

As described in previous chapters, VEEV IE 68U201 was the enzootic virus utilized for these studies. A full-length 68U201 virus expressing GFP (see chapter 2) was used for oral exposure and a 68U201 replicon particle expressing GFP (see chapters 2 and 4) was utilized for IT inoculation. Virus inoculum and back titers from viremic hosts were titered on Vero cells.

Oral infection of *Cx. taeniopus*

Viremic exposure

To develop a natural viremia, mice or hamsters were inoculated SC with 1000 plaque-forming units (PFU), held for 24 hours, and anesthetized by IP administration of sodium pentobarbital (50 mg/kg) immediately prior to mosquito exposure. Mice were bled from the retro-orbital sinus, and exposed to mosquitoes for approximately one hour.

Artificial viremia exposure

CD-1 mice utilized for the artificial viremic exposure were anesthetized by IP inoculation of 50 mg/kg sodium pentobarbital (ca. 0.04 ml per 10-week old mouse), and 200 µl of a stock virus was inoculated into the tail-vein of the animal (see chapter 4).

Virus was allowed to circulate for 5-10 minutes prior to collecting blood and exposing the animal to the mosquitoes. Mosquitoes were allowed to feed for ca. one hour after which, blood was collected from the animal again to detect any loss of circulating viral concentration.

Intrathoracic inoculation of *Cx. taeniopus*

A cohort of 50 adult females was subjected to intrathoracic inoculation of approximately 1 μ l of a strain 68U201 GFP stock or the replicon 68U201 repGFP. Mosquitoes were incubated at 27° C with a relative humidity of 70-75%.

Sampling and cryosectioning

Following exposure, 10 mosquitoes each were sampled at 12h, 24h, 36h, 48h, 60h, 72h, day 4, day 6, day 10, and day 14 for processing and analysis. At each time point, mosquitoes were cold-anesthetized and placed in 70% EtOH for 30 seconds to one minute before being transferred to a PBS solution. Each individual was placed in a drop of 4% PFA in a Tissue Tek cryomold (VWR, Radnor, PA) and legs and wings were removed before filling the cryomold with 4% PFA. Mosquitoes were submerged until they remained at the bottom of the mold and were stored protected from light at 4°C for 48 hours prior to removal from biosafety level three containment. At biosafety level two, mosquitoes were washed twice with PBS before being covered with Tissue Tek OCT compound (Fisher Scientific, Pittsburgh, PA). Mosquitoes were allowed to soak, protected from light, at 4°C overnight prior to being frozen on dry ice. Frozen blocks

were stored at -80 and held for cryosectioning. Four to six μm sections were cut using a Leica cryostat with a chamber temperature of - 23°C.

Fluorescent microscopy

Mosquito midgut samples were analyzed on an Olympus BX61 fluorescent microscope.

RESULTS

Intrathoracic exposure.

Unfortunately, all intrathoracic exposure attempts were unsuccessful, as our colony of *Cx. taeniopus* mosquitoes does not seem able to survive the procedure. This was surprising considering these type of inoculations had been performed on colonies of *Cx. taeniopus* mosquitoes in the past [110]. I systematically adjusted multiple variables, including the mosquito anesthesia method (cold versus CO₂), the physical inoculation method (microinjector versus manual injection), use of a dissecting microscope to improve precision of the inoculation site, and had other laboratory members try as well, but in the end I was unable to find a way to successfully inoculate these mosquitoes. Considering these troubles, I chose to focus on the oral exposure route for identifying the route of viral midgut escape.

Oral exposure.

Cx. taeniopus mosquitoes were initially exposed to mice viremic with VEEV strain 68U201 GFP and collected at multiple time points for cryosectioning and

microscopy. However, back titer of the viremic exposure dose showed an average exposure of $3.3 \log_{10}$ FU/ml, which indicates that either 68U201 GFP does not replicate well in mice or GFP expression is low. Regardless, that exposure dose is below the estimated ID50 to be for wild type 68U201 virus in this mosquito, so the exposure was repeated using an artificial viremia derived from a tail-vein inoculation of a 10-week old CD1 mouse. The artificial viremia resulted in an average exposure dose of $6.4 \log_{10}$ FU/ml, which is a dose previously shown (chapter 2) to infect all exposed *Cx. taeniopus* mosquitoes.

Dissemination.

Ten mosquitoes each were selected at 12h, 24h, 36h, 48h, 60h, 72h, 84h, d4, d6, d8, d10, and d14 for fixation and cryosectioning to evaluate the dissemination of the virus from the midgut into the hemocoel. Samples evaluated at 12h were not found to express any GFP, which is likely due to limited replication having occurred in the first 12 hours. By 24 and 36 hours, GFP could be observed in the epithelium layer of the posterior midgut. The same pattern of fluorescence was seen for hours 48 through day 4 and no regions outside of the abdominal midgut expressed GFP at levels above background (figure 5-2).

Cryosectioning and Microscopy.

There were several obstacles encountered as a result of the chosen methodology. I quickly recognized that cryosectioning of mosquito samples presents additional

challenges as compared to cryosectioning tissue sections or even other arthropods such as ticks [215]. The primary challenge was maintaining integrity of the section. Frequently, the mosquito tissues would drop out of the section while the slice was occurring and be lost or largely displaced during the transfer to the glass slide. This was moderately managed with careful control of the chamber temperature. If the sample was too cold, the slice would curl up, which was also a significant problem as I found it difficult to consistently keep the cryostat at a cold enough temperature (between -22 and -24°C)

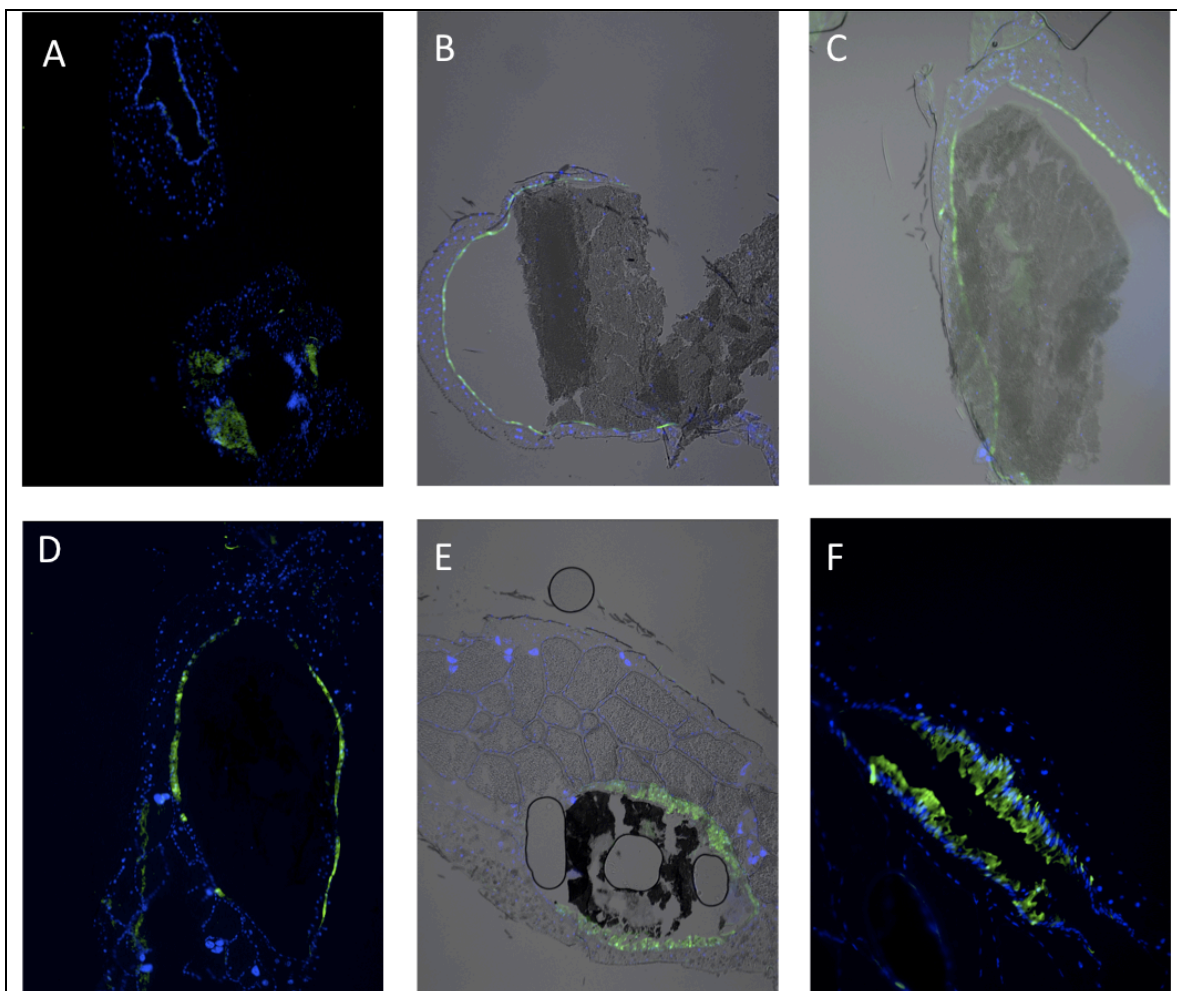


Figure 5-2: GFP in *Cx. taeniopus* at serial time points

A) Negative control B) 24 hours post infection C) 36 hours D) 48 hours E) 72 hours F) 4 days. Viewed on an Olympus BX61 (10x).

to alleviate this problem. I also determined that taking thinner slices (4-6 μm) was ideal for keeping the sample together during the sectioning at the cost of increased fragility during the transfer to the slide, which resulted in images with tears. The problems of integrity and fragility appeared to be worse in mosquitoes without an engorged midgut. These combined difficulties culminated in frequently damaged slices that made identification of various mosquito organs challenging.

An additional challenge with this method was distinguishing background from true signal with this method. All mosquitoes examined, even the negative controls (figure 5-2A) showed high levels of background GFP and some particular regions showed more background than others for undetermined reasons. In order to differentiate true GFP signal from background, I included filters for fluorescence excited at a range outside of the GFP excitation and those locations that showed both filter colors were deemed to be nonspecific (figure 5-3).

DISCUSSION

The goal of this study was to identify the route of dissemination utilized by enzootic VEEV in *Cx. taeniopus* mosquitoes. Previous studies have primarily utilized immunohistochemistry (IHC) [133,153,216] or electron microscopy [109,154,217-219] for this purpose, but a few have shown the potential of GFP labeled virus [153,176,177,220-222]. While insertion of a fluorescent reporter in a flavivirus has been

shown to result in genomic instability and replicative attenuation in a mosquito model as early as day four following infection, similar fluorescent constructs in CHIKV, SINV, ONNV have generally shown an increased genomic stability and minimal replicative attenuation in model mosquito vectors [176,177,221,222]. Knowing that enzootic VEEV has been shown to disseminate within four days of infection in *Cx. taeniopus* [109], I anticipated that the 68U201 GFP construct would allow for highly sensitive observation of early infection and secondary sites of infection in *Cx. taeniopus*. I was unable to observe dissemination beyond initial infection and replication sites within the midgut through day 4 post-infection. This could be a result of either genetic instability resulting in the deletion of portions of the GFP insert, rendering it invisible, or replicative attenuation due to the inclusion of the 1 kb GFP insert, which accounts for an addition of approximately 10% to the original size of the VEEV genome. Direct comparison of 68U201 GFP and the parental 68U201 replication *in vitro* in Vero cells indicated no differences in replicative ability. However, sc needle inoculation of 68U201 GFP resulted in a highly diminished ($> 2 \log_{10}$ FU/ml reduction) viremia 24 hours post infection as compared to the wild type, which indicates a significant *in vivo* replicative attenuation in a mouse model. In order to resolve whether the lack of observed GFP dissemination in *Cx. taeniopus* is due to *in vivo* replication attenuation therefore delayed dissemination or a result of compensating mutations rendering the GFP insert defective, I orally exposed a small cohort of *Cx. taeniopus* mosquitoes to 68U201 GFP and examined

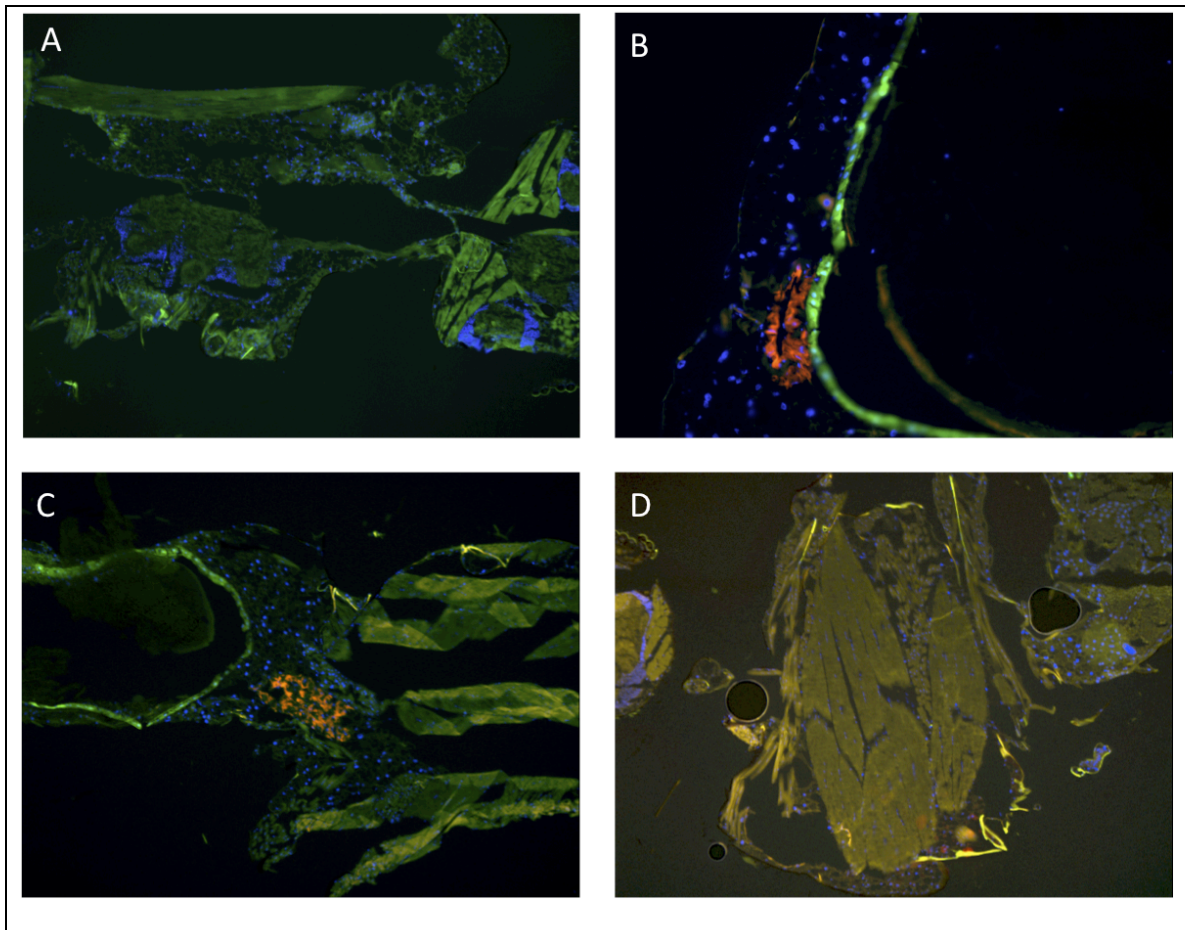


Figure 5-3: Example of high levels of background and nonspecific fluorescence

A) A 48 hour negative control image showing GFP background B) 36 hour mosquito with positive GFP midgut signal and nonspecific red excitation C) 48 hour mosquito with specific GFP, nonspecific red excitation, and mixed red and green background excitation in the thorax region D) 60 mosquito with high mixed nonspecific excitation of green and red in the thorax (positive midgut not shown)

them at day 7 for disseminated infection and the presence of GFP expression. It was discovered that at day 7, 90% of mosquitoes had a disseminated infection and GFP was still being expressed. This suggests that the dissemination is likely delayed and occurs beyond day 4 post-infection.

While utilization of virus constructs expressing GFP for characterizing infection and dissemination allows for a highly sensitive assay, there are several disadvantages to this method. Primarily, there is a potential for the additional GFP genetic load to result in decrease in replicative efficiency that may bias temporal dissemination and potentially viral tropism. Other significant disadvantages pertain to the sectioning and integrity of samples. I have established, in accordance with histology core employees, that cryosectioning of mosquitoes has specific challenges that are unique to this insect that result in high variability of sample quality. Similarly, it is possible that the 48 hour incubation in 4% PFA necessary to irrefutably inactivate VEEV could have contributed to the background expression. While these studies and my findings with GFP expressing replicons in chapter four exhibit the advantageous sensitivity of fluorescent protein, the other disadvantageous make this particular method less useful than other methods including immunohistochemistry and electron microscopy. Immunohistochemistry has been utilized successfully to follow the pathway of dissemination of epizootic VEEV, yellow fever virus (YFV), and West Nile virus (WNV) [153,201,217], however it does lack the sensitivity of electron microscopy. Electron microscopy examining

dissemination of 68U201 in *Cx. taeniopus* has been performed previously, and general patterns and timing of IE VEEV dissemination, it did not look closely at how the virus escaped the midgut [109]. If time allowed, I would attempt to repeat this study utilizing immunohistochemistry methods in conjunction with electron microscopy thoroughly examine how IE VEEV escapes the midgut. However, I find it highly interesting that inclusion of a GFP construct within the 68U201 genome appeared to result in severe attenuation and would welcome the opportunity to examine this in more detail to evaluate the degree of attenuation *in vitro* and *in vivo* models as well as characterize any detectable effects on specific RNA species synthesis.

CHAPTER 6: TRANSMISSION POTENTIAL OF TWO CHIMERIC WESTERN EQUINE ENCEPHALITIS VACCINE CANDIDATES IN CULEX TARSALIS⁴

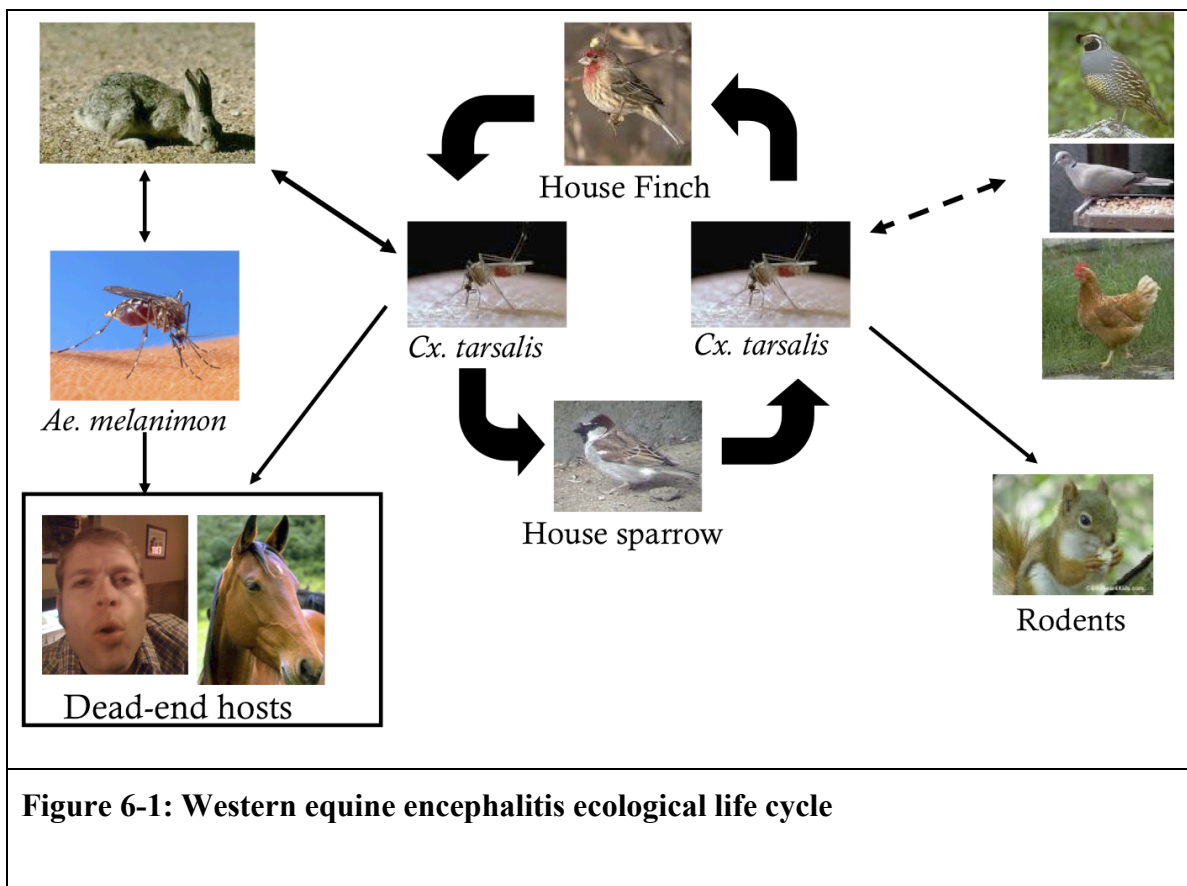
INTRODUCTION

Like Venezuelan equine encephalitis virus, Western equine encephalitis virus (WEEV) is a mosquito-borne alphavirus pathogen that can cause fatal neurologic disease. Clinical cases, which can cost anywhere from \$21,000 to \$3 million dollars to treat [223], can leave a survivor with mild to severe sequelae. Unlike other alphaviruses, WEEV a descendant of an ancient recombination event believed to have occurred between an ancestral Eastern equine encephalitis-like virus and a Sindbis-like progenitor virus [224,225]. While the incidence of WEEV human and equine cases has fallen significantly in the past 30 years [226,227], it is still considered an important public health risk as there is no licensed vaccine available, the overwintering ecology of the virus has yet to be established, public health control measures should an outbreak occur are expensive, and there is little ongoing surveillance to rapidly detect an upsurge in cases and prevent re-

⁴The data in this chapter were previously published in the American Journal of Tropical Medicine and Hygiene and is reproduced here with copyright permission from the journal. The citation for the article is: Kenney JL, Adams AP, Weaver SC (2010) Transmission potential of two chimeric Western equine encephalitis vaccine candidates in *Culex tarsalis*. *Am J Trop Med Hyg* 82: 354-359.

emergence of the virus. WEEV is also potential bioterrorism agent and is classified as an NIAID category B select agent [228].

WEEV primarily cycles between passerine birds such as sparrows and house finches, and the primary mosquito vector, *Cx. tarsalis* [229-233]. A secondary cycle, which has yet to be thoroughly examined, is believed to exist between *Aedes melanimon* [232,234,235] mosquitoes and hares (*Lepus californicus*) [229,236]. Other implicated mosquito vectors that are able to transmit WEEV include *Ae. dorsalis* [229,237,238] and *Culiseta inornata* [233] (figure 6-1).



As the population of *Cx. tarsalis* females increases throughout the summer, the proportion of mosquitoes feeding on mammals increases, which leads to an increased risk of WEEV transmission to humans and domestic animals [239,240].

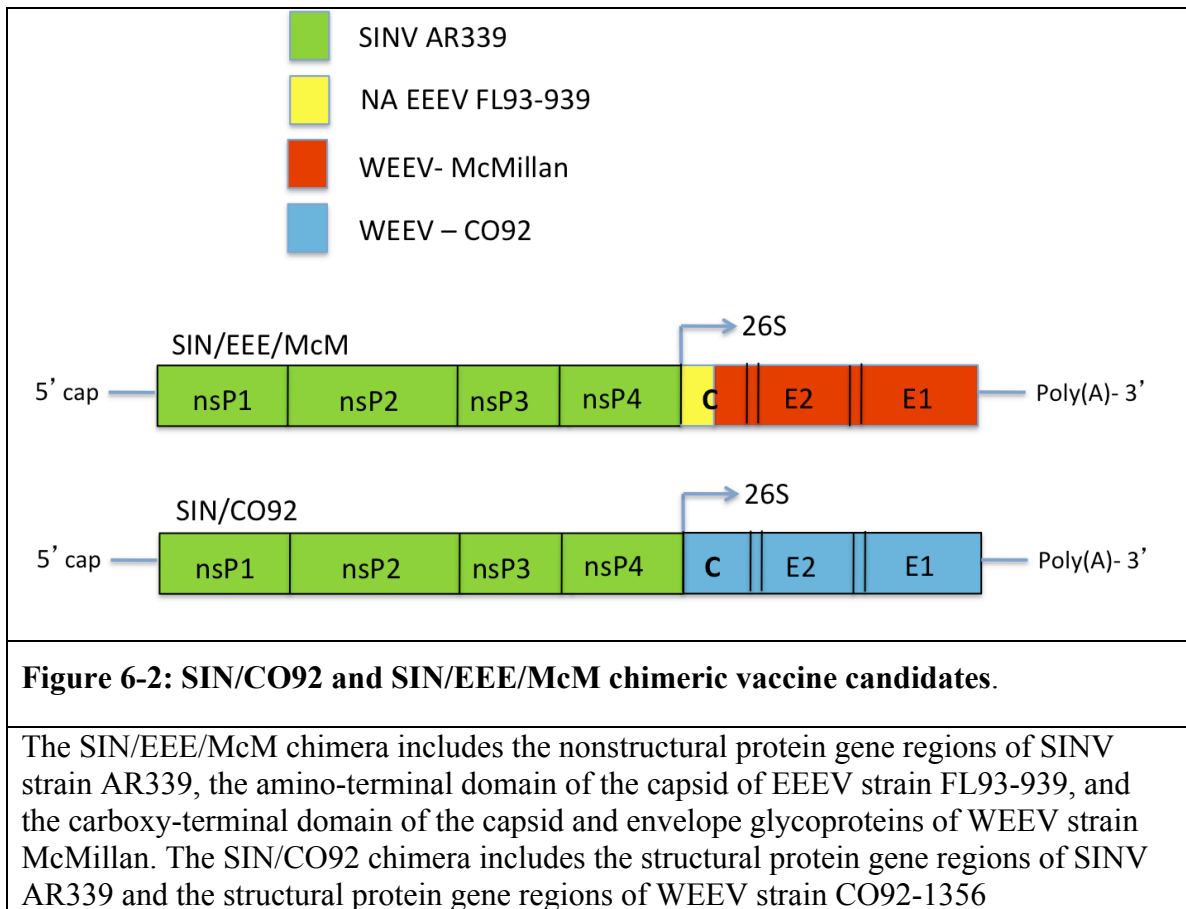
While there is no licensed WEEV vaccine for human immunization of individuals at risk such as laboratory professionals or veterinarians, there are several commercial vaccines available for use in equids. These vaccines consist of formalin-inactivated, wild-type WEEV prepared from chicken embryo fibroblast cultures and are typically delivered as a bivalent eastern equine encephalitis virus (EEEV)/WEEV formulation or even a trivalent Venezuelan equine encephalitis virus (VEEV)/EEEV/WEEV preparation [199]. As they are inactivated, effective immunization requires two initial doses followed by annual boosters. However, inactivated vaccines are not ideal for public health following either a natural WEE outbreak or potential bioweapon exposure due the multiple requirement and the typically slow and short-lived immune responses that recipients generate [229].

In order to develop a safer, more efficacious vaccine candidate, live-attenuated chimeric WEEV vaccine candidates have been developed [164]. Alphaviruses contain a single stranded, positive-sense RNA genome with four nonstructural proteins (nsP1-4), encoded by an open reading frame in the 5' two-thirds of the genome, and a structural polyprotein that is translated from a subgenomic (26S) RNA and cleaved into the capsid and envelope glycoproteins, E2 and E1. The backbone of the first chimeric vaccine, SIN/CO92, consists of the 3'- and 5'-UTRs and nonstructural protein genes of Sindbis

virus (SINV) strain AR339 (figure 6-2). The structural protein genes are derived from WEEV strain CO92-1356. The second strain, SIN/EEE/McM, has a similar genetic makeup with two exceptions: a) the amino-terminal half of the capsid gene, including the 5'-UTR of the subgenomic RNA, is derived from EEEV strain FL93-939 [241], and b) the remainder of the structural protein genes is derived from the WEEV McMillan strain. The amino-terminal half of the EEEV capsid gene was included to enhance virus packaging without the attenuating effects that would occur if a SINV or WEEV N-terminal capsid gene was present to interact with the nsP2 packaging signal [242]. The high replication efficiency observed previously with a SIN/EEEV chimeric virus indicated that the EEEV-specific capsid has strong RNA-binding activity during virus assembly [164,166,243]. Both chimeric SIN/WEEV viruses replicated efficiently in both African green monkey (Vero) cells and *Ae. albopictus* (C710) cells, and were highly attenuated, immunogenic, and efficacious in mouse models of WEE [164].

The primary disadvantage to live attenuated vaccine candidates is the risk of reversion to virulence and transmissibility, which could lead to outbreaks of disease as demonstrated by the live-attenuated poliovirus vaccine [244]. This risk is under greater scrutiny for genetically modified viruses that might evolve in unpredictable ways during circulation in nature. For arboviruses, transmission typically requires the generation of a host viremia sufficient for infection of the vector, followed by replication and dissemination in the vector, and shedding into the saliva. Although neither chimeric WEEV vaccine produces viremia in mice, it is nonetheless important to establish their

ability to infect WEEV vectors as a measure of environmental safety. Any live virus vaccine, when administered on a large scale, has the potential to produce a viremia in a compromised host. However, if infection or transmission by the mosquito vector cannot occur, the risk of progression to a public health concern would be minimal.



To evaluate the environmental safety of these chimeric WEEV vaccine candidates, and to assess the contributions of different alphavirus genes and cis-acting sequence elements to vector infectivity, I orally exposed the primary WEEV mosquito vector, *Cx. tarsalis*, to high-titered artificial blood meals to assess the ability of these chimeric viruses to infect, disseminate, and be transmitted to naïve mice. This mosquito species was selected because it is the principal WEEV vector in North America [233], where these vaccine candidates would be used if approved for equids or humans.

METHODS

Viruses

Three wild-type alphavirus strains and two chimeric vaccine candidates were compared in this study. The wild-type strains included: 1) SINV strain AR339, 2) WEEV strain CO92-1356, which was isolated in 1992 from *Cx. tarsalis* mosquitoes in Colorado, and 3) WEEV strain McMillan, which was isolated in 1941 from a human in Ontario, Canada. The first chimeric vaccine candidate (SIN/CO92) consisted of nonstructural protein genes derived from SINV strain AR339 and structural protein genes derived from WEEV strain CO92 (figure 6-2). The second vaccine candidate (SIN/EEE/McM) also contained SINV strain AR339 nonstructural protein genes, but derived the N-terminal half of its capsid gene from the North American EEEV strain FL93-939 [245] and the remainder of the capsid as well as the envelope glycoprotein

genes from WEEV strain McMillan (figure 6-2). Cloning and electroporation of each chimeric virus were performed as described previously [164].

Oral mosquito infections.

Cx. tarsalis eggs from a colony generated at the University of California, Davis were hatched and reared using standard methods to generate a laboratory-based colony [246]. Five cohorts of 50 adult females (1-3 replicates per virus), 5-6 days after emergence from the pupal state, were allowed to feed for 45 min on an artificial blood meal containing 33% (v/v) defibrinated sheep erythrocytes (Colorado Serum Company, Denver, Co), 33% (v/v) heat-inactivated fetal bovine serum (FBS) (Omega Scientific, Inc., Tarzana, CA), 33% (v/v) of each individual virus in cell culture fluid (resulting in a final concentration of approximately $6 \log_{10}$ PFU/ml), and 1% (v/v) of 0.25 μ M adenosine triphosphate. Artificial blood meals were encased in a collagen membrane and warmed in a Hemotek feeder (Discovery Workshops, Accrington, United Kingdom) prior to being placed on the screened lids of 0.45-liter paper cartons. After feeding, mosquitoes were cold-anesthetized and engorged specimens were held at 27° C with a relative humidity of 70-75% for an extrinsic incubation period of 11-14 days.

Intrathoracic mosquito infections.

Two cohorts of 30 adult females were subjected to intrathoracic inoculation of approximately 1 μ l of $6 \log_{10}$ PFU/ml of SINV, SIN/EEE/McM, or wild-type WEEV strain McMillan (WEEV-McM). Mosquitoes were held for an extrinsic incubation period

of 8 days at 27° C with a relative humidity of 70-75% prior to being presented to naïve suckling mice for blood feeding.

Mosquito processing

After extrinsic incubation, legs and wings were removed from cold-anesthetized mosquitoes and placed in an Eppendorf tube with 350 µl of Dulbecco's modified Eagle's essential medium (DMEM) with 10% FBS, and amphotericin B (50µg/ml). When salivation was performed, the proboscis of each immobilized mosquito was inserted into a 10 µl capillary tube containing immersion oil (Cargille Laboratories, Cedar Grove, NJ) to induce salivation for approximately 45 min. Following salivation, mosquito bodies and legs/wings were triturated for 4 min in 350 µl of DMEM, 10% FBS, and amphotericin B using a Mixer Mill 300 (Retsch, Newton, PA). Collected saliva was added to an Eppendorf tube containing 100 µl of 10% FBS/DMEM and centrifuged prior to transfer of the supernatants. Collected supernatants from each sample were analyzed for virus content by the induction of cytopathic effects (CPE) on Vero cells [247].

Transmission to mice

Because artificial saliva collection assayed by cell culture CPE has limited sensitivity to detect transmission potential [248], I also exposed some mosquitoes to naïve murine hosts. Following completion of the extrinsic incubation period, mosquito cohorts were allowed to feed for 45 min on a group of five 6-day-old mice placed on the screened lid of the incubation carton. For all experiments, it was noted that no mosquito

engorged fully on the suckling mice, but probing was considered exposure because mosquitoes salivate while locating a blood vessel. In subsequent experiments, each individual mosquito was allowed to probe on an individual mouse in order to follow which mosquitoes probed on a particular mouse. Individual mosquitoes were cold-anesthetized and separated into individual wire-top tubes through which they could probe. Mice were placed adjacent to the wire top and mosquitoes were allowed to probe. As a control, an additional cohort of mice was exposed to uninfected mosquitoes. Mice were then returned to their cages and observed for survival for three weeks. Survivors were bled and analyzed for neutralizing antibodies to assess exposure to virus. Positive and negative control serum samples were included for all 80% plaque reduction neutralization tests (PRNT₈₀).

Statistical analyses

Initial body infection, dissemination into the hemocoel, and salivary infection as a measure of transmission potential were compared between virus groups using a 2x3 Chi Square for Independence Test using the software program, InStat (version 3.0) (GraphPad, San Diego, CA). Experimental replicates were combined for final analysis between groups. Results were considered significant if the *P*-value of less than 0.05 was achieved.

RESULTS

Orally exposed *Cx. tarsalis* infection and dissemination.

Overall, *Cx. tarsalis* body infection rates varied greatly among the parental virus strains [SINV, WEEV-CO92, WEEV-McM; 92%, 73%, and 0%, respectively (table 6-1)]. The SIN/CO92 vaccine candidate strain showed a significantly decreased rate of body infection as compared to both of its parents ($P < 0.0025$). Similarly, comparison of SINV, WEEV-CO92, and SIN/CO92 showed a significant difference in dissemination rates into the hemocoel, with 86%, 60%, and 8%, respectively ($P < 0.0001$). The McMillan-derived vaccine candidate strain, as well as the parental WEEV strain, failed to infect or disseminate in any *Cx. tarsalis* following oral exposure.

Intrathoracic exposure to WEEV-McM and SIN/EEE/McM

To determine whether McMillan-derived viruses can replicate within *Cx. tarsalis* mosquitoes, intrathoracic inoculations bypassing the midgut were also performed. Bodies of all surviving mosquitoes inoculated with SINV, WEEV-McM, or SIN/EEE/McM, were examined for infection (table 6-1). In contrast to oral exposure to WEEV-McM and SIN/EEE/McM (table 6-1), the intrathoracic route infected all mosquitoes. As expected, all SINV mosquitoes were also infected.

Virus	Blood meal titer (log ₁₀ PFU/ml)	No. engorged	No. infected (% infected)		
			Body	Legs/wings	Saliva
SINV	6.9	22	22 (100)	21 (95)	2 (20) ^a
	7	7	5 (71)	5 (71)	0 (0)
	6.2	7 ^g	6 (85)	5 (71)	-
Total		36	33 (92)	31/36 (86)	2/17 (12)^b
SIN/CO92	6.1	20	9 (45)	2 (10)	0 (0) ^c
	6.3	10	4 (40)	1 (10)	0 (0)
	6.2	7 ^g	1 (14)	0 (0)	-
Total		37	14 (37)	3 (8)	0/20 (0)^d
WEEV CO92	6.2	20	17 (85)	14 (70)	0 (0) ^e
	6	16	9 (56)	8 (50)	4 (25)
	5.6	2 ^g	2 (100)	1 (50)	-
Total		38	28 (73)	23 (60)	4/26 (15)^f
SIN/EEE/McM	6.6	27	0 (0)	0 (0)	0 (0)
WEEV McM	5.9	26	0 (0)	0 (0)	0 (0)

Table 6-1: Rates of infection and dissemination

^a10 mosquitoes were selected for salivary analysis at the time of processing, and upon analysis, it was found that all 10 had disseminated infection.

^bTotal represents the number out of the sample of 17 tested for salivary infection

^c10 mosquitoes were selected for salivary analysis at the time of processing, and upon analysis, it was found that only 2 of the 10 chosen had disseminated infection.

^dTotal represents the number out of the sample of 20 tested for salivary infection

^e10 mosquitoes were selected for salivary analysis at the time of processing, and upon analysis, it was found that only 6 of the 10 chosen had disseminated infection.

^fTotal represents the number out of the sample of 26 tested for salivary infection

^gThe number engorged in these groups indicates the number of orally exposed mosquitoes that were later presented to suckling mice.

Mosquito transmission following oral exposure.

SIN/CO92 and its parental virus strains were evaluated for transmission potential by examining the saliva of exposed mosquitoes using the capillary method. When the SIN/CO92 vaccine candidate strain was compared to SINV and WEEV-CO92, there were no statistically significant differences in transmission potential based on infectious saliva content. SINV, SIN/CO92, and WEEV-CO92 had 12%, 0%, and 15%, saliva infection rate respectively. However, due to the known insensitivity of saliva assays for transmission potential [248], other cohorts of orally exposed mosquitoes were allowed to feed on groups of five naïve 6-day-old mice, which were followed for 3 weeks for survival (figure 6-3) and seroconversion. The parental WEEV-CO92 strain produced rapid mortality in mice, which all succumbed to infection by 3 days after exposure to infected mosquitoes. SINV strain AR339 was also transmitted by *Cx. tarsalis* to mice, resulting in 40% mortality by day 6 post-exposure. The mice exposed to mosquitoes that fed on the vaccine candidate SIN/CO92 showed no mortality up to 3 weeks following exposure to infected mosquitoes. Similarly, mice exposed to mosquitoes that fed on WEEV McM and vaccine candidate SIN/EEE/McM also showed no mortality (figure 6-3). However, it was determined that none of the exposed mosquitoes acquired either of these two vaccines, further supporting their poor infectivity for *Cx. tarsalis*.

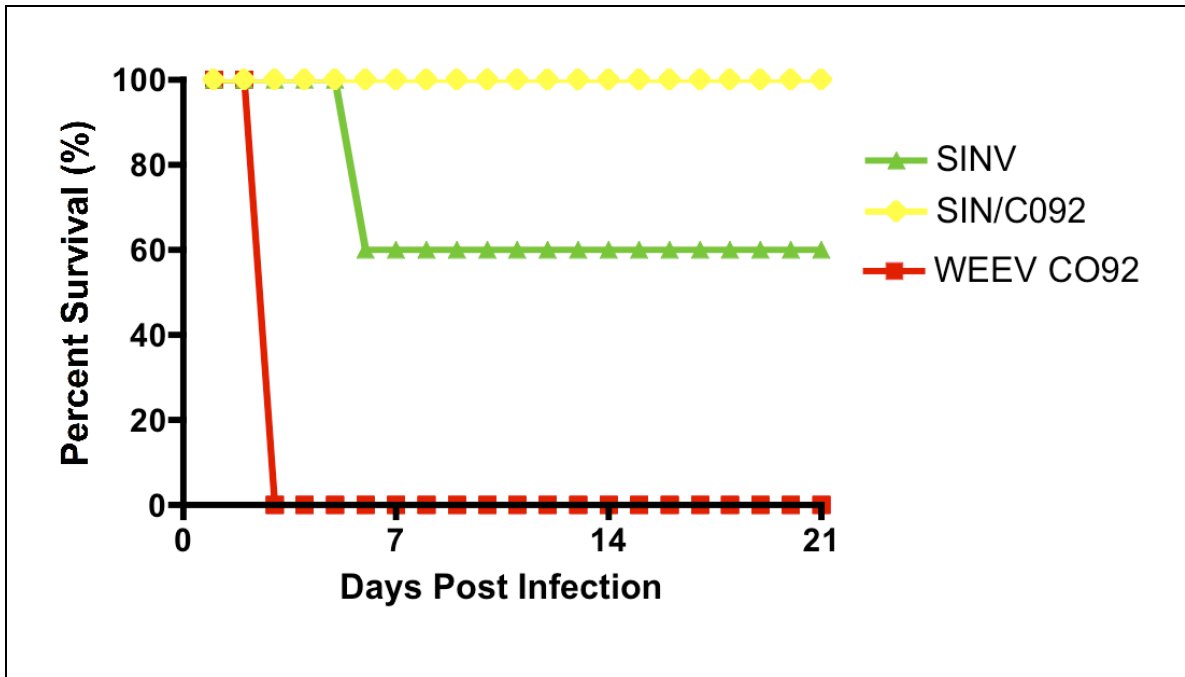


Figure 6-3: Survival of suckling mice from orally exposed *Cx. tarsalis*

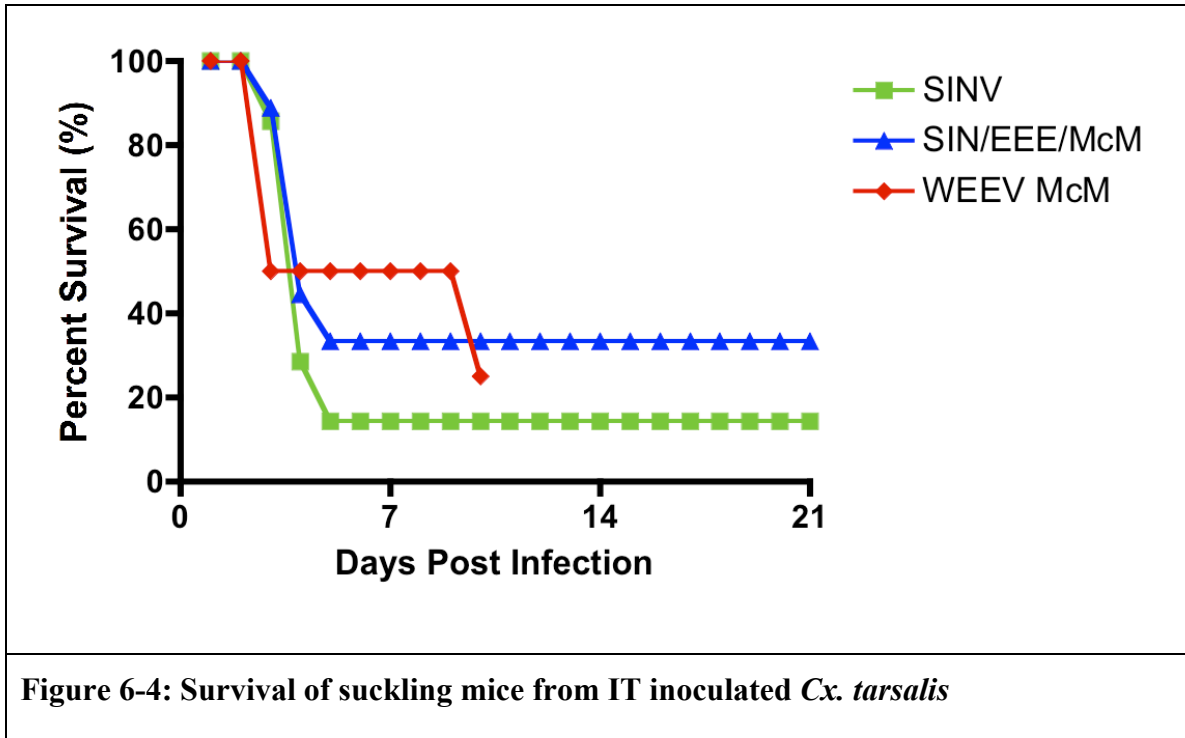
To determine whether mice that survived mosquito probing or feeding had been infected with either SINV or SIN/CO92, serum was collected from the mice 3 weeks post-mosquito exposure and assayed for neutralizing antibodies. There were no antibodies detected in the surviving mice, suggesting these mice were never exposed to virus during mosquito probing or feeding. Alternatively, it was also possible that the mosquitoes that contained infectious saliva were not the individuals that probed on the mice. Therefore, the SIN/CO92 mouse transmission experiment was repeated in order to expose each individual mosquito to an individual suckling mouse. In this experiment, seven SIN/CO92 orally exposed mosquitoes that survived the extrinsic incubation period

were each exposed to one suckling mouse and probing was observed. While it was noted that each of the seven mosquitoes probed, all of the suckling mice survived, and subsequent tests indicated that none of the seven mosquitoes had disseminated infections with SIN/CO92. Future studies should examine the transmission ability of IT inoculated *Cx. tarsalis* for this chimeric vaccine candidate.

Mosquito transmission following intrathoracic inoculation.

Mosquitoes that were intrathoracically inoculated with either SIN/EEE/McM, SINV, or McM were examined for the ability to transmit virus. Suckling mice were exposed to individual mosquitoes and probing/feeding behavior was noted (table 6-2). Subsequent CPE assays indicated that all mosquitoes in each virus group were infected. As observed in the previous experiments with orally exposed mosquitoes, SINV was transmitted to suckling mice. Of the nine mice presented to individual mosquitoes in the SINV group, seven (78%) were probed upon. Six of the seven SINV-exposed mice (86%) succumbed to disease by day 5 post-exposure (figure 6-4) and the single surviving mouse was seropositive (antibody titer=1:20). Of 10 SIN/EEE/McM-infected mosquitoes, nine (90%) probed on individual mice. Of these nine SIN/EEE/McM-exposed mice, six succumbed to disease (67%) by day 5 post-infection (figure 6-4). Of the three surviving SIN/EEE/McM-exposed mice, two were seropositive (1:20 and 1:40) and one was seronegative. In the McM group, three of the seven infected mosquitoes (43%) probed on individual mice. Two of the three mice succumbed to disease (67%) by

day 3 post-infection. The single surviving mouse was killed by the mother at day 10 post-infection; however, this mouse never displayed signs of disease and was seronegative.



CONCLUSIONS AND SUMMARY

All currently available WEEV vaccines are inactivated strains that are only licensed for veterinary use (i.e., horses), are poorly immunogenic, not consistently efficacious, and require multiple doses to achieve seroconversion.[229,249] Therefore, recent efforts have focused on developing live-attenuated vaccine strains that will be highly immunogenic and efficacious after a single dose. The purpose of this study was to assess whether, in the event that a human or equid became viremic after vaccination,

these recently developed chimeric WEEV strains have the potential to be introduced into a mosquito-borne transmission cycle. Using the primary WEEV mosquito vector, *Cx. tarsalis*, I evaluated the potential for each chimeric vaccine candidate strain (SIN/CO92 and SIN/EEE/McM) to infect, disseminate, and be transmitted when compared to parental virus strains (SINV and WEEV).

Experimental infections of house sparrows and white-crowned sparrows, primary avian hosts of WEEV, with various wild type strains of WEEV showed that these birds can generate a viremia ranging from 3.6 to 6.5 log₁₀ PFU/ml [250]. I found that the parental SINV strain AR339, WEEV strain CO92, as well as the chimeric vaccine candidate strain SIN/CO92, were infectious for *Cx. tarsalis* following exposure to doses approaching the peak viremia observed in experimentally infected avian hosts. Similarly, SIN/CO92 was able to disseminate in mosquitoes, albeit at a much lower rate when compared to the parental strains. Interestingly, *Cx. tarsalis* was refractory to WEEV strain McMillan as well as the McMillan-derived chimeric vaccine candidate strain. This is likely due to unaccounted mouse brain passages since its isolation in 1941. I speculate that this strain was selected for neurovirulence in rodents, and as a result, lost its ability to efficiently infect mosquitoes. A similar phenomenon has been observed with a neurovirulent SINV strain, which is unable to infect the midgut epithelial cells of *Ae. aegypti* mosquitoes, whereas a wild-type SINV strain can. The amino acids responsible for this difference in SINV infection capability have been mapped to the E2 glycoprotein [251-254]. Ablation of *Cx. tarsalis* mosquito infection ability by inclusion of the

McMillan derived carboxy-terminal region of capsid and remaining structural proteins indicates that these regions include determinants for infection of *Cx. tarsalis*. Previous sequencing comparisons between the structural regions of CO92 and McMillan identify a total of 13 amino acid differences that may play a role in vector competence [164]. One in particular, Arg to Lys difference at amino acid 250 of the capsid has been shown to be important for mouse virulence [255], and could potentially result in a fitness cost that reduces mosquito infectivity. Outside of the capsid, the authors identified eight amino acid differences between CO92 and McMillan in the E2 glycoprotein, one in the 6K, and three in the E1 glycoprotein that might also contribute to the inability of McMillan virus to infect *Cx. tarsalis* [164]. Based on pre-established determinants for vector infection and other alphaviruses, it is likely that mutations in the E1 or E2 glycoprotein play a role in vector infection [69,256].

The SIN/EEE/McM vaccine candidate exhibited the same inability to orally infect *Cx. tarsalis* as the parental WEEV McM strain, which is a promising safety characteristic of this vaccine candidate. Further examination indicated that both WEEV strain McMillan and SIN/EEE/McM can replicate in *Cx. tarsalis* when the midgut is bypassed by an intrathoracic inoculation. Previous studies have shown that there is a dose-dependent midgut infection barrier within *Cx. tarsalis* as it relates to strains of WEEV [192]. However, in our studies, oral doses as high as 6.0 log₁₀ PFU/ml were unable to overcome this putative threshold barrier.

The enhancement of alphavirus dissemination in mosquitoes co-infected with filarial worms has been reported and could allow for the transmission of the chimeric vaccine candidates I studied [257]. However, the *Brugia spp.* that are known to enhance dissemination do not circulate in the same geographic regions as WEEV and have not been found in equids [258]. To our knowledge, no studies have been performed indicating WEEV viral dissemination enhancement in horses (the most likely non-human vaccine host) co-infected with filarial worms. However, this concern could be easily alleviated by a simple blood smear to determine an equid's parasitic status prior to WEEV vaccination, or treatment with a dewormer prior to vaccination. Additionally, because horses do not become viremic from wild-type WEEV [229], the risk of an equid developing viremia sufficient for transmission with an attenuated vaccine candidate strain is further diminished. Therefore, it is highly unlikely that *Cx. tarsalis* could acquire infection from a host vaccinated with either a McMillan- or CO92-derived vaccine candidate strain.

Next, I examined the transmissibility of each vaccine candidate when compared to parental strains by utilizing three measures: 1) presence of virus in *Cx. tarsalis* saliva as measured by cell culture assay, 2) survival of neonatal mice following exposure to infected *Cx. tarsalis*, and 3) seroconversion of surviving mice following exposure to infected mosquitoes. Rates of saliva infection were lower than expected when considering the typical transmission potential for wild-type viruses. For example, transmission potential measured by capillary method for mosquitoes exposed to WEEV

CO92 showed that only 15% of mosquitoes with disseminated infection had virus in the saliva, which seems unusually low for a vector known to be highly competent for this strain of virus. However, orally exposed mosquitoes were able to transmit WEEV CO92 to 100% of naïve mice, indicating that saliva collection resulted in a significant underestimation of transmission potential for this virus. Previous studies have shown viral transmission detection from newborn mice is more sensitive than capillary saliva collection followed by cell culture-based assays, and our findings support these observations [245]. The mouse assay is a true measure of transmission, while detection of virus in the salivary glands is only a predictor of transmission potential. Hence, capillary salivary assays were used minimally throughout the study. Exposure of the WEEV CO92-fed mosquito group to naïve suckling mice resulted in rapid mortality of all mice by day 3 post-exposure, indicating transmission. Forty percent of mice succumbed to SINV following exposure to orally infected mosquitoes. At the time of exposure, the number of infected mosquitoes was unknown because assays were performed only after mosquitoes were killed. Therefore, I deemed it necessary to distinguish if the 60% of surviving mice had been infected by evaluating their serum for neutralizing antibodies 3 weeks post-exposure. The PRNT₈₀ results indicated that none of the surviving mice in this cohort had been infected with SINV. Similarly, all surviving mice from the SIN/CO92 exposure group were seronegative. Whether this was due to the fact that these mice were only exposed to uninfected mosquitoes, or whether the mosquitoes were

infected but unable to transmit, was not clear, and so, further experiments were performed to resolve this uncertainty.

In the subsequent experiments, individual mosquitoes were allowed to feed on an individual naïve suckling mouse in order to correlate mosquito infection status with

SINV			
Mouse	Exposure	Date of Death	Survival Serostatus
1	probed	D4	-
2	probed	-	1:20
3	probed	D4	-
4	probed	D3	-
5	Not exposed	-	Neg
6	Not exposed	-	Neg
7	probed	D5	-
8	probed	D4	-
9	probed	D4	-

SINV/EEE/McM			
Mouse	Exposure	Date of Death	Survival Serostatus
1	probed	-	1:40
2	probed	D4	-
3	Not exposed	-	Neg
4	probed	-	1:20
5	probed	-	Neg
6	probed	D4	-
7	probed	D3	-
8	probed	D4	-
9	probed	D4	-
10	probed	D5	-

McM			
Mouse	Exposure	Date of Death	Survival Serostatus
1	probed	D11*	Neg
2	Not exposed	D11*	-
3	probed	D3^	-
4	probed	D3^	-
5	Not exposed	-	Neg
6	Not exposed	-	Neg
7	Not exposed	-	Neg
Mother	consumed 3 and 4	D10*	1:20

* Killed by surrogate mother

^ Killed by original mother when showing signs of illness

Table 6-2: Probing status and survival of suckling mice exposed to IT inoculated mosquitoes

mouse exposure (table 6-2). None of the mosquitoes in the SIN/CO92 oral exposure group acquired a disseminated infection. While we did demonstrate in previous studies that SIN/CO92 is able to disseminate in *Cx. tarsalis* mosquitoes, we observed these rates to be very low, even at relatively high oral doses (6 log₁₀ PFU/ml or higher). Due to these low rates of dissemination, we were unable to generate a cohort of mosquitoes with the potential to transmit to naïve mice.

In summary, while both vaccine WEE candidate strains do not appear to be transmitted by the primary WEEV mosquito vector, *Cx. tarsalis*, only the SIN/EEE/McM strain was completely unable to infect this species following oral exposure. This vaccine candidate, therefore, should be regarded as having superior environmental safety. These results corroborate previous findings that chimeric alphaviruses have reduced infectivity in mosquito vectors [197,198], further supporting their safety as vaccine candidates.

CHAPTER 7: FINAL CONCLUSIONS AND FUTURE DIRECTIONS

SUMMARY

The primary goal of this dissertation was to elucidate mechanisms by which enzootic VEEV interacts in its enzootic vector. Significant amounts of work have been done examining the interaction between epizootic VEEV strains and their primary mosquito vectors, which is valuable as these are the strains and vectors most commonly implicated in human and equid outbreaks. Recently it has been shown that the disease burden of enzootic VEEV is likely highly underestimated so it is more important than ever to fully understand the intricacies of the enzootic virus cycle as well [162]. Given the numerous differences between the temporal and ecological cycles of epizootic and enzootic strains, it is logical to assume they pose different challenges to public health. Epizootic viruses emerge periodically for short periods, during which they can infect a wide range of bridge or epizootic vectors, typically with a high threshold of infection, and be disseminated in geographic locations where humans and domestic animals are likely to be present and become exposed. Enzootic VEEV, subtype IE in particular, is believed to persist continually in a mosquito and wild-mammalian host cycle in an established ecological niche characterized by abundant shade, pools of fresh water, and in some cases co-habitation of aquatic plants. Such distinct ecological cycles are bound to generate

different selective pressures acting on each viral type. Similarly, phylogenies of VEEV show that IE viruses form a monophyletic group that shares a common ancestor with other subtype I and II type viruses in the VEEV complex and suggest that IE viruses diverged from other subtype I viruses before IC, ID, and IAB [8]. It is also interesting to note that until recently, VEE outbreak strains have not been linked to IE viruses.

When considering the mechanism by which enzootic IE VEEV theoretically became adapted to being maintained by *Cx. taeniopus*, there are a number of possible scenarios. It has recently been suggested that alphaviruses originated from an aquatic environment prior to being introduced into the New World (Forrester et al., unpublished). The most likely scenario for long distance movement and introduction ancestral genomes into the New World is one in which avian hosts are involved. Coastal regions of Mexico are plausible termination points for migration pathways that could coincide with introduction of viruses to these locations. Parasites that traveled with the bird species could have introduced the virus into the ecosystem as they expanded to utilize resident fauna as hosts. Alternatively, resident parasite species (including mosquitoes) could have acquired the novel viruses from these migratory birds and subsequently introduced it into their preferred hosts (or a wide range of hosts depending on the fastidiousness of the parasite) where it was able to replicate enough to permit specialization into a niche. *Cx. taeniopus* was likely a moderately competent vector even for ancestral IE VEEV strains for the virus to have utilized this mosquito as a long-term host. I speculate that the ancestral IE VEEV strain was able to initially infect *Cx. taeniopus* mosquitoes or

acquired mutations to allow for infection, but probably acquired mutations to allow for enhanced replication within the vector over many generations. Considering that other North American encephalitides have been shown to cause sloughing or cytopathology in mosquito vectors, it is possible that ancestral IE VEEV also had deleterious effects on *Cx. taeniopus* initially and has since adapted to a more commensal relationship, although no studies examining the effect of IE infection on *Cx. taeniopus* fecundity have been performed to date.

These theoretical natural history, in conjunction with historical data that shows *Cx. taeniopus* mosquitoes to be highly competent vectors, suggests that this virus and its enzootic vector have been co-existing in close proximity and likely in a stable, sylvatic habitat for some time. Therefore, I hypothesized that the enzootic virus/vector interaction is likely vastly different from what is known about the epizootic virus/vector interaction.

Viral determinants of enzootic infection

The first aim I pursued was designed to identify the viral determinants allowing enzootic IE strains to efficiently infect the primary vector *Cx. taeniopus* while in contrast epizootic strains show poor infection rates. Studies of multiple vector-borne alphaviruses have repeatedly indicated that the determinants for vector infection reside in the structural proteins, specifically the E1 or E2 glycoproteins [69,187,251,252,254,256]. Specifically, determinants for SINV and epizootic IE either fall between residues 200 to 229 [252] or were specifically linked to a mutation at residue 218 in the E2 [187], respectively.

However, CHIKV virus adaption to the *Ae. albopictus* vector has been mapped to residue 226 in the E1 glycoprotein.

After comparing the infection and dissemination of two pairs of enzootic/epizootic VEEV chimeras, I was able to conclude that the high specificity that enzootic IE VEEV has for *Cx. taeniopus* mosquitoes exhibited by enzootic IE VEEV cannot solely be mapped to the E2 glycoprotein, or even to the structural proteins only. In fact, it is possible the 3' UTR may play a role and act synergistically with other regions of the genome, although more chimeric studies would need to be utilized to fully explain this relationship. Based on infection rates, I was unable to statistically differentiate the contribution of the nonstructural and structural ORFs for vector specificity, although the two chimeras with IE-derived nonstructural proteins achieved higher infection rates than the other two chimeras. Recent studies examining West Nile virus adaptation to *Cx. pipiens* mosquitoes showed that serial passage *in vivo* results an increased replication efficiency within *Cx. pipiens* as well as more mutations found in the nonstructural protein genes than in the structural regions [259]. Studies of ID and IC VEEV indicated that adaptation to one host is constrained in a dual-host (mosquito-vertebrate) cycle, suggesting that it would be unlikely for IE virus to make fitness gains in the mosquito vector while persisting in a dual-host cycle [260]. However, these studies only examined the effects of ten dual-passages and did not have the advantage of a colonized enzootic mosquito vector to utilize for the ID virus, so it is possible that a longer dual-host passaging study in the ecologically relevant vector may indicate fitness gains in the

vector do occur. Although, even the most comparable laboratory model cannot simulate the selective pressures and huge numbers of viral lineages that have occurred in the natural ecological cycle over hundreds or thousands of years.

The infection determinant findings with enzootic IE were a stark contrast to the infection and dissemination capabilities of two chimeric WEEV vaccine candidates in *Cx. tarsalis* in which findings implicated only the structural proteins were important determinants of infection. It has been estimated that the recombination event that gave rise to WEEV and other closely related recombinant New World alphaviruses occurred relatively recently compared to when alphaviruses are estimated to have been introduced into the New World [261]. This, in concert with the knowledge that WEEV strains have been shown to cause midgut lesions in *Cx. tarsalis* suggests that WEEV strains may not be adapted to their insect vector. It is also likely that because WEEV viruses are transmitted by birds, which are highly mobile compared to small mammals and rodents, and that WEEV is not limited to persist in a single ecological niche. This is exemplified by the fact WEEV has been described to cycle in at least two distinct ecological cycles (*Cx. tarsalis* and birds and *Ae. melanimon* and hares) and similarly has been isolated from a wide variety of other avian species [239]. This suggests, that WEEV is not solely highly adapted to a single vector within a specialized ecological niche, but rather utilizes at least two vector types and potentially many species of avian reservoir hosts. I believe the contrasting phylogenetic and natural histories of IE VEEV and WEEV provide plausible explanations for the observed differences in genetic determinants for enzootic

IE vector infection and WEEV vector infection. Specifically, I think these findings support the assertion that IE VEEV is adapted to its vector.

Supplemental studies to bolster the support that enzootic IE VEEV has distinct determinants for vector infection compared to epizootic viruses are necessary. In future studies with these chimeras, it may be valuable to titrate replication in mosquitoes at time points throughout the extrinsic incubation period to gain more information about how each chimera replicates in the mosquito vector over time. Another way to examine the roll of the nonstructural proteins in the *Cx. taeniopus* mosquito model would be to utilize mixed IE and IAB replicons and helpers to distinguish the importance of binding and entry versus replication efficiency within the midgut epithelium. This could be achieved by fusion of a reporter such as GFP or luciferase to nsp3 produced by the replicon to quantitate nonstructural polyprotein expression. This experiment could also provide insight as to why it was very rare to achieve 100% infection of *Cx. taeniopus* midgut cells. For example, the two chimeras with IAB-derived nonstructural proteins never achieved greater than 75% infection even at the highest doses. This lack of saturated infection has been observed before with chimeric alphavirus vaccines strains that were able to infect and disseminate at diminished rates as compared to the parent strains [197-199]. Considering the infection rates are just diminished and infection is not abolished it is likely due to multiple, potentially synergistic or dependent elements. One possibility is that inclusion of a capsid protein that is not matched to other *cis*-acting VEEV elements of the genome results in a diminished down-regulation of host cell transcription. This

could be examined in the mosquito utilizing chimeric viruses with heterologous portions of the capsid in a IE backbone.

Initial midgut infection and cell susceptibility

In the second aim I characterized *in vivo* the initial IE VEEV infection of *Cx. taeniopus* midgut epithelial cells. Utilizing GFP-expressing replicon particles to visualize the initial infection, my findings supported my hypothesis that initial infection takes place in the posterior region of the midgut. My results showed that virions do not have a predilection for one particular region of the *Cx. taeniopus* posterior midgut. Previous methods, primarily utilizing immunohistochemistry for epizootic IC virus in *Ae. taeniorhynchus* or electron microscopy of IE VEEV in *Cx. taeniopus*, have localized initial infection to the region of the brush border, but lack of sensitivity of these methods has prevented detailed characterization of the specific initial locations within the posterior midgut [109,153]. To further explore the theory that the interaction between *Cx. taeniopus* and IE viral strains is vastly different than what is known about how epizootic strains (particularly IC VEEV) behave within an epizootic vector *Ae. taeniorhynchus*, I estimated the number of susceptible midgut cells in the enzootic vector. I used two experimental designs to predict this number. The first was to look at the number of cells infected at various doses to see if there was an upper threshold to the dose response. At the highest doses achievable by the artificial viremia exposure method, I observed an average of 1012 cells infected per midgut with some midguts showing as many as 1757

cells infected. It is interesting that even at the highest exposure doses, the number of cells counted to be infected appears to be only a fraction of the entire midgut. However, some higher resolution images (figure 4-5a) show the regions examined have nearly every cell infected, indicating that the potential for higher proportions of midgut cell infection exists. It must also be recognized that the number of virus particles that a mosquito imbibes is also a reduced compared to what was circulating in the artificial viremia model. For instance, if a mosquito was exposed to a blood meal with a viral concentration of $7.0 \log_{10}$ PFU/ml, and imbibes an estimated 5 μ l of infectious blood, the mosquito is actually acquiring only approximately 5000 PFU within its midgut. This could explain why, even at the highest doses, not every midgut cell was observed to be infected.

This observation of thousands of midgut cells being infected, considering that the estimated number of IC VEEV-susceptible *Ae. taeniorhynchus* midgut cells is approximately 100 [161], suggests that *Cx. taeniopus* does not have a limited population of susceptible midgut cells. The second method to estimate the population of susceptible midgut cells utilized oral infection of mixed 68U201 replicon particles expressing either GFP or CFP. Using the observed probabilities of the cells being infected with each individual replicon, I used basic binomial probability theories to predict the expected number of co-infected cells per midgut assuming the independence of infection with the two replicons. Since I saw no co-infected cells, my observed value did not exceed my predicted value, thus indicating that it is highly unlikely that there is a subpopulation of more susceptible epithelial cells in the *Cx. taeniopus* midgut epithelia. Another way to

look at this result was to compare my observed co-infection probabilities to the observed probabilities in the epizootic mosquito model (*Ae. taeniorhynchus* and IC VEEV) that has been shown to have a small subpopulation of susceptible cells. Utilizing a Poisson distribution to account for calculations of very low probabilities, I determined that the probability of observing less than one co-infected cell in a mosquito with only a small population of susceptible cells (given the observed co-infection probabilities observed in *Ae. taeniorhynchus*) would be extremely low (5.1×10^{-12}), which supports my original hypothesis that in the case of IE VEEV, *Cx. taeniopus* does not have a restricted population of susceptible midgut epithelial cells.

However, it is a little surprising to see such a low rate of co-infection, especially with such high concentrations of singly infected cells throughout these dual infection experiments. It cannot be ruled out that there is some exclusion mechanism that prevents dual infection of *Cx. taeniopus* midgut cells. This would be interesting considering that both replicons were administered at the same time so the exclusion would likely be limited to early virus-cell interactions such as attachment or penetration. However, studies examining homologous virus interference with SINV showed that exclusion is not established at attachment or penetration but rather at translation. *In vitro* studies in BHK cells as well as *Ae. albopictus* cells indicate that the excluded virus is translated, but not replicated [262-265]. Such an exclusion could prevent dual fluorescent expression in *Cx. taeniopus* midgut epithelial cells, assuming the determinants for exclusion are present in the replicon particle. This could also explain the low incidence of co-infected C6/36 cells

observed in my control. Examination of RNA replication following simultaneous or sequential transfection of homologous replicons or full-length 68U201 could help identify if exclusion is occurring and whether it functions to prevent the superinfecting virus from replicating. Regardless of whether interference is inhibiting co-infection, it was clearly observed that the number of susceptible cells in the *Cx. taeniopus* midgut is greater than 2000, which is very different than what is observed in the epizootic *Ae. taeniorhynchus* model.

The findings from characterizing the initial midgut infection in *Cx. taeniopus* indicate a vast difference in how enzootic and epizootic strains utilize their mosquito vectors. Perpetuation of the enzootic cycle is most limited by the availability of susceptible (young) naïve rodent hosts to generate a viremia for the next mosquito to be orally infected. In addition to only a limited portion of the rodent host population being naïve, not all infected rodents will generate a viremia high enough and long enough duration to infect a *Cx. taeniopus* mosquito despite its high sensitivity. There are many factors that define the capacity of a mosquito to act as a vector for a pathogen as defined by the MacDonal vector capacity formula [266]. In the case of *Cx. taeniopus* we know it is highly susceptible to infection at low exposure and like other New World encephalitides it has been shown to transmit virus within four days from infection, and appears able to survive a minimum of 14 days following infection based on laboratory observations. Survival of infected vectors is a highly relevant variable as even a mosquito with 100% susceptibility will not be a competent vector if they are unable to survive long

enough to transmit the virus to susceptible hosts. It is likely that recent ecological changes in areas where IE VEEV circulates [267] have had an effect on populations of *Cx. taeniopus* mosquitoes, but ecological studies would be required to assess their survival in the field. We also cannot account for the population density of *Cx. taeniopus* in relation to the primary reservoir host, how frequently *Cx. taeniopus* feeds on the IE VEEV reservoir host, the longevity of *Cx. taeniopus* in nature, or the density of naïve and viremic rodent hosts. It is reasonable to hypothesize that a vector that is highly susceptible to low titer exposure and can maintain circulation would be an ideal enzootic vector. Therefore, the more midgut cells that are infected at a low dose, the more likely the vector will be able to generate a high enough viral concentration to transmit to an aging population of naïve rodents.

In contrast, the epizootic cycle is maintained by a number of highly viremic equine hosts. When populations of epizootic vector mosquitoes erupt during an epizootic, there is an abundance of mosquitoes being exposed to large sources (large domestic animals) of infectious blood meals so even if the infection rate is relatively low (or the number of midgut cells infected is relatively small), there are still enough infected mosquitoes to perpetuate the cycle.

It would be very interesting to examine the midgut infection dynamics of other *Cx. (Melanoconions)* mosquitoes with ID VEEV strains. Despite being enzootic, ID strains are inherently different from enzootic IE strains in that they have a long history of association with emerging outbreak strains indicating that ID VEEV strains either persist

in an ecological niche similar to or in close vicinity to ideal epizootic hosts and vectors, and/or are compatible with a wider range of mosquito vectors than IE enzootic viruses. Studies of an enzootic foci in Venezuela [268] and recent ID outbreaks in Peru [163,269] indicate that *Cx. (Melanoconion)* mosquitoes known to be competent for ID strains are circulating in areas that overlap with human populations, which suggests narrowing geographic distance between sylvatic forest regions and developed landscapes is a large contributor to emergence. Considering that ID viruses must persist in a rodent-dependent cycle, I would hypothesize that these strains would also be well adapted to establish an infection in a mosquito vector given low exposure titers. Similarly, it would be interesting to characterize the midgut infection of the recently emerged epizootic-IE viruses that have caused disease in horses and can readily infect the epizootic vector in both *Cx. taeniopus* and *Ae. taeniorhynchus*.

Dissemination pathway

My third aim was designed to elucidate the pattern of dissemination in *Cx. taeniopus* using a highly sensitive reporter, oral feeds, and IT inoculations. Unfortunately, this experimental design proved to be very problematic. Although there are many examples of utilizing GFP as a reporter in alphaviruses during mosquito infections [176-178,222], I observed a delayed dissemination rate in IE VEEV expressing GFP. While it cannot be ruled out that the attenuating effects of the GFP affect the pathway as well as the time frame of dissemination, I believe that the sensitivity of a GFP

reporter is an indispensable tool. However, considering the potential bias that GFP might introduce, I would likely utilize immunohistochemistry and electron microscopy to further examine dissemination in *Cx. taeniopus*. Immunohistochemistry would allow for identification of the general pathway and specific time points of dissemination from the midgut so that electron microscopy could be utilized to focus in on that specific time point to identify the specific route of infection. By narrowing the time frame with immunohistochemistry, the electron microscopy could be used more effectively and likely yield more useful results.

FINAL CONCLUSIONS

In summary, I believe the findings of my dissertation demonstrate that the interaction between the enzootic mosquito vector and its companion virus differs from that of the relationship between the vector and virus in the epizootic cycle. Specifically, my results support the hypothesis that a long adaptation of IE viruses to *Cx. taeniopus* mosquitoes plays a role in this difference, but there are still many questions to be addressed. One question in particular, is what is the emergence potential of enzootic IE viruses? Historically, they have not been phylogenetically linked to outbreak strains; however, the recent emergence of epizootic-like IE strains is anomalous. Of particular interest and concern is the ability for these epizootic IE viruses to utilize both *Cx. taeniopus* and *Ae. taeniorhynchus* as vectors. It would be interesting to evaluate the fitness through competition assays of epizootic and enzootic IE strains in each vector. It

has been proposed that massive deforestation and land use change has diminished the habitat of *Cx. taeniopus* in Coastal regions of southern Mexico to the extent that areas that were formerly sylvatic habitat are encroached upon or in close proximity to habitats where epizootic mosquito vectors such as *Ae. taeniorhynchus* are abundant [187]. This change in habitat and available vectors may have selected for IE strains that can efficiently infect epizootic vectors and spawned the emergence of IE strains that can infect horses. Examination of epizootic IE strains indicate that they can cause disease in equids, but do not generate high viremia titers [122]; however, a more recent study with a small group of horses saw high viremias ($7.0 \log_{10}$ PFU/ml) generated in experimentally infected horses (A.P. Adams, personal communication). All the phenotype of these epizootic-like IE viruses in equids needs to be examined in more detail, current findings suggests the potential for these viruses to adapt to an epizootic cycle and generate new outbreaks, which underscores the importance of understanding the different determinants required for a IE strain to be successfully transmitted by either *Cx. taeniopus* or *Ae. taeniorhynchus*. This information could also allow for informed vaccine strategies for future development of VEEV candidates. Knowing the determinants of both epizootic and enzootic vector determinants would allow for the generation of a vaccine that is unable to be reintroduced into either cycle should a vaccinated host become viremic, which is important because recent outbreaks suggest that enzootic and epizootic habitats are likely in close proximity due to clearing of forests for agricultural use [267].

REFERENCES

1. Griffin DE (2007) Alphaviruses. In: Knipe DM, Howley PM, editors. *Fields Virology*. Fifth ed. pp. 1023-1067.
2. Strauss JH, Strauss EG (1994) The alphaviruses: gene expression, replication, and evolution. *Microbiol Rev* 58: 491-562.
3. Rice CM, Strauss JH (1982) Association of sindbis virion glycoproteins and their precursors. *J Mol Biol* 154: 325-348.
4. Ziemiecki A, Garoff H (1978) Subunit composition of the membrane glycoprotein complex of Semliki Forest virus. *J Mol Biol* 122: 259-269.
5. Kuhn RJ (2006) *Togaviridae: The Viruses and Their Replication*. *Fields' Virology*. 5th ed. Philadelphia, PA: Wolters Kluwer Health/Lippincott Williams & Wilkins, c2007. pp. 1001-1022.
6. Ludwig GV, Kondig JP, Smith JF (1996) A putative receptor for Venezuelan equine encephalitis virus from mosquito cells. *J Virol* 70: 5592-5599.
7. Bernard KA, Klimstra WB, Johnston RE (2000) Mutations in the E2 glycoprotein of Venezuelan equine encephalitis virus confer heparan sulfate interaction, low morbidity, and rapid clearance from blood of mice. *Virology* 276: 93-103.
8. Brault AC, Powers AM, Holmes EC, Woelk CH, Weaver SC (2002) Positively charged amino acid substitutions in the e2 envelope glycoprotein are associated with the emergence of venezuelan equine encephalitis virus. *J Virol* 76: 1718-1730.
9. Weaver SC, Brault AC, Kang W, Holland JJ (1999) Genetic and fitness changes accompanying adaptation of an arbovirus to vertebrate and invertebrate cells. *J Virol* 73: 4316-4326.
10. Byrnes AP, Griffin DE (1998) Binding of Sindbis virus to cell surface heparan sulfate. *J Virol* 72: 7349-7356.
11. Gardner JP, Frolov I, Perri S, Ji Y, MacKichan ML, zur Megede J, Chen M, Belli BA, Driver DA, Sherrill S, et al. (2000) Infection of human dendritic cells by a sindbis virus replicon vector is determined by a single amino acid substitution in the E2 glycoprotein. *J Virol* 74: 11849-11857.

12. Klimstra WB, Ryman KD, Johnston RE (1998) Adaptation of Sindbis virus to BHK cells selects for use of heparan sulfate as an attachment receptor. *J Virol* 72: 7357-7366.
13. Gardner CL, Ebel GD, Ryman KD, Klimstra WB (2011) Heparan sulfate binding by natural eastern equine encephalitis viruses promotes neurovirulence. *Proc Natl Acad Sci U S A* 108: 16026-16031.
14. DeTulleo L, Kirchhausen T (1998) The clathrin endocytic pathway in viral infection. *EMBO J* 17: 4585-4593.
15. White J, Kartenbeck J, Helenius A (1980) Fusion of Semliki forest virus with the plasma membrane can be induced by low pH. *J Cell Biol* 87: 264-272.
16. Wahlberg JM, Bron R, Wilschut J, Garoff H (1992) Membrane fusion of Semliki Forest virus involves homotrimers of the fusion protein. *J Virol* 66: 7309-7318.
17. Sherman MB, Weaver SC (2010) Structure of the recombinant alphavirus Western equine encephalitis virus revealed by cryoelectron microscopy. *J Virol* 84: 9775-9782.
18. Singh I, Helenius A (1992) Role of ribosomes in Semliki Forest virus nucleocapsid uncoating. *J Virol* 66: 7049-7058.
19. Strauss EG, Rice CM, Strauss JH (1983) Sequence coding for the alphavirus nonstructural proteins is interrupted by an opal termination codon. *Proc Natl Acad Sci U S A* 80: 5271-5275.
20. Sawicki DL, Sawicki SG (1980) Short-lived minus-strand polymerase for Semliki Forest virus. *J Virol* 34: 108-118.
21. Sawicki DL, Sawicki SG, Keranen S, Kaariainen L (1981) Specific Sindbis virus-coded function for minus-strand RNA synthesis. *J Virol* 39: 348-358.
22. Li GP, Rice CM (1989) Mutagenesis of the in-frame opal termination codon preceding nsP4 of Sindbis virus: studies of translational readthrough and its effect on virus replication. *J Virol* 63: 1326-1337.
23. Ding MX, Schlesinger MJ (1989) Evidence that Sindbis virus NSP2 is an autoprotease which processes the virus nonstructural polyprotein. *Virology* 171: 280-284.
24. Hardy WR, Strauss JH (1989) Processing the nonstructural polyproteins of sindbis virus: nonstructural proteinase is in the C-terminal half of nsP2 and functions both in cis and in trans. *J Virol* 63: 4653-4664.
25. Ahola T, Kaariainen L (1995) Reaction in alphavirus mRNA capping: formation of a covalent complex of nonstructural protein nsP1 with 7-methyl-GMP. *Proc Natl Acad Sci U S A* 92: 507-511.
26. Ahola T, Kujala P, Tuittila M, Blom T, Laakkonen P, Hinkkanen A, Auvinen P (2000) Effects of palmitoylation of replicase protein nsP1 on alphavirus infection. *J Virol* 74: 6725-6733.

27. Peranen J, Laakkonen P, Hyvonen M, Kaariainen L (1995) The alphavirus replicase protein nsP1 is membrane-associated and has affinity to endocytic organelles. *Virology* 208: 610-620.
28. Wang YF, Sawicki SG, Sawicki DL (1991) Sindbis virus nsP1 functions in negative-strand RNA synthesis. *J Virol* 65: 985-988.
29. De I, Sawicki SG, Sawicki DL (1996) Sindbis virus RNA-negative mutants that fail to convert from minus-strand to plus-strand synthesis: role of the nsP2 protein. *J Virol* 70: 2706-2719.
30. Hahn YS, Strauss EG, Strauss JH (1989) Mapping of RNA- temperature-sensitive mutants of Sindbis virus: assignment of complementation groups A, B, and G to nonstructural proteins. *J Virol* 63: 3142-3150.
31. Suopanki J, Sawicki DL, Sawicki SG, Kaariainen L (1998) Regulation of alphavirus 26S mRNA transcription by replicase component nsP2. *J Gen Virol* 79 (Pt 2): 309-319.
32. Bird LE, Subramanya HS, Wigley DB (1998) Helicases: a unifying structural theme? *Curr Opin Struct Biol* 8: 14-18.
33. Gomez de Cedron M, Ehsani N, Mikkola ML, Garcia JA, Kaariainen L (1999) RNA helicase activity of Semliki Forest virus replicase protein NSP2. *FEBS Lett* 448: 19-22.
34. Takkinen K (1986) Complete nucleotide sequence of the nonstructural protein genes of Semliki Forest virus. *Nucleic Acids Res* 14: 5667-5682.
35. Ulmanen I (1978) Assembly of Semliki Forest virus nucleocapsid: detection of a precursor in infected cells. *J Gen Virol* 41: 353-365.
36. Vasiljeva L, Valmu L, Kaariainen L, Merits A (2001) Site-specific protease activity of the carboxyl-terminal domain of Semliki Forest virus replicase protein nsP2. *J Biol Chem* 276: 30786-30793.
37. Fazakerley JK, Boyd A, Mikkola ML, Kaariainen L (2002) A single amino acid change in the nuclear localization sequence of the nsP2 protein affects the neurovirulence of Semliki Forest virus. *J Virol* 76: 392-396.
38. Peranen J, Rikkonen M, Liljestrom P, Kaariainen L (1990) Nuclear localization of Semliki Forest virus-specific nonstructural protein nsP2. *J Virol* 64: 1888-1896.
39. Kaariainen L, Ahola T (2002) Functions of alphavirus nonstructural proteins in RNA replication. *Prog Nucleic Acid Res Mol Biol* 71: 187-222.
40. Varjak M, Zusinaite E, Merits A (2010) Novel Functions of the Alphavirus Nonstructural Protein nsP3 C-Terminal Region. *J Virol* 84: 2352-2364.
41. Li GP, Rice CM (1993) The signal for translational readthrough of a UGA codon in Sindbis virus RNA involves a single cytidine residue immediately downstream of the termination codon. *J Virol* 67: 5062-5067.
42. Koonin EV, Dolja VV (1993) Evolution and taxonomy of positive-strand RNA viruses: implications of comparative analysis of amino acid sequences. *Crit Rev Biochem Mol Biol* 28: 375-430.

43. O'Reilly EK, Kao CC (1998) Analysis of RNA-dependent RNA polymerase structure and function as guided by known polymerase structures and computer predictions of secondary structure. *Virology* 252: 287-303.
44. Aliperti G, Schlesinger MJ (1978) Evidence for an autoprotease activity of sindbis virus capsid protein. *Virology* 90: 366-369.
45. Frolov I, Hardy R, Rice CM (2001) Cis-acting RNA elements at the 5' end of Sindbis virus genome RNA regulate minus- and plus-strand RNA synthesis. *Rna* 7: 1638-1651.
46. Hardy RW (2006) The role of the 3' terminus of the Sindbis virus genome in minus-strand initiation site selection. *Virology* 345: 520-531.
47. Kuhn RJ, Hong Z, Strauss JH (1990) Mutagenesis of the 3' nontranslated region of Sindbis virus RNA. *J Virol* 64: 1465-1476.
48. Lemm JA, Rice CM (1993) Roles of nonstructural polyproteins and cleavage products in regulating Sindbis virus RNA replication and transcription. *J Virol* 67: 1916-1926.
49. Lemm JA, Rice CM (1993) Assembly of functional Sindbis virus RNA replication complexes: requirement for coexpression of P123 and P34. *J Virol* 67: 1905-1915.
50. Garoff H, Huylebroeck D, Robinson A, Tillman U, Liljestrom P (1990) The signal sequence of the p62 protein of Semliki Forest virus is involved in initiation but not in completing chain translocation. *J Cell Biol* 111: 867-876.
51. Sefton BM (1977) Immediate glycosylation of Sindbis virus membrane proteins. *Cell* 10: 659-668.
52. Liljestrom P, Garoff H (1991) Internally located cleavable signal sequences direct the formation of Semliki Forest virus membrane proteins from a polyprotein precursor. *J Virol* 65: 147-154.
53. Mulvey M, Brown DT (1996) Assembly of the Sindbis virus spike protein complex. *Virology* 219: 125-132.
54. de Curtis I, Simons K (1988) Dissection of Semliki Forest virus glycoprotein delivery from the trans-Golgi network to the cell surface in permeabilized BHK cells. *Proc Natl Acad Sci U S A* 85: 8052-8056.
55. Skoging U, Vihinen M, Nilsson L, Liljestrom P (1996) Aromatic interactions define the binding of the alphavirus spike to its nucleocapsid. *Structure* 4: 519-529.
56. Zhang W, Mukhopadhyay S, Pletnev SV, Baker TS, Kuhn RJ, Rossmann MG (2002) Placement of the structural proteins in Sindbis virus. *J Virol* 76: 11645-11658.
57. Liljestrom P, Lusa S, Huylebroeck D, Garoff H (1991) In vitro mutagenesis of a full-length cDNA clone of Semliki Forest virus: the small 6,000-molecular-weight membrane protein modulates virus release. *J Virol* 65: 4107-4113.
58. Garoff H, Hewson R, Opstelten DJ (1998) Virus maturation by budding. *Microbiol Mol Biol Rev* 62: 1171-1190.

59. Ou JH, Strauss EG, Strauss JH (1983) The 5'-terminal sequences of the genomic RNAs of several alphaviruses. *J Mol Biol* 168: 1-15.
60. Niesters HG, Strauss JH (1990) Mutagenesis of the conserved 51-nucleotide region of Sindbis virus. *J Virol* 64: 1639-1647.
61. Niesters HG, Strauss JH (1990) Defined mutations in the 5' nontranslated sequence of Sindbis virus RNA. *J Virol* 64: 4162-4168.
62. Fayzuln R, Frolov I (2004) Changes of the secondary structure of the 5' end of the Sindbis virus genome inhibit virus growth in mosquito cells and lead to accumulation of adaptive mutations. *J Virol* 78: 4953-4964.
63. Gorchakov R, Hardy R, Rice CM, Frolov I (2004) Selection of functional 5' cis-acting elements promoting efficient sindbis virus genome replication. *J Virol* 78: 61-75.
64. Kulasegaran-Shylini R, Atasheva S, Gorenstein DG, Frolov I (2009) Structural and functional elements of the promoter encoded by the 5' untranslated region of the Venezuelan equine encephalitis virus genome. *J Virol* 83: 8327-8339.
65. Ou JH, Rice CM, Dalgarno L, Strauss EG, Strauss JH (1982) Sequence studies of several alphavirus genomic RNAs in the region containing the start of the subgenomic RNA. *Proc Natl Acad Sci U S A* 79: 5235-5239.
66. Levis R, Schlesinger S, Huang HV (1990) Promoter for Sindbis virus RNA-dependent subgenomic RNA transcription. *J Virol* 64: 1726-1733.
67. Hardy RW, Rice CM (2005) Requirements at the 3' end of the sindbis virus genome for efficient synthesis of minus-strand RNA. *J Virol* 79: 4630-4639.
68. Weaver SC, Ferro C, Barrera R, Boshell J, Navarro JC (2004) Venezuelan Equine Encephalitis. *Annu Rev Entomol* 49: 141-174.
69. Brault AC, Powers AM, Weaver SC (2002) Vector infection determinants of Venezuelan equine encephalitis virus reside within the E2 envelope glycoprotein. *J Virol* 76: 6387-6392.
70. Oberste MS, Fraire M, Navarro R, Zepeda C, Zarate ML, Ludwig GV, Kondig JF, Weaver SC, Smith JF, Rico-Hesse R (1998) Association of Venezuelan equine encephalitis virus subtype IE with two equine epizootics in Mexico. *Am J Trop Med Hyg* 59: 100-107.
71. Walton TE, Alvarez O, Buckwalter PM, Johnson KM (1973) Experimental infection of horses with enzootic and epizootic strains of Venezuelan equine encephalomyelitis virus. *J Infect Dis* 128: 271-282.
72. de la Monte SM, Castro F, Bonilla NS, de Urdaneta AG, Hutchins GM (1985) The systemic pathology of Venezuelan equine encephalitis in humans. *Am J Trop Med Hyg* 34: 194-202.
73. Lord RD (1974) History and geographic distribution of Venezuelan equine encephalitis. *Bull Pan Am Health Organ* 8: 100-110.
74. Beck CE, Wyckoff RW (1938) Venezuelan equine encephalomyelitis. *Science* 88: 530.

75. Sanmartin-Barberi C, Groot H, Osorno-Mesa E (1954) Human epidemic in Colombia caused by the Venezuelan equine encephalomyelitis virus. *Am J Trop Med Hyg* 3: 283-293.
76. Weaver SC, Pfeiffer M, Marriott K, Kang W, Kinney RM (1999) Genetic evidence for the origins of Venezuelan equine encephalitis virus subtype IAB outbreaks. *Am J Trop Med Hyg* 60: 441-448.
77. Groot H. The health and economic impact of Venezuelan equine encephalitis; 1972; Washington, DC. Pan Am. Health Org.
78. Rico-Hesse R, Weaver SC, de Siger J, Medina G, Salas RA (1995) Emergence of a new epidemic/epizootic Venezuelan equine encephalitis virus in South America. *Proc Natl Acad Sci U S A* 92: 5278-5281.
79. Anishchenko M, Bowen RA, Paessler S, Austgen L, Greene IP, Weaver SC (2006) Venezuelan encephalitis emergence mediated by a phylogenetically predicted viral mutation. *Proc Natl Acad Sci U S A* 103: 4994-4999.
80. Rivas F, Diaz LA, Cardenas VM, Daza E, Bruzon L, Alcala A, De la Hoz O, Caceres FM, Aristizabal G, Martinez JW, et al. (1997) Epidemic Venezuelan equine encephalitis in La Guajira, Colombia, 1995. *J Infect Dis* 175: 828-832.
81. Rosenbloom M, Leikin JB, Vogel SN, Chaudry ZA (2002) Biological and chemical agents: a brief synopsis. *Am J Ther* 9: 5-14.
82. Lamb A (2001) Biological weapons: the facts not the fiction. *Clin Med* 1: 502-504.
83. Berge TO, Bankds IS, Tigertt WD (1961) Attenuation of Venezuelan equine encephalomyelitis virus by in vitro cultivation in guinea pig heart cells. *Am J Hyg* 73: 209-218.
84. Kinney RM, Johnson BJ, Welch JB, Tsuchiya KR, Trent DW (1989) The full-length nucleotide sequences of the virulent Trinidad donkey strain of Venezuelan equine encephalitis virus and its attenuated vaccine derivative, strain TC-83. *Virology* 170: 19-30.
85. Alevizatos AC, McKinney RW, Feigin RD (1967) Live, attenuated Venezuelan equine encephalomyelitis virus vaccine. I. Clinical effects in man. *Am J Trop Med Hyg* 16: 762-768.
86. Burke DS, Ramsburg HH, Edelman R (1977) Persistence in humans of antibody to subtypes of Venezuelan equine encephalomyelitis (VEE) virus after immunization with attenuated (TC-83) VEE virus vaccine. *J Infect Dis* 136: 354-359.
87. McKinney RW, Berge TO, Sawyer WD, Tigertt WD, Crozier D (1963) Use of an Attenuated Strain of Venezuelan Equine Encephalomyelitis Virus for Immunization in Man. *Am J Trop Med Hyg* 12: 597-603.
88. McKinney RW (1972) Venezuelan equine encephalitis. *Pan American Health Organization* 243: 369-376.
89. Johnson KM, Martin DH (1974) Venezuelan equine encephalitis. *Adv Vet Sci Comp Med* 18: 79-116.

90. Pittman PR, Makuch RS, Mangiafico JA, Cannon TL, Gibbs PH, Peters CJ (1996) Long-term duration of detectable neutralizing antibodies after administration of live-attenuated VEE vaccine and following booster vaccination with inactivated VEE vaccine. *Vaccine* 14: 337-343.
91. Kenney JL, Volk SM, Pandya J, Wang E, Liang X, Weaver SC (2011) Stability of RNA virus attenuation approaches. *Vaccine* 29: 2230-2234.
92. Ludwig G, Turell MJ, Vogel P, Kondig JP, Kell WK, al. e (2001) Comparative neurovirulence of attenuated and non-attenuated strains of Venezuelan equine encephalitis virus in mice. *Am J Trop Med Hyg* 64: 49-55.
93. Fine DL, Roberts BA, Terpening SJ, Mott J, Vasconcelos D, House RV (2008) Neurovirulence evaluation of Venezuelan equine encephalitis (VEE) vaccine candidate V3526 in nonhuman primates. *Vaccine* 26: 3497-3506.
94. Sharma A, Gupta P, Glass PJ, Parker MD, Maheshwari RK (2011) Safety and protective efficacy of INA-inactivated Venezuelan equine encephalitis virus: implication in vaccine development. *Vaccine* 29: 953-959.
95. Wang E, Bowen RA, Medina G, Powers AM, Kang W, Chandler LM, Shope RE, Weaver SC (2001) Virulence and viremia characteristics of 1992 epizootic subtype IC Venezuelan equine encephalitis viruses and closely related enzootic subtype ID strains. *Am J Trop Med Hyg* 65: 64-69.
96. Chamberlain RW. Venezuelan equine encephalitis: infection of mosquitoes and transmission. ; 1971; Washington, DC Pan American Health Organization. pp. 144-154.
97. Grayson MA, Galindo P (1972) Experimental transmission of Venezuelan equine encephalitis virus by *Deinocerites pseudus* Dyar and Knab, 1909. *J Med Entomol* 9: 196-200.
98. Sellers RF, Bergold GH, Suarez OM, Morales A (1965) Investigations During Venezuelan Equine Encephalitis Outbreaks in Venezuela--1962-1964. *Am J Trop Med Hyg* 14: 460-469.
99. Sudia WD, Newhouse VF, Beadle ID, Miller DL, Johnston JG, Jr., Young R, Calisher CH, Maness K (1975) Epidemic Venezuelan equine encephalitis in North America in 1971: vector studies. *Am J Epidemiol* 101: 17-35.
100. Walton TE, Grayson MA (1989) Venezuelan equine encephalomyelitis. In: Monath TP, editor. *The Arboviruses: Epidemiology and Ecology*. Boca Raton, FL: CRC.
101. Turell MJ, Barth J, Coleman RE (1999) Potential for Central American mosquitoes to transmit epizootic and enzootic strains of Venezuelan equine encephalitis virus. *J Am Mosq Control Assoc* 15: 295-298.
102. Kramer LD, Scherer WF (1976) Vector competence of mosquitoes as a marker to distinguish Central American and Mexican epizootic from enzootic strains of Venezuelan encephalitis virus. *Am J Trop Med Hyg* 25: 336-346.
103. Deardorff ER, Forrester NL, Travassos-da-Rosa AP, Estrada-Franco JG, Navarro-Lopez R, Tesh RB, Weaver SC (2009) Experimental infection of potential

- reservoir hosts with Venezuelan equine encephalitis virus, Mexico. *Emerg Infect Dis* 15: 519-525.
104. Carrara AS, Coffey LL, Aguilar PV, Moncayo AC, Da Rosa AP, Nunes MR, Tesh RB, Weaver SC (2007) Venezuelan equine encephalitis virus infection of cotton rats. *Emerg Infect Dis* 13: 1158-1165.
 105. Carrara AS, Gonzales G, Ferro C, Tamayo M, Aronson J, Paessler S, Anishchenko M, Boshell J, Weaver SC (2005) Venezuelan equine encephalitis virus infection of spiny rats. *Emerg Infect Dis* 11: 663-669.
 106. Deardorff ER, Weaver SC (2010) Vector competence of *Culex* (*Melanoconion*) *taeniopus* for equine-virulent subtype IE strains of Venezuelan equine encephalitis virus. *Am J Trop Med Hyg* 82: 1047-1052.
 107. Scherer WF, Cupp EW, Dziem GM, Breener RJ, Ordonez JV (1982) Mesenteronal infection threshold of an epizootic strain of Venezuelan encephalitis virus in *Culex* (*Melanoconion*) *taeniopus* mosquitoes and its implication to the apparent disappearance of this virus strain from an enzootic habitat in Guatemala. *Am J Trop Med Hyg* 31: 1030-1037.
 108. Scherer WF, Weaver SC, Taylor CA, Cupp EW, Dickerman RW, Rubino HH (1987) Vector competence of *Culex* (*Melanoconion*) *taeniopus* for allopatric and epizootic Venezuelan equine encephalomyelitis viruses. *Am J Trop Med Hyg* 36: 194-197.
 109. Weaver SC (1986) Electron microscopic analysis of infection patterns for Venezuelan equine encephalomyelitis virus in the vector mosquito, *Culex* (*Melanoconion*) *taeniopus*. *Am J Trop Med Hyg* 35: 624-631.
 110. Weaver SC, Scherer WF, Cupp EW, Castello DA (1984) Barriers to dissemination of venezuelan encephalitis viruses in the middle american enzootic vector mosquito, *Culex* (*Melanoconion*) *taeniopus*. *Am J Trop Med Hyg* 33: 953-960.
 111. Scherer WF, Cupp EW, Lok JB, Brenner RJ, Ordonez JV (1981) Intestinal threshold of an enzootic strain of Venezuelan encephalitis virus in *Culex* (*Melanoconion*) *taeniopus* mosquitoes and its implications to vector competency and vertebrate amplifying hosts. *Am J Trop Med Hyg* 30: 862-869.
 112. Ferro C, Boshell J, Moncayo AC, Gonzalez M, Ahumada ML, Kang W, Weaver SC (2003) Natural enzootic vectors of Venezuelan equine encephalitis virus, Magdalena Valley, Colombia. *Emerg Infect Dis* 9: 49-54.
 113. Aitken TH (1972) Habits of some mosquito hosts of VEE (Mucambo) virus from northeastern South America, including Trinidad. *Proceedings of workshop-symposium on Venezuelan encephalitis virus*. Washington, DC. pp. 254-256.
 114. Chamberlain RW, Sudia WD, Coleman PH, Work TH (1964) Venezuelan Equine Encephalitis Virus from South Florida. *Science* 145: 272-274.
 115. Galindo P, Grayson MA (1971) *Culex* (*Melanoconion*) *aikenii*: natural vector in Panama of endemic Venezuelan encephalitis. *Science* 172: 594-595.

116. Galindo P, Grayson MA. Endemic vectors of Venezuelan encephalitis; 1972; Washington: Pan American Health Organization. Scientific Publ. pp. 249-253.
117. Ortiz DI, Anishchenko M, Weaver SC (2005) Susceptibility of *Psorophora confinnis* (Diptera: Culicidae) to infection with epizootic (subtype IC) and enzootic (subtype ID) Venezuelan Equine encephalitis viruses. *J Med Entomol* 42: 857-863.
118. Calisher CH, Maness KC (1974) Virulence of Venezuelan equine encephalomyelitis virus subtypes for various laboratory hosts. *Appl Microbiol* 28: 881-884.
119. Scherer WF, Chin J (1977) Responses of guinea pigs to infections with strains of Venezuelan encephalitis virus, and correlations with equine virulence. *Am J Trop Med Hyg* 26: 307-312.
120. Walton TE, Alvarez O, Jr., Buckwalter RM, Johnson KM (1972) Experimental infection of horses with an attenuated Venezuelan equine encephalomyelitis vaccine (strain TC-83). *Infect Immun* 5: 750-756.
121. Walton TE, Alvarez O, Jr., Buckwalter RM, Johnson KM (1973) Experimental infection of horses with enzootic and epizootic strains of Venezuelan equine encephalomyelitis virus. *J Infect Dis* 128: 271-282.
122. Gonzalez-Salazar D, Estrada-Franco JG, Carrara AS, Aronson JF, Weaver SC (2003) Equine amplification and virulence of subtype IE Venezuelan equine encephalitis viruses isolated during the 1993 and 1996 Mexican epizootics. *Emerg Infect Dis* 9: 161-168.
123. Jahrling PB, Scherer F (1973) Histopathology and distribution of viral antigens in hamsters infected with virulent and benign Venezuelan encephalitis viruses. *Am J Pathol* 72: 25-38.
124. Jahrling PB, Scherer WF (1973) Growth curves and clearance rates of virulent and benign Venezuelan encephalitis viruses in hamsters. *Infect Immun* 8: 456-462.
125. Greene IP, Paessler S, Anishchenko M, Smith DR, Brault AC, Frolov I, Weaver SC (2005) Venezuelan equine encephalitis virus in the guinea pig model: evidence for epizootic virulence determinants outside the E2 envelope glycoprotein gene. *Am J Trop Med Hyg* 72: 330-338.
126. Martin DH, Dietz WH, Alvarez O, Jr., Johnson KM (1982) Epidemiological significance of Venezuelan equine encephalomyelitis virus in vitro markers. *Am J Trop Med Hyg* 31: 561-568.
127. Spotts DR, Reich RM, Kalkhan MA, Kinney RM, Roehrig JT (1998) Resistance to alpha/beta interferons correlates with the epizootic and virulence potential of Venezuelan equine encephalitis viruses and is determined by the 5' noncoding region and glycoproteins. *J Virol* 72: 10286-10291.
128. Eldridge BF (2005) Mosquitoes, the Culicidae. In: Marquardt WC, editor. *Biology of Disease Vectors*. second ed. Amsterdam: Elsevier Academic Press.

129. Clements AN (2000) Mosquitoes: life cycle, biology, disease transmission. The biology of mosquitoes: development, nutrition and reproduction. New York, NY: CABI publishing. pp. xiii-xxii.
130. Nielsen ET, Nielsen AT (1953) Field Observations on the Habits of *Aedes Taeniorhynchus*. *Ecology* 34: 141-156.
131. Sirivanakarn S (1982) A review of the systematics and a proposed scheme of internal classification of the new world subgenus *Melanoconion* of *Culex* (Diptera; Culicidae). *Mosquito Systematics* 14: 265-333.
132. Christophers SR (1901) Anatomy and histology of the adult female mosquito. London: Harrison and Sons. 20 p.
133. Romoser WS, Faran ME, Bailey CL (1987) Newly recognized route of arbovirus dissemination from the mosquito (Diptera: Culicidae) midgut. *J Med Entomol* 24: 431-432.
134. Jobling B, Lewis DJ (1987) Anatomical Drawings of biting flies. London: British Museum (Natural History).
135. Volkman LE (1997) Nucleopolyhedrovirus interactions with their insect hosts. *Adv Virus Res* 48: 313-348.
136. Wigglesworth VB (1977) Structural changes in the epidermal cells of *Rhodnius* during tracheole capture. *J Cell Sci* 26: 161-174.
137. Maina J (1989) Scanning and transmission electron microscopic study of tracheal air sac system in a grasshopper *Chrotogonus senegalensis* (Kraus) - Orthoptera: Acrididae: Pyrgomorphae. *Anatomical Record* 223: 393-405.
138. Houk EJ, Obie F, Hardy JL (1979) Peritrophic membrane formation and the midgut barrier to arboviral infection in the mosquito, *Culex tarsalis* Coquillett (Insecta, Diptera). *Acta Trop* 36: 39-45.
139. Scherer WF, Weaver SC, Taylor CA, Cupp EW (1986) Vector incompetency: its implication in the disappearance of epizootic Venezuelan equine encephalomyelitis virus from Middle America. *J Med Entomol* 23: 23-29.
140. Hardy JL, Reeves WC, Sjogren RD (1976) Variations in the susceptibility of field and laboratory populations of *Culex tarsalis* to experimental infection with western equine encephalomyelitis virus. *Am J Epidemiol* 103: 498-505.
141. Houk EJ, Arcus YM, Hardy JL, Kramer LD (1990) Binding of western equine encephalomyelitis virus to brush border fragments isolated from mesenteron epithelial cells of mosquitoes. *Virus Res* 17: 105-117.
142. Klimstra WB, Nangle EM, Smith MS, Yurochko AD, Ryman KD (2003) DC-SIGN and L-SIGN can act as attachment receptors for alphaviruses and distinguish between mosquito cell- and mammalian cell-derived viruses. *J Virol* 77: 12022-12032.
143. Reddy J, Locke M (1990) The size limited penetration of gold particles through insect basal laminae. *J Insect Physiol* 36: 397-408.

144. Miles JA, Pillai JS, Maguire T (1973) Multiplication of Whataroa virus in mosquitoes. *J Med Entomol* 10: 176-185.
145. Kramer LD, Hardy JL, Presser SB (1983) Effect of temperature of extrinsic incubation on the vector competence of *Culex tarsalis* for western equine encephalomyelitis virus. *Am J Trop Med Hyg* 32: 1130-1139.
146. Reisen WK, Meyer RP, Presser SB, Hardy JL (1993) Effect of temperature on the transmission of western equine encephalomyelitis and St. Louis encephalitis viruses by *Culex tarsalis* (Diptera: Culicidae). *J Med Entomol* 30: 151-160.
147. Reinhardt C, Hecker H (1973) Structure and function of the basal lamina and of the cell junctions in the midgut epithelium (stomach) of female *Aedes aegypti* L. (Insecta, Diptera). *Acta Trop* 30: 213-236.
148. Hecker H, Freyvogel TA, Briegel H, Steiger R (1971) The ultrastructure of midgut epithelium in *Aedes aegypti* (L). (Insecta, Diptera) males. *Acta Trop* 28: 275-290.
149. Weaver SC, Lorenz LH, Scott TW (1992) Pathologic changes in the midgut of *Culex tarsalis* following infection with Western equine encephalomyelitis virus. *Am J Trop Med Hyg* 47: 691-701.
150. Weaver SC, Scott TW, Lorenz LH, Lerdthusnee K, Romoser WS (1988) Togavirus-associated pathologic changes in the midgut of a natural mosquito vector. *J Virol* 62: 2083-2090.
151. Weaver SC, Scott TW, Lorenz LH, Repik PM (1991) Detection of eastern equine encephalomyelitis virus deposition in *Culiseta melanura* following ingestion of radiolabeled virus in blood meals. *Am J Trop Med Hyg* 44: 250-259.
152. Romoser WS, Wasieloski LP, Jr., Pushko P, Kondig JP, Lerdthusnee K, Neira M, Ludwig GV (2004) Evidence for arbovirus dissemination conduits from the mosquito (Diptera: Culicidae) midgut. *J Med Entomol* 41: 467-475.
153. Smith DR, Arrigo NC, Leal G, Muehlberger LE, Weaver SC (2007) Infection and dissemination of Venezuelan equine encephalitis virus in the epidemic mosquito vector, *Aedes taeniorhynchus*. *Am J Trop Med Hyg* 77: 176-187.
154. Weaver SC, Lorenz LH, Scott TW (1993) Distribution of western equine encephalomyelitis virus in the alimentary tract of *Culex tarsalis* (Diptera: Culicidae) following natural and artificial blood meals. *J Med Entomol* 30: 391-397.
155. Volkman L (1997) Nucleopolyhedrovirus interactions with their insect hosts. *Adv Virus Res* 48: 313-348.
156. Hecker H (1977) Structure and function of midgut epithelial cells in culicidae mosquitoes (insecta, diptera). *Cell Tissue Res* 184: 321-341.
157. Barrett JW, Brownwright AJ, Primavera MJ, Palli SR (1998) Studies of the nucleopolyhedrovirus infection process in insects by using the green fluorescence protein as a reporter. *J Virol* 72: 3377-3382.

158. Engelhard EK, Kam-Morgan LN, Washburn JO, Volkman LE (1994) The insect tracheal system: a conduit for the systemic spread of *Autographa californica* M nuclear polyhedrosis virus. *Proc Natl Acad Sci U S A* 91: 3224-3227.
159. Kirkpatrick BA, Washburn JO, Engelhard EK, Volkman LE (1994) Primary infection of insect tracheae by *Autographa californica* M nuclear polyhedrosis virus. *Virology* 203: 184-186.
160. Bowers DF, Abell BA, Brown DT (1995) Replication and tissue tropism of the alphavirus Sindbis in the mosquito *Aedes albopictus*. *Virology* 212: 1-12.
161. Smith DR, Adams AP, Kenney JL, Wang E, Weaver SC (2008) Venezuelan equine encephalitis virus in the mosquito vector *Aedes taeniorhynchus*: infection initiated by a small number of susceptible epithelial cells and a population bottleneck. *Virology* 372: 176-186.
162. Aguilar PV, Estrada-Franco JG, Navarro-Lopez R, Ferro C, Haddow AD, Weaver SC (2011) Endemic Venezuelan equine encephalitis in the Americas: hidden under the dengue umbrella. *Future Virol* 6: 721-740.
163. Aguilar PV, Adams AP, Suarez V, Beingolea L, Vargas J, Manock S, Freire J, Espinoza WR, Felices V, Diaz A, et al. (2009) Genetic characterization of Venezuelan equine encephalitis virus from Bolivia, Ecuador and Peru: identification of a new subtype ID lineage. *PLoS Negl Trop Dis* 3: e514.
164. Atasheva S, Wang E, Adams AP, Plante KS, Ni S, Taylor K, Miller ME, Frolov I, Weaver SC (2009) Chimeric alphavirus vaccine candidates protect mice from intranasal challenge with western equine encephalitis virus. *Vaccine* 27: 4309-4319.
165. Paessler S, Fayzulin RZ, Anishchenko M, Greene IP, Weaver SC, Frolov I (2003) Recombinant sindbis/Venezuelan equine encephalitis virus is highly attenuated and immunogenic. *J Virol* 77: 9278-9286.
166. Wang E, Petrakova O, Adams AP, Aguilar PV, Kang W, Paessler S, Volk SM, Frolov I, Weaver SC (2007) Chimeric Sindbis/eastern equine encephalitis vaccine candidates are highly attenuated and immunogenic in mice. *Vaccine* 25: 7573-7581.
167. Kim DY, Atasheva S, Foy NJ, Wang E, Frolova EI, Weaver S, Frolov I (2011) Design of chimeric alphaviruses with a programmed, attenuated, cell type-restricted phenotype. *J Virol* 85: 4363-4376.
168. Wang E, Kim DY, Weaver SC, Frolov I (2011) Chimeric chikungunya viruses are nonpathogenic in highly sensitive mouse models but efficiently induce a protective immune response. *J Virol* 85: 9249-9252.
169. Wang E, Volkova E, Adams AP, Forrester N, Xiao SY, Frolov I, Weaver SC (2008) Chimeric alphavirus vaccine candidates for chikungunya. *Vaccine* 26: 5030-5039.
170. Kuhn RJ, Griffin DE, Owen KE, Niesters HG, Strauss JH (1996) Chimeric Sindbis-Ross River viruses to study interactions between alphavirus nonstructural and structural regions. *J Virol* 70: 7900-7909.

171. Powers AM, Brault AC, Kinney RM, Weaver SC (2000) The use of chimeric Venezuelan equine encephalitis viruses as an approach for the molecular identification of natural virulence determinants. *J Virol* 74: 4258-4263.
172. Kinney RM, Chang GJ, Tsuchiya KR, Sneider JM, Roehrig JT, Woodward TM, Trent DW (1993) Attenuation of Venezuelan equine encephalitis virus strain TC-83 is encoded by the 5'-noncoding region and the E2 envelope glycoprotein. *J Virol* 67: 1269-1277.
173. Davis NL, Powell N, Greenwald GF, Willis LV, Johnson BJ, Smith JF, Johnston RE (1991) Attenuating mutations in the E2 glycoprotein gene of Venezuelan equine encephalitis virus: construction of single and multiple mutants in a full-length cDNA clone. *Virology* 183: 20-31.
174. Breslauer KJ, Frank R, Blocker H, Marky LA (1986) Predicting DNA duplex stability from the base sequence. *Proc Natl Acad Sci U S A* 83: 3746-3750.
175. Owczarzy R, You Y, Moreira BG, Manthey JA, Huang L, Behlke MA, Walder JA (2004) Effects of sodium ions on DNA duplex oligomers: improved predictions of melting temperatures. *Biochemistry* 43: 3537-3554.
176. Brault AC, Foy BD, Myles KM, Kelly CL, Higgs S, Weaver SC, Olson KE, Miller BR, Powers AM (2004) Infection patterns of o'nyong nyong virus in the malaria-transmitting mosquito, *Anopheles gambiae*. *Insect Mol Biol* 13: 625-635.
177. Tsetsarkin K, Higgs S, McGee CE, De Lamballerie X, Charrel RN, Vanlandingham DL (2006) Infectious clones of Chikungunya virus (La Reunion isolate) for vector competence studies. *Vector Borne Zoonotic Dis* 6: 325-337.
178. Foy BD, Myles KM, Pierro DJ, Sanchez-Vargas I, Uhlirova M, Jindra M, Beaty BJ, Olson KE (2004) Development of a new Sindbis virus transducing system and its characterization in three Culicine mosquitoes and two Lepidopteran species. *Insect Mol Biol* 13: 89-100.
179. Pierro DJ, Myles KM, Foy BD, Beaty BJ, Olson KE (2003) Development of an orally infectious Sindbis virus transducing system that efficiently disseminates and expresses green fluorescent protein in *Aedes aegypti*. *Insect Mol Biol* 12: 107-116.
180. Romoser WS, Turell MJ, Lerdthusnee K, Neira M, Dohm D, Ludwig G, Wasieloski L (2005) Pathogenesis of Rift Valley fever virus in mosquitoes--tracheal conduits & the basal lamina as an extra-cellular barrier. *Arch Virol Suppl*: 89-100.
181. Bredenbeek PJ, Frolov I, Rice CM, Schlesinger S (1993) Sindbis virus expression vectors: packaging of RNA replicons by using defective helper RNAs. *J Virol* 67: 6439-6446.
182. Turell MJ, Jones JW, Sardelis MR, Dohm DJ, Coleman RE, Watts DM, Fernandez R, Calampa C, Klein TA (2000) Vector competence of Peruvian mosquitoes (Diptera: Culicidae) for epizootic and enzootic strains of Venezuelan equine encephalomyelitis virus. *J Med Entomol* 37: 835-839.

183. Sudia WD, Newhouse VF, Henderson BE (1971) Experimental infection of horses with three strains of Venezuelan equine encephalomyelitis virus. II. Experimental vector studies. *Am J Epidemiol* 93: 206-211.
184. Turell MJ, Ludwig GV, Beaman JR (1992) Transmission of Venezuelan equine encephalomyelitis virus by *Aedes sollicitans* and *Aedes taeniorhynchus* (Diptera: Culicidae). *J Med Entomol* 29: 62-65.
185. Turell MJ, O'Guinn ML, Navarro R, Romero G, Estrada-Franco JG (2003) Vector competence of Mexican and Honduran mosquitoes (Diptera: Culicidae) for enzootic (IE) and epizootic (IC) strains of Venezuelan equine encephalomyelitis virus. *J Med Entomol* 40: 306-310.
186. Turell MJ (1999) Vector competence of three Venezuelan mosquitoes (Diptera: Culicidae) for an epizootic IC strain of Venezuelan equine encephalitis virus. *J Med Entomol* 36: 407-409.
187. Brault AC, Powers AM, Ortiz D, Estrada-Franco JG, Navarro-Lopez R, Weaver SC (2004) Venezuelan equine encephalitis emergence: enhanced vector infection from a single amino acid substitution in the envelope glycoprotein. *Proc Natl Acad Sci U S A* 101: 11344-11349.
188. Voss JE, Vaney MC, Duquerroy S, Vonrhein C, Girard-Blanc C, Crublet E, Thompson A, Bricogne G, Rey FA (2010) Glycoprotein organization of Chikungunya virus particles revealed by X-ray crystallography. *Nature* 468: 709-712.
189. Weaver SC, Bellew LA, Rico-Hesse R (1992) Phylogenetic analysis of alphaviruses in the Venezuelan equine encephalitis complex and identification of the source of epizootic viruses. *Virology* 191: 282-290.
190. Austin FJ, Scherer WF (1971) Studies of viral virulence. I. Growth and histopathology of virulent and attenuated strains of Venezuelan encephalitis virus in hamsters. *Am J Pathol* 62: 195-210.
191. Houk EJ, Hardy JL, Chiles RE (1981) Permeability of the midgut basal lamina in the mosquito, *Culex tarsalis* Coquillett (Insecta, Diptera). *Acta Trop* 38: 163-171.
192. Kramer LD, Hardy JL, Presser SB, Houk EJ (1981) Dissemination Barriers For Western Equine Encephalomyelitis Virus in *Culex Tarsalis* Infected After Ingestion of Low Viral Doses. *Am J Trop Med Hyg* 30: 190-197.
193. Weaver SC, Reisen WK (2010) Present and future arboviral threats. *Antiviral Res* 85: 328-345.
194. Estrada-Franco JG, Navarro-Lopez R, Freier JE, Cordova D, Clements T, Moncayo A, Kang W, Gomez-Hernandez C, Rodriguez-Dominguez G, Ludwig GV, et al. (2004) Venezuelan equine encephalitis virus, southern Mexico. *Emerg Infect Dis* 10: 2113-2121.
195. Garmashova N, Atasheva S, Kang W, Weaver SC, Frolova E, Frolov I (2007) Analysis of Venezuelan equine encephalitis virus capsid protein function in the inhibition of cellular transcription. *J Virol* 81: 13552-13565.

196. Fernandez Z, Moncayo AC, Carrara AS, Forattini OP, Weaver SC (2003) Vector competence of rural and urban strains of *Aedes* (*Stegomyia*) *albopictus* (Diptera: Culicidae) from Sao Paulo State, Brazil for IC, ID, and IF subtypes of Venezuelan equine encephalitis virus. *J Med Entomol* 40: 522-527.
197. Arrigo NC, Watts DM, Frolov I, Weaver SC (2008) Experimental infection of *Aedes sollicitans* and *Aedes taeniorhynchus* with two chimeric Sindbis/Eastern equine encephalitis virus vaccine candidates. *Am J Trop Med Hyg* 78: 93-97.
198. Darwin JR, Kenney JL, Weaver SC (2011) Transmission Potential of Two Chimeric Chikungunya Vaccine Candidates in the Urban Mosquito Vectors, *Aedes aegypti* and *Ae. albopictus*. *Am J Trop Med Hyg* 84: 1012-1015.
199. Kenney JL, Adams AP, Weaver SC (2010) Transmission potential of two chimeric western equine encephalitis vaccine candidates in *Culex tarsalis*. *Am J Trop Med Hyg* 82: 354-359.
200. Vanlandingham DL, Tsetsarkin K, Klingler KA, Hong C, McElroy KL, Lehane MJ, Higgs S (2006) Determinants of vector specificity of o'nyong nyong and chikungunya viruses in *Anopheles* and *Aedes* mosquitoes. *Am J Trop Med Hyg* 74: 663-669.
201. McElroy KL, Girard YA, McGee CE, Tsetsarkin KA, Vanlandingham DL, Higgs S (2008) Characterization of the antigen distribution and tissue tropisms of three phenotypically distinct yellow fever virus variants in orally infected *Aedes aegypti* mosquitoes. *Vector Borne Zoonotic Dis* 8: 675-687.
202. Ortiz DI, Weaver SC (2004) Susceptibility of *Ochlerotatus taeniorhynchus* (Diptera: Culicidae) to infection with epizootic (subtype IC) and enzootic (subtype ID) Venezuelan equine encephalitis viruses: evidence for epizootic strain adaptation. *J Med Entomol* 41: 987-993.
203. Weaver SC, Scherer WF, Taylor CA, Castello DA, Cupp EW (1986) Laboratory vector competence of *Culex* (*Melanoconion*) *cedeciei* for sympatric and allopatric Venezuelan equine encephalomyelitis viruses. *Am J Trop Med Hyg* 35: 619-623.
204. Hardy JL, Houk EJ, Kramer LD, Reeves WC (1983) Intrinsic factors affecting vector competence of mosquitoes for arboviruses. *Annu Rev Entomol* 28: 229-262.
205. Houk EJ, Kramer LD, Hardy JL, Presser SB (1986) An interspecific mosquito model for the mesenteron infection barrier to western equine encephalomyelitis virus (*Culex tarsalis* and *Culex pipiens*). *Am J Trop Med Hyg* 35: 632-641.
206. Chao L (1990) Fitness of RNA virus decreased by Muller's ratchet. *Nature* 348: 454-455.
207. Duarte E, Clarke D, Moya A, Domingo E, Holland J (1992) Rapid fitness losses in mammalian RNA virus clones due to Muller's ratchet. *Proc Natl Acad Sci U S A* 89: 6015-6019.

208. Escarmis C, Davila M, Charpentier N, Bracho A, Moya A, Domingo E (1996) Genetic lesions associated with Muller's ratchet in an RNA virus. *J Mol Biol* 264: 255-267.
209. Novella IS, Elena SF, Moya A, Domingo E, Holland JJ (1995) Size of genetic bottlenecks leading to virus fitness loss is determined by mean initial population fitness. *J Virol* 69: 2869-2872.
210. Scott TW, Hildreth SW, Beaty BJ (1984) The distribution and development of eastern equine encephalitis virus in its enzootic mosquito vector, *Culiseta melanura*. *Am J Trop Med Hyg* 33: 300-310.
211. Chamberlain RW, Sudia WD (1961) Mechanism of transmission of viruses by mosquitoes. *Annu Rev Entomol* 6: 371-390.
212. McLintock J (1978) Mosquito-virus relationships of American encephalitides. *Annu Rev Entomol* 23: 17-37.
213. Boorman J (1960) Observations on the amount of virus present in the haemolymph of *Aedes aegypti* infected with Uganda S, yellow fever and Semliki Forest viruses. *Trans R Soc Trop Med Hyg* 54: 362-365.
214. Chandler LJ, Blair CD, Beaty BJ (1998) La Crosse virus infection of *Aedes triseriatus* (Diptera: Culicidae) ovaries before dissemination of virus from the midgut. *J Med Entomol* 35: 567-572.
215. Escobar K (2011) Personal communication. Galveston.
216. Romoser WS, Faran ME, Bailey CL, Lerdthusnee K (1992) An immunocytochemical study of the distribution of Rift Valley fever virus in the mosquito *Culex pipiens*. *Am J Trop Med Hyg* 46: 489-501.
217. Girard YA, Klingler KA, Higgs S (2004) West Nile virus dissemination and tissue tropisms in orally infected *Culex pipiens quinquefasciatus*. *Vector Borne Zoonotic Dis* 4: 109-122.
218. Houk EJ, Kramer LD, Hardy JL, Chiles RE (1985) Western equine encephalomyelitis virus: in vivo infection and morphogenesis in mosquito mesenteron epithelial cells. *Virus Res* 2: 123-138.
219. Weaver SC, Scott TW, Lorenz LH (1990) Patterns of eastern equine encephalomyelitis virus infection in *Culiseta melanura* (Diptera: Culicidae). *J Med Entomol* 27: 878-891.
220. McGee CE, Shustov AV, Tsetsarkin K, Frolov IV, Mason PW, Vanlandingham DL, Higgs S (2010) Infection, dissemination, and transmission of a West Nile virus green fluorescent protein infectious clone by *Culex pipiens quinquefasciatus* mosquitoes. *Vector Borne Zoonotic Dis* 10: 267-274.
221. Olson KE, Myles KM, Seabaugh RC, Higgs S, Carlson JO, Beaty BJ (2000) Development of a Sindbis virus expression system that efficiently expresses green fluorescent protein in midguts of *Aedes aegypti* following per os infection. *Insect Mol Biol* 9: 57-65.

222. Vanlandingham DL, Tsetsarkin K, Hong C, Klingler K, McElroy KL, Lehane MJ, Higgs S (2005) Development and characterization of a double subgenomic chikungunya virus infectious clone to express heterologous genes in *Aedes aegypti* mosquitoes. *Insect Biochem Mol Biol* 35: 1162-1170.
223. (2005) Arboviral Encephalitides. In: Disease CfDCaPDoV-BI, editor. Fact Sheet: Western Equine Encephalitis.
224. Hahn CS, Lustig S, Strauss EG, Strauss JH (1988) Western equine encephalitis virus is a recombinant virus. *Proc Natl Acad Sci U S A* 85: 5997-6001.
225. Weaver SC, Hagenbaugh A, Bellew LA, Netesov SV, Volchkov VE, Chang GJ, Clarke DK, Gousset L, Scott TW, Trent DW, et al. (1993) A comparison of the nucleotide sequences of eastern and western equine encephalomyelitis viruses with those of other alphaviruses and related RNA viruses. *Virology* 197: 375-390.
226. Forrester NL, Kenney JL, Deardorff E, Wang E, Weaver SC (2008) Western Equine Encephalitis submergence: lack of evidence for a decline in virus virulence. *Virology* 380: 170-172.
227. Zhang M, Fang Y, Brault AC, Reisen WK (2011) Variation in western equine encephalomyelitis viral strain growth in mammalian, avian, and mosquito cells fails to explain temporal changes in enzootic and epidemic activity in California. *Vector Borne Zoonotic Dis* 11: 269-275.
228. (2007) NIAID Category B Select Agents. NIAID Biodefense Research.
229. Reisen WK, Monath TP (1988) Western Equine Encephalomyelitis. Boca Raton, Florida: CRC Press.
230. Chamberlain RW (1962) Vector relationships of the arthropod-borne encephalitides in North America. *Ann NY Acad Sci* 70.
231. Hess A, Hayes R (1967) Seasonal dynamics of western encephalitis virus. *Am J Med Sci* 253.
232. Reeves WC, Hammon WM, Longshore WA, Jr., Mc CH, Geib AF (1962) Epidemiology of the arthropod-borne viral encephalitides in Kern County, California, 1943-1952. *Publ Public Health Univ Calif* 4: 1-257.
233. Hammon WM, Reeves WC, Gray M (1943) Mosquito Vectors and Inapparent Animal Reservoirs of St. Louis and Western Equine Encephalitis Viruses. *Am J Public Health Nations Health* 33: 201-207.
234. Jensen T, Washino RK (1991) An assessment of the biological capacity of a Sacramento Valley population of *Aedes melanimon* to vector arboviruses. *Am J Trop Med Hyg* 44: 355-363.
235. Hardy J, Reeves WC, Bruen JP, Presser SB (1979) Vector competence of *Culex tarsalis* and other mosquito species for western equine encephalomyelitis virus. *Arct Trop Arbo* 10.
236. Hardy JL, Bruen JP (1974) *Aedes melanimon* as a vector of WEE virus in California. *Proc Mosq Control Assoc* 42.

237. Kramer LD, Reisen WK, Chiles RE (1998) Vector competence of *Aedes dorsalis* (Diptera: Culicidae) from Morro Bay, California, for western equine encephalomyelitis virus. *J Med Entomol* 35: 1020-1024.
238. Reisen WK, Lothrop HD, Chiles RE (1998) Ecology of *Aedes dorsalis* (Diptera: Culicidae) in relation to western equine encephalomyelitis virus in the Coachella Valley of California. *J Med Entomol* 35: 561-566.
239. Hardy JL (1987) The ecology of western equine encephalomyelitis virus in the Central Valley of California, 1945-1985. *Am J Trop Med Hyg* 37: 18S-32S.
240. Olson JG, Reeves WC, Emmons RW, Milby MM (1979) Correlation of *Culex tarsalis* population indices with the incidence of St. Louis encephalitis and western equine encephalomyelitis in California. *Am J Trop Med Hyg* 28: 335-343.
241. Aguilar PV, Paessler S, Carrara AS, Baron S, Poast J, Wang E, Moncayo AC, Anishchenko M, Watts D, Tesh RB, et al. (2005) Variation in interferon sensitivity and induction among strains of eastern equine encephalitis virus. *J Virol* 79: 11300-11310.
242. Frolova E, Frolov I, Schlesinger S (1997) Packaging signals in alphaviruses. *J Virol* 71: 248-258.
243. Atasheva S, Wang E, Adams AP, Plant KS, Ni S, Taylor K, Miller ME, Frolov I, Weaver SC (2009) Chimeric alphavirus vaccine candidates provide complete protection in mice after intranasal challenge with western equine encephalitis virus. Vaccine: under review.
244. Fine PEM, Carneiro IAM (1999) Transmissibility and Persistence of Oral Polio Vaccine Viruses: Implications for the Global Poliomyelitis Eradication Initiative. *Am J Epidemiol* 150: 1001-1021.
245. Aguilar PV, Adams AP, Wang E, Kang W, Carrara AS, Anishchenko M, Frolov I, Weaver SC (2008) Structural and nonstructural protein genome regions of eastern equine encephalitis virus are determinants of interferon sensitivity and murine virulence. *J Virol* 82: 4920-4930.
246. Gerberg EJ, Barnard DR, Ward RA (1994) Manual for mosquito rearing and experimental techniques. Bulletin No. 5. Lake Charles, Louisiana: American Mosquito Control Association. 98 p.
247. Beaty BJ, Calisher CH, Shope RE (1989) Arboviruses. In: Schmidt NJ, Emmons RW, editors. Diagnostic procedures for viral, rickettsial and chlamydial infections, 6th edition. Washington, D. C.: American Public Health Association. pp. 797-855.
248. Smith DR, Carrara AS, Aguilar PV, Weaver SC (2005) Evaluation of methods to assess transmission potential of Venezuelan equine encephalitis virus by mosquitoes and estimation of mosquito saliva titers. *Am J Trop Med Hyg* 73: 33-39.

249. Walldridge BM, Wenzel JG, Ellis AC, Rowe-Morton SE, Bridges ER, D'Andrea G, Wint R (2003) Serologic responses to eastern and western equine encephalomyelitis vaccination in previously vaccinated horses. *Vet Ther* 4: 242-248.
250. Reisen WK, Fang Y, Brault AC (2008) Limited interdecadal variation in mosquito (Diptera: Culicidae) and avian host competence for Western equine encephalomyelitis virus (Togaviridae: Alphavirus). *Am J Trop Med Hyg* 78: 681-686.
251. Pierro DJ, Powers EL, Olson KE (2008) Genetic determinants of Sindbis virus mosquito infection are associated with a highly conserved alphavirus and flavivirus envelope sequence. *J Virol* 82: 2966-2974.
252. Myles KM, Pierro DJ, Olson KE (2003) Deletions in the putative cell receptor-binding domain of Sindbis virus strain MRE16 E2 glycoprotein reduce midgut infectivity in *Aedes aegypti*. *J Virol* 77: 8872-8881.
253. Myles KM, Pierro DJ, Olson KE (2004) Comparison of the transmission potential of two genetically distinct Sindbis viruses after oral infection of *Aedes aegypti* (Diptera: Culicidae). *J Med Entomol* 41: 95-106.
254. Pierro DJ, Powers EL, Olson KE (2007) Genetic determinants of Sindbis virus strain TR339 affecting midgut infection in the mosquito *Aedes aegypti*. *J Gen Virol* 88: 1545-1554.
255. Nagata LP, Hu WG, Parker M, Chau D, Rayner GA, Schmaltz FL, Wong JP (2006) Infectivity variation and genetic diversity among strains of Western equine encephalitis virus. *J Gen Virol* 87: 2353-2361.
256. Tsetsarkin KA, Vanlandingham DL, McGee CE, Higgs S (2007) A single mutation in chikungunya virus affects vector specificity and epidemic potential. *PLoS Pathog* 3: e201.
257. Vaughan JA, Turell MJ (1996) Dual host infections: enhanced infectivity of eastern equine encephalitis virus to *Aedes* mosquitoes mediated by *Brugia microfilariae*. *Am J Trop Med Hyg* 54: 105-109.
258. (2000) Helminthiases. In: Meyers WM, Neafie RC, Marty AM, Wear DJ, editors. *Pathology of Infectious Diseases*. Washington, D.C.: Armed Forces Institute of Pathology. pp. 245-306.
259. Ciota AT, Lovelace AO, Jia Y, Davis LJ, Young DS, Kramer LD (2008) Characterization of mosquito-adapted West Nile virus. *J Gen Virol* 89: 1633-1642.
260. Coffey LL, Vasilakis N, Brault AC, Powers AM, Triplet F, Weaver SC (2008) Arbovirus evolution in vivo is constrained by host alternation. *Proc Natl Acad Sci U S A* 105: 6970-6975.
261. Weaver SC, Kang W, Shirako Y, Rumenapf T, Strauss EG, Strauss JH (1997) Recombinational history and molecular evolution of western equine encephalomyelitis complex alphaviruses. *J Virol* 71: 613-623.

262. Adams RH, Brown DT (1985) BHK cells expressing Sindbis virus-induced homologous interference allow the translation of nonstructural genes of superinfecting virus. *J Virol* 54: 351-357.
263. Igarashi A, Koo R, Stollar V (1977) Evolution and properties of *Aedes albopictus* cell cultures persistently infected with sindbis virus. *Virology* 82: 69-83.
264. Stollar V, Shenk TE (1973) Homologous viral interference in *Aedes albopictus* cultures chronically infected with Sindbis virus. *J Virol* 11: 592-595.
265. Johnston RE, Wan K, Bose HR (1974) Homologous interference induced by Sindbis virus. *J Virol* 14: 1076-1082.
266. MacDonald GH (1957) *The epidemiology and control of malaria*: Oxford University Press, London.
267. De Jong BHJ, Cairns MA, Haggerty PK, Ramirez-Marcial N, Ochoa-Gaona S, Mendoza-Vega J, Gonzalez-Espinosa II, March-Mifsut II (1999) Land-Use Change and Carbon Flux Between 1970s and 1990s in Central Highlands of Chiapas, Mexico. *Environ Manage* 23: 373-385.
268. Barrera R, Torres N, Freier JE, Navarro JC, Garcia CZ, Salas R, Vasquez C, Weaver SC (2001) Characterization of enzootic foci of Venezuelan equine encephalitis virus in western Venezuela. *Vector Borne Zoonotic Dis* 1: 219-230.
269. Aguilar PV, Greene IP, Coffey LL, Medina G, Moncayo AC, Anishchenko M, Ludwig GV, Turell MJ, O'Guinn ML, Lee J, et al. (2004) Endemic Venezuelan equine encephalitis in northern Peru. *Emerg Infect Dis* 10: 880-888.

Vita

Joan Louise Kenney was born on April 3, 1979 to John and Ann Kenney. She graduated from Shawnee Mission East High School in Prairie Village, KS in 1997 and matriculated at Tulane University for her undergraduate degree. After receiving her Bachelor of Science studying Ecology and Evolution, Joanie acquired a Master in Public Health degree at Yale University School of Public Health. While at Yale in Durland Fish's lab, she studied examined co-infection of multiple tick-borne pathogens in the black-legged tick (*Ixodes scapularis*) and the white footed mouse (*Peromyscus leucopus*). Joanie was awarded a CDC/NCID/APHL pre-doctoral Emerging Infectious Disease Fellowship and worked in the state public health laboratory under Pascale Leonard in New Mexico developing surveillance systems for multiple vector-borne pathogens throughout her fellowship. After completing her fellowship, she decided to acquire a Ph.D degree and was accepted as a starting graduate student at the University of Texas Medical Branch in 2005. While working in Scott Weaver's lab, Joanie was awarded the Robert Gross Memorial award from the American Society of Biological Safety and the UTMB Center for Tropical Diseases Scholarship award in addition to multiple training fellowships. Through her research at UTMB, Joanie has gained valuable laboratory experience in a vast number of techniques and procedures and has had many opportunities to improve her scientific writing through paper and grant submissions.

After November 11th, Joanie can be contacted at 3632 S. Timberline Rd. #C304, Fort Collins, CO 80525. Email: joaniekenney@mac.com

Education

B.S., May 2001, Tulane University, New Orleans, LA

MPH, May 2003, Yale University School of Public Health, New Haven, CT

Publications

Smith, D. R., A. P. Adams, **J. L. Kenney**, E. Wang, and S. C. Weaver. 2008. Venezuelan equine encephalitis virus in the mosquito vector *Aedes taeniorhynchus*: infection initiated by a small number of susceptible epithelial cells and a population bottleneck. *Virology* **372**:176-86.

Forrester NL, **Kenney JL**, Deardorff E, Wang E, Weaver SC, 2008. Western Equine Encephalitis submergence: lack of evidence for a decline in virus virulence. *Virology* **380**: 170-2.

Vasilakis N, Deardorff ER, **Kenney JL**, Rossi SL, Hanley KA, Weaver SC, 2009. Mosquitoes Put the Brake on Arbovirus Evolution: Experimental Evolution Reveals Slower Mutation Accumulation in Mosquito Than Vertebrate Cells. *PLoS Pathog* **5**: e1000467.

Kenney JL, Adams AP, Weaver SC, 2010. Evaluation of transmission potential of two chimeric western equine encephalitis vaccine candidates in *Culex tarsalis*. *American Journal of Tropical Medicine and Hygiene*. **82**(2): 354-9

Kenney, JL, Volk S, Wang E, Pandya J, Xiaodong R, Weaver SC. 2011. Stability of alphavirus attenuation approaches. *Vaccine*. **29**: 2230-2234

Darwin JR, Kenney JL, Weaver SC (2011) Transmission potential of two chimeric chikungunya vaccine candidates in the urban mosquito vectors, *Aedes aegypti* and *Ae. albopictus*. *Am J Trop Med Hyg* **84**: 1012-1015.

Kenney, JL, Adams AP, Gorchakov R, Leal G, Weaver SC. 2011. Determinants of infection and dissemination in the enzootic mosquito vector, *Cx. taeniopus*. *PLOS Neg Trop Dis*. In Revisions.

PERMISSIONS

Hi Joanie,

Thanks for sending that across - there is no need to fax a copy. If you require me to send you a high-res copy of the image, there will be a nominal service fee of £2.50 + VAT, however if the version you already have is sufficient, all that you need to do is to ensure that the image is clearly and correctly credited to: 'Wellcome Library, London'. Just let me know if you would like the high-res.

All the best,
Al.

-----Original Message-----

From: Kenney, Joan L. [<mailto:jkkenney@UTMB.EDU>]

Sent: 06 October 2011 17:35

To: McCartney, Alasdair

Subject: Re: permission to use material in my dissertation

Thanks Al,

This is the image I am using. There are a few handwritten bits around the labels, but otherwise it was scanned directly from the hard copy (a photocopy of the original) we have in the lab. Here is the form. I'll have to find a fax machine to send the signature on. Let know if am missing anything on the form.

Thanks,
Joanie

On 10/6/11 9:34 AM, "McCartney, Alasdair" <A.McCartney@wellcome.ac.uk> wrote:

Dear Joan,

Thank you for your email. Would it be possible for you to forward me a copy of the image, as I can't seem to identify it from the links you've provided below. Could you also complete and return the attached form.

All the best,
Al.

Al McCartney

Picture Researcher, Historical Collection The Wellcome Trust

215 Euston Road, London NW1 2BE

Tele: +44 (0) 207 611 8643

Fax: +44 (0) 207 611 8577

mailto: A.McCartney@wellcome.ac.uk

<http://www.wellcome.ac.uk>

We are a global charitable foundation dedicated to achieving extraordinary improvements in human and animal health. We support the brightest minds in biomedical research and the medical humanities. Our breadth of support includes public engagement, education and the application of research to improve health. We are independent to both political and commercial interests.

**ELSEVIER LICENSE
TERMS AND CONDITIONS**

Sep 14, 2011

This is a License Agreement between Joan L Kenney ("You") and Elsevier ("Elsevier") provided by Copyright Clearance Center ("CCC"). The license consists of your order details, the terms and conditions provided by Elsevier, and the payment terms and conditions.

All payments must be made in full to CCC. For payment instructions, please see information listed at the bottom of this form.

Supplier	Elsevier Limited The Boulevard, Langford Lane Kidlington, Oxford, OX5 1GB, UK
Registered Company Number	1982084
Customer name	Joan L Kenney
Customer address	102 Strand Street Galveston, TX 77550
License number	2747870419632
License date	Sep 14, 2011
Licensed content publisher	Elsevier
Licensed content publication	Virology
Licensed content title	Venezuelan equine encephalitis virus in the mosquito vector <i>Aedes taeniorhynchus</i> : Infection initiated by a small number of susceptible epithelial cells and a population bottleneck
Licensed content author	Darci R. Smith, A. Paige Adams, Joan L. Kenney, Eryu Wang, Scott C. Weaver
Licensed content date	1 March 2008
Licensed content volume number	372
Licensed content issue number	1
Number of pages	11
Start Page	176
End Page	186
Type of Use	reuse in a thesis/dissertation
Portion	figures/tables/illustrations

[Print This Page](#)

**AMERICAN SOCIETY FOR MICROBIOLOGY LICENSE
TERMS AND CONDITIONS**

Sep 14, 2011

This is a License Agreement between Joan L Kenney ("You") and American Society for Microbiology ("American Society for Microbiology") provided by Copyright Clearance Center ("CCC"). The license consists of your order details, the terms and conditions provided by American Society for Microbiology, and the payment terms and conditions.

All payments must be made in full to CCC. For payment instructions, please see information listed at the bottom of this form.

License Number	2747870941523
License date	Sep 14, 2011
Licensed content publisher	American Society for Microbiology
Licensed content publication	Infection and Immunity
Licensed content title	Growth Curves and Clearance Rates of Virulent and Benign Venezuelan Encephalitis Viruses in Hamsters
Licensed content author	Peter B. Jahrling, William F. Scherer
Licensed content date	Sep 1, 1973
Volume	8
Issue	3
Start page	456
End page	462
Type of Use	Dissertation/Thesis
Format	Print and electronic
Portion	Figures/tables/images
Number of figures/tables	1
Order reference number	
Title of your thesis / dissertation	Venezuelan equine encephalitis in the enzootic mosquito vector, Culex taeniopus
Expected completion date	Oct 2011
Estimated size(pages)	120
Billing Type	Invoice
Billing Address	102 Strand Street

[Print This Page](#)

Subject

Figure inclusion in dissertation properly cited

Discussion Thread

	10/1
	9/20
Response Via Email (Juleen Deaner)	11
	09:2
	9 AM

Dear Joan,

Your request has been granted for use of Image 30.5 and image 31.1 from Knipe D.M., Fields Virology, 5th edition in your PhD dissertation entitled "Venezuelan equine encephalitis virus in the enzootic mosquito, Culex taeniopus." You will receive a formal letter of permission shortly.

Thank you,

Juleen Deaner

Fields 5e: 978-0-7817-8668-3

	10/1
	8/20
Customer By Email (Joan L. Kenney)	11
	05:5
	6 PM

In response to Juleen Deaner's question. The dissertation will have a maximum print of 5 copies, but likely only 2. The dissertation will be available electronically through the University website, but with password protection. Five members of my committee will be reviewing it.

Thanks,
Joan Kenney

From: Wolters Kluwer Rights and Permissions <permissions@lww.com>
Reply-To: Wolters Kluwer Rights and Permissions <permissions@lww.com>
Date: Tue, 18 Oct 2011 16:04:40 -0400
To: Joanie Kenney <jkenney@utmb.edu>
Subject: Figure inclusion in dissertation properly cited [Incident: 110926-000890]

	10/1
Response Via Email (Juleen Deaner)	8/20
	11

